AD-A218 105

DOCUMENTATION PAGE

Form Approved
OMB No. 0704-0188

1a. REPORT SECURITY CLASSIFICATION: UNCLASSIFIED	1b. RESTRICTIVE MARKINGS: NONE
2a. SECURITY CLASSIFICATION AUTHORITY	3. DISTRIBUTION/AVAILABILITY OF REPORT: APPROVED FOR PUBLIC RELEASE; DISTRIBUTION UNLIMITED.
2b. DECLASSIFICATION/DOWNGRADING SCHEDULE	
4. PERFORMING ORGANIZATION REPORT NUMBER(S)	5. MONITORING ORGANIZATION REPORT NUMBER(S): AFIT/CI/CIA- 89-104
6a. NAME OF PERFORMING ORGANIZATION: AFIT STUDENT AT TX A&M Univ / 6b. OFFICE SYMBOL (If applicable)	7a. NAME OF MONITORING ORGANIZATION: AFIT/CIA
6c. ADDRESS (City, State, and ZIP Code)	7b. ADDRESS (City, State, and ZIP Code): Wright-Patterson AFB OH 45433-6583
8a. NAME OF FUNDING/SPONSORING ORGANIZATION / 8b. OFFICE SYMBOL (If applicable)	9. PROCUREMENT INSTRUMENT IDENTIFICATION NUMBER
8c. ADDRESS (City, State, and ZIP Code)	10. SOURCE OF FUNDING NUMBERS: PROGRAM ELEMENT NO. / PROJECT NO. / TASK NO. / WORK UNIT ACCESSION NO.

11. TITLE (Include Security Classification) (UNCLASSIFIED)
DESIGN OF A HIGH ANGLE OF ATTACK ROBOTIC STING MOUNT FOR TESTS IN A LOW SPEED WIND TUNNEL

12. PERSONAL AUTHOR(S)
TOMMY JACK KUBLER

13a. TYPE OF REPORT	13b. TIME COVERED	14. DATE OF REPORT (Year, Month, Day)	15. PAGE COUNT
THESIS/DISSERTATION	FROM _____ TO _____	1989	143

16. SUPPLEMENTARY NOTATION
APPROVED FOR PUBLIC RELEASE IAW AFR 190-1
ERNEST A. HAYGOOD, 1st Lt, USAF
Executive Officer, Civilian Institution Programs

17. COSATI CODES			18. SUBJECT TERMS (Continue on reverse if necessary and identify by block number)
FIELD	GROUP	SUB-GROUP	

19. ABSTRACT (Continue on reverse if necessary and identify by block number)

20. DISTRIBUTION/AVAILABILITY OF ABSTRACT	21. ABSTRACT SECURITY CLASSIFICATION
☒ UNCLASSIFIED/UNLIMITED ☐ SAME AS RPT. ☐ DTIC USERS	UNCLASSIFIED

22a. NAME OF RESPONSIBLE INDIVIDUAL	22b. TELEPHONE (Include Area Code)	22c. OFFICE SYMBOL
ERNEST A. HAYGOOD, 1st Lt, USAF	(513) 255-2259	AFIT/CI

DD Form 1473, JUN 86 — Previous editions are obsolete. — SECURITY CLASSIFICATION OF THIS PAGE

AFIT/CI "OVERPRINT"

ABSTRACT

DESIGN OF A HIGH ANGLE OF ATTACK ROBOTIC STING MOUNT FOR TESTS IN A LOW SPEED WIND TUNNEL

A Thesis

by

TOMMY JACK KUBLER, CAPTAIN, US AIR FORCE

Submitted to the Office of Graduate Studies of
Texas A&M University
in partial fulfillment of the requirements for the degree of

MASTER OF SCIENCE

August 1989

Major Subject: Aerospace Engineering

143 pages

ABSTRACT

Design of a High Angle of Attack Robotic Sting Mount for

Tests in a Low Speed Wind Tunnel. (August 1989)

Tommy Jack Kubler, B.S., Texas A&M University

Chair of Advisory Committee: Dr. Thomas C. Pollock

A sting mounting system designed for high angle of attack (AOA) testing has been developed for the 7×10 foot low-speed wind tunnel (LSWT) at Texas A&M University (TAMU). The mechanism was able to position the model from -15° to +90° of pitch with accuracy to within 0.2°, while keeping the model near the center of the test section. Compatible with the current turntable apparatus, the high angle of attack robotic sting (HARS) retained the turntable's full range of yaw movement of ±90°. All model positioning was done without shutting the tunnel down to manually alter the sting or mounting apparatus. Pitch adjustment progressed at about 4° per second, with final position tuning taking nearly 15 seconds. The mechanism consisted of two square steel telescoping tube struts that were joined at the ends in the test section by a cross-link that held the existing TAMU LSWT small Langley sting. Wind tunnel blockage and flow irregularities near the model were minimized by mounting drive hardware under the tunnel floor. An IBM/AT compatible microcomputer equipped with an analog-to-digital conversion board provided position control, drive motor signaling, and input signal filtering.

DESIGN OF A HIGH ANGLE OF ATTACK ROBOTIC STING MOUNT FOR TESTS IN A LOW SPEED WIND TUNNEL

INTRODUCTION

Current aerodynamic challenges of design include high angle-of-attack (AOA) systems capable of sustained and controllable flight at moderate to low air speeds.[1] At the same time as more emphasis is being placed upon controllability, the ability to flight test designs is encountering ever increasing difficulty. Budgetary cutbacks are not alone in demanding more efficiency in the testing cycle. Users are demanding more results from flight tests, namely, demonstrated reliability and maintainable systems. This emphasis on assessing operational capabilities, as the weapon systems reach that level of development, is making less time available to explore the airframe's performance envelope.[2] Wind tunnel testing will now have an even more important role in the evaluation of new high AOA systems to insure that the aerodynamic performance and control characteristics are well understood and documented. Former testing methods are being reexamined for applicability in today's testing arena and new techniques are being researched to overcome the liabilities of the past.

PREVIOUS RESEARCH

Wind tunnel model mounting practices vary widely, depending

Journal model is the Journal of Aircraft

upon the the testing facility practices and the type of tests performed. The most common practice is the use of strut(s) or a tail sting. A sting is a slender rod extending along the models longitudinal axis from the base of the model, such as the tail cone or exhaust nozzle. Single strut arrangements, generally, have their centerline closely aligned with the aerodynamic center of the model. For high AOA tests, they extend from the midsection of the fuselage at angles ranging from 45 to 90 degrees. Multiple struts are also used, attaching to the fuselage and wings at angles approaching perpendicular. Since the mid-1970s, high AOA testing has found substantial differences in stability data derived from the use of different mount systems. One important fact that has become apparent; sting mounting systems are superior to strut systems, stability data differing by up to 30% for AOA above 65 degrees.[3] Mounting system supports, too, contribute destabilizing effects. Greater at low air speeds[3,4], some of the problems found in lateral-directional stability characteristics have been linked to premature vortex bursting induced by the mount support or other obstacles located downstream of the model[5]. While wind tunnel wall interference may contribute to the forementioned deviations, for most investigations the effects are from support interference. A review of current ground facility testing support systems by Ericsson and Reding in 1981 concluded that all techniques cause interference of one kind or another, strut supports significantly.[6] The elimination of interference is not realistic, but it can be minimized.[6]

NASA wind tunnel facilities have several designs used in high AOA investigations. For their 30X60 ft Langley tunnel, NASA

has a scimitar shaped track onwhich a driver/instrumentation package rides.[7] To maintain the aerodynamic center of the model in the middle of the tunnel, this design places the drive package within a cord length of the model. As discussed in reference 5, this is not far enough from the test article to provide clean, unimpinged flow about the model. In 1978, NASA announced the development of a new rotation-balance apparatus for measuring airplane spin aerodynamics in their 12-foot pressure tunnel at the Ames Research Center.[8] Capable of testing AOAs up to 100 degrees and angle of sideslip to 30 degrees, the sting/balance/mount assembly utilizes an extremely complex articulated mounting system and three different struts for high AOA simulations. The effects of rotating the large apparatus structure behind the model, unfortunatly, has been shown to cause significant support interference with vortex shedding.[9] This system, besides giving undesirable flow disturbance, would be prohibitively expensive to construct, present the undesirable use of a strut for model support and cause certain flow problems in the Texas A&M University (TAMU) Low Speed Wind Tunnel (LSWT). Flow blockage is a more critical factor in the TAMU LSWT as it has neither the cross sectional area of the NASA/Ames wind tunnel, nor their five atmosphere pressurization ability.

A three phase research program sponsored by General Dynamics/Fort Worth (GD/FW) began in 1983 in the TAMU LSWT. These tests collected data up to approximately 68 degrees AOA and side-slip angles from -10 to +10 degrees. Throughout the experimental phases of this previous work, wind tunnel data collection was

hampered by the mounting arrangement for the test model. In order to obtain a suitable matrix of variations in both AOA and sideslip, the model had to be mounted with wings vertical. This introduced an asymmetric flow field immediately downstream (within about five feet) of the model center. Since the interaction of shed vortices with this support structure is quite unpredictable, there are unknown effects from this support structure on the measured model force data. Attempts have been made to quantify these effects, but lack of an efficient way to change one of the flow angles has restricted the number of comparative measurements that can be made in the limited tunnel time. This constraint originates in the requirement to shut down the tunnel to set the sting to a new angle by repositiong pins at the base of the sting. Simply stated, data collection across both AOA and sideslip was very tedious.

PROPOSAL FOR RESEARCH

In January, 1988 a contract for research that would complement this earlier work was signed by the Texas Engineering Experiment Station (TEES) and GD/FWs Internal Research and Development Group. This new series of windtunnel tests are to go beyond the 68 degree capability of the TAMU LSWT, to 90 degrees. This research study requires the development of a new model mounting mechanism; the development of that mechanism is the focus of this proposal. Investigations by Johnson, Grafton, and Yip[5] and by Ericsson[9] found that current mounting systems have a number of undesirable effects on test items. The 7X10 foot TAMU LSWT is one of the more common sizes in the country. An

improved mounting system developed for the TAMU LSWT would have wide spread applicability in other wind tunnel facilities as well. While it would be TAMUs responsibility to design and construct a mechanism to facilitate the testing, GD/FW will fund up to 70% of the costs and the remainder arranged by TEES.

A number items define the design:

1. This design must allow a model undergoing high AOA testing to sweep through a series of angles of attack and sideslip without shutting down the tunnel to set one of the flow direction angles, AOA to range from 0 to 90 deg.

2. The design must fit on the present turntable without affecting rotations for sideslip up to 50^{o} in either direction.

3. The model must be mounted wings level in the tunnel to minimize effects on lateral-directional coefficients.

4. The model must be maintained in the center of the tunnel where the dynamic pressure variation does not exceed 0.4%.

5. The mechanical system must be remotely controlled from the operators control room.

6. AOA to be positioned to within 0.25 deg repeatably.

7. The sting mechanism must support a 200 lb model throughout the envelope described above.

Since no structural blueprints were available for the external pyramidal balance of the TAMU LSWT, physical relationships of the balance had to be surveyed and plotted. This inspection promised possibilities of including a design that mounted below the floor of the tunnel. Current sting/support designs and a number of brainstorming results were evaluated on

merits of possible tunnel blockage characteristics, flow inpingement upon the model, and; to a lessor degree; time and expense of construction.

Of several designs that were considered, one proposal ranks extremely well in all light of evaluations. Figure 1 shows the proposed sting mount, referred to as the High Angle-of-attack Robotic Sting (HARS), installed in the tunnel to scale. The mechanism consists of two square steel tubing telescoping struts which retract at differing rates. They are joined at the ends in the test section by a crosslink that holds the existing small sting. Driving the struts are a pair of electric motors geared down to a central drive screw in each strut. HARS avoids the interference with the model and the high tunnel blockage factor associated with some other model mounting methods by mounting drive hardware under the floor of the tunnel.

This design allows a model to be positioned at any desired AOA ranging from -15 to 90 degrees while allowing sideslip to be varied +-90 degrees at the same time via the test section turntable without shutting down the tunnel. Because the model would have a transient position in relation to the resolving center of the tunnel's balance structure, HARS cannot effectly use the external pyramidal balance, any model would necessarily have to use an internal balance compatible to the standard Langley sting mount.

The design can use variable gearing to the drive screw to control the rate of strut extension/retraction. Properly sized motors could allow future dynamic tests to be performed using the new mount. Backlash and other critical clearances that affect

position accuracy are to be controlled by a variety of means. The extension position nut which is moved via the drive screw can made in two parts, separated by shim stock to provide zero backlash. To control clearance between the strut extensions and their housings, adjustable nylon wear pads will separate the inner and outer tubes. Longitudinal play in the drive screws can be removed by installing a proper thickness thrust washer between the spur gear that rotates the drive screw and the mounting plate which carries the electric motors and other spur gears. Backlash in the spur gears would be unavoidable but would have a negligable effect on sting postioning.

An IBM/AT compatable microcomputer with an analog-to-digital (A/D) board will act as controller for the mechanism, providing position reading, drive motor signaling, and signal filtering. Position feedback can be given by linear potentiometers, which provide a predictable voltage drop for a percentage length extension, read through A/D ports. D/A conversion on the same board can supply a drive motor control signal. A D/A signal would be boosted by an amplifier capable of supplying power to the electric motors. A pair of microswitches on each strut protect against movement past physical limits that would damage the sting or model. In the event that any protective link should malfunction, a master power disable switch is used to shut off power to the system.

Computer code to control the mechanism will have to be user friendly and continuously sampling position to insure position accuracy. AOA is to be controlled manually or by loading an

external data file. Variables that affect the degree of movement and other characteristics of the mount will be externally defined to allow mount tuning without software modification. The final AOA position would be displayed on the screen upon the conclusion of the move. Logic sampling of the A/D ports for positioning data will need to provide for transiant voltage signals and line noise, to be filtered within the software.

For the completed design, these items will be supplied and documented:

1. Technical drawings used in the manufacture of the mechanism.

2. Listing of any computer code used in the control hardware.

3. Operation guide to installation and maintenance of the mechanism

4. Electrical schematics and requirements.

REFERENCES

[1]Vinceint, John, "New Technologies for a European Fighter," AEROSPACE AMERICA, 24 (Sept 86), 34.

[2]Wright, Orville, Jr., "Squeezing the Testing Cycle," AEROSPACE AMERICA, 26 (Feb 88), 17-19.

[3]Dietz, W. E., Jr. and Altstatt, M. C., "Experimental Investigation of Support Interface on an Ogive Cylinder at High Incidence," AIAA Paper 78-165, 16th Aerospace Sciences Meeting,

Jan 16-18, 1978.

[4]Mouch, Thomas N. and Nelson, Robert C., "The Influence of Aerodynamic Interference on High Angle of Attack Wind Tunnel Testing," AIAA Paper 78-827, 1978.

[5]Johnson, Joseph L., Grafton, Sue B. and Yip, Long P., "Exploratory Investigation of the Effects of Vortex Bursting on the High Angle-of-Attack Lateral-Directional Stability Characteristics of Highly-Swept Wings," AIAA Paper 80-0463, March 1980.

[6]Ericsson, Lars E. and Reding, J. P., "Support Interference in Static and Dynamic Tests," ICIASF '81 Record, pp. 213-223.

[7]Rae, William H., Jr., and Pope, Alan, Low-Speed Wind Tunnel Testing (New York: John Wiley & Sons, 1984), p. 175.

[8]Malcolm, Gerald N., "New Rotation-Balance Apparatus for Measuring Airplane Spin Aerodynamics in the Wind Tunnel," AIAA Paper 78-835, 1978.

[9]Ericsson, L. E., "Reflections Regarding Recent Rotary Rig Results," AIAA Paper 86-0123, AIAA 24th Aerospace Sciences Meeting, Jan 6-9, 1986.

DESIGN OF A HIGH ANGLE OF ATTACK ROBOTIC STING MOUNT FOR TESTS IN A LOW SPEED WIND TUNNEL

INTRODUCTION

Current aerodynamic challenges of design include high angle-of-attack (AOA) systems capable of sustained and controllable flight at moderate to low air speeds.[1] At the same time as more emphasis is being placed upon controllability, the ability to flight test designs is encountering ever increasing difficulty. Budgetary cutbacks are not alone in demanding more efficiency in the testing cycle. Users are demanding more results from flight tests, namely, demonstrated reliability and maintainable systems. This emphasis on assessing operational capabilities, as the weapon systems reach that level of development, is making less time available to explore the airframe's performance envelope.[2] Wind tunnel testing will now have an even more important role in the evaluation of new high AOA systems to insure that the aerodynamic performance and control characteristics are well understood and documented. Former testing methods are being reexamined for applicability in today's testing arena and new techniques are being researched to overcome the liabilities of the past.

PREVIOUS RESEARCH

Wind tunnel model mounting practices vary widely, depending

Journal model is the Journal of Aircraft

upon the the testing facility practices and the type of tests performed. The most common practice is the use of strut(s) or a tail sting. A sting is a slender rod extending along the models longitudinal axis from the base of the model, such as the tail cone or exhaust nozzle. Single strut arrangements, generally, have their centerline closely aligned with the aerodynamic center of the model. For high AOA tests, they extend from the midsection of the fuselage at angles ranging from 45 to 90 degrees. Multiple struts are also used, attaching to the fuselage and wings at angles approaching perpendicular. Since the mid-1970s, high AOA testing has found substantial differences in stability data derived from the use of different mount systems. One important fact that has become apparent; sting mounting systems are superior to strut systems, stability data differing by up to 30% for AOA above 65 degrees.[3] Mounting system supports, too, contribute destabilizing effects. Greater at low air speeds[3,4], some of the problems found in lateral-directional stability characteristics have been linked to premature vortex bursting induced by the mount support or other obstacles located downstream of the model[5]. While wind tunnel wall interference may contribute to the forementioned deviations, for most investigations the effects are from support interference. A review of current ground facility testing support systems by Ericsson and Reding in 1981 concluded that all techniques cause interference of one kind or another, strut supports significantly.[6] The elimination of interference is not realistic, but it can be minimized.[6]

NASA wind tunnel facilities have several designs used in high AOA investigations. For their 30X60 ft Langley tunnel, NASA

has a scimitar shaped track onwhich a driver/instrumentation package rides.[7] To maintain the aerodynamic center of the model in the middle of the tunnel, this design places the drive package within a cord length of the model. As discussed in reference 5, this is not far enough from the test article to provide clean, unimpinged flow about the model. In 1978, NASA announced the development of a new rotation-balance apparatus for measuring airplane spin aerodynamics in their 12-foot pressure tunnel at the Ames Research Center.[8] Capable of testing AOAs up to 100 degrees and angle of sideslip to 30 degrees, the sting/balance/mount assembly utilizes an extremely complex articulated mounting system and three different struts for high AOA simulations. The effects of rotating the large apparatus structure behind the model, unfortunatly, has been shown to cause significant support interference with vortex shedding.[9] This system, besides giving undesirable flow disturbance, would be prohibitively expensive to construct, present the undesirable use of a strut for model support and cause certain flow problems in the Texas A&M University (TAMU) Low Speed Wind Tunnel (LSWT). Flow blockage is a more critical factor in the TAMU LSWT as it has neither the cross sectional area of the NASA/Ames wind tunnel, nor their five atmosphere pressurization ability.

A three phase research program sponsored by General Dynamics/Fort Worth (GD/FW) began in 1983 in the TAMU LSWT. These tests collected data up to approximately 68 degrees AOA and side-slip angles from -10 to +10 degrees. Throughout the experimental phases of this previous work, wind tunnel data collection was

hampered by the mounting arrangement for the test model. In order to obtain a suitable matrix of variations in both AOA and sideslip, the model had to be mounted with wings vertical. This introduced an asymmetric flow field immediately downstream (within about five feet) of the model center. Since the interaction of shed vortices with this support structure is quite unpredictable, there are unknown effects from this support structure on the measured model force data. Attempts have been made to quantify these effects, but lack of an efficient way to change one of the flow angles has restricted the number of comparative measurements that can be made in the limited tunnel time. This constraint originates in the requirement to shut down the tunnel to set the sting to a new angle by repositiong pins at the base of the sting. Simply stated, data collection across both AOA and sideslip was very tedious.

PROPOSAL FOR RESEARCH

In January, 1988 a contract for research that would complement this earlier work was signed by the Texas Engineering Experiment Station (TEES) and GD/FWs Internal Research and Development Group. This new series of windtunnel tests are to go beyond the 68 degree capability of the TAMU LSWT, to 90 degrees. This research study requires the development of a new model mounting mechanism; the development of that mechanism is the focus of this proposal. Investigations by Johnson, Grafton, and Yip[5] and by Ericsson[9] found that current mounting systems have a number of undesirable effects on test items. The 7X10 foot TAMU LSWT is one of the more common sizes in the country. An

improved mounting system developed for the TAMU LSWT would have wide spread applicability in other wind tunnel facilities as well. While it would be TAMUs responsibility to design and construct a mechanism to facilitate the testing, GD/FW will fund up to 70% of the costs and the remainder arranged by TEES.

A number items define the design:

1. This design must allow a model undergoing high AOA testing to sweep through a series of angles of attack and sideslip without shutting down the tunnel to set one of the flow direction angles, AOA to range from 0 to 90 deg.

2. The design must fit on the present turntable without affecting rotations for sideslip up to 50^{o} in either direction.

3. The model must be mounted wings level in the tunnel to minimize effects on lateral-directional coefficients.

4. The model must be maintained in the center of the tunnel where the dynamic pressure variation does not exceed 0.4%.

5. The mechanical system must be remotely controlled from the operators control room.

6. AOA to be positioned to within 0.25 deg repeatably.

7. The sting mechanism must support a 200 lb model throughout the envelope described above.

Since no structural blueprints were available for the external pyramidal balance of the TAMU LSWT, physical relationships of the balance had to be surveyed and plotted. This inspection promised possibilities of including a design that mounted below the floor of the tunnel. Current sting/support designs and a number of brainstorming results were evaluated on

merits of possible tunnel blockage characteristics, flow inpingement upon the model, and; to a lessor degree; time and expense of construction.

Of several designs that were considered, one proposal ranks extremely well in all light of evaluations. Figure 1 shows the proposed sting mount, referred to as the High Angle-of-attack Robotic Sting (HARS), installed in the tunnel to scale. The mechanism consists of two square steel tubing telescoping struts which retract at differing rates. They are joined at the ends in the test section by a crosslink that holds the existing small sting. Driving the struts are a pair of electric motors geared down to a central drive screw in each strut. HARS avoids the interference with the model and the high tunnel blockage factor associated with some other model mounting methods by mounting drive hardware under the floor of the tunnel.

This design allows a model to be positioned at any desired AOA ranging from -15 to 90 degrees while allowing sideslip to be varied +-90 degrees at the same time via the test section turntable without shutting down the tunnel. Because the model would have a transient position in relation to the resolving center of the tunnel's balance structure, HARS cannot effectly use the external pyramidal balance, any model would necessarily have to use an internal balance compatible to the standard Langley sting mount.

The design can use variable gearing to the drive screw to control the rate of strut extension/retraction. Properly sized motors could allow future dynamic tests to be performed using the new mount. Backlash and other critical clearances that affect

position accuracy are to be controlled by a variety of means. The extension position nut which is moved via the drive screw can made in two parts, separated by shim stock to provide zero backlash. To control clearance between the strut extensions and their housings, adjustable nylon wear pads will separate the inner and outer tubes. Longitudinal play in the drive screws can be removed by installing a proper thickness thrust washer between the spur gear that rotates the drive screw and the mounting plate which carries the electric motors and other spur gears. Backlash in the spur gears would be unavoidable but would have a negligable effect on sting postioning.

An IBM/AT compatable microcomputer with an analog-to-digital (A/D) board will act as controller for the mechanism, providing position reading, drive motor signaling, and signal filtering. Position feedback can be given by linear potentiometers, which provide a predictable voltage drop for a percentage length extension, read through A/D ports. D/A conversion on the same board can supply a drive motor control signal. A D/A signal would be boosted by an amplifier capable of supplying power to the electric motors. A pair of microswitches on each strut protect against movement past physical limits that would damage the sting or model. In the event that any protective link should malfunction, a master power disable switch is used to shut off power to the system.

Computer code to control the mechanism will have to be user friendly and continuously sampling position to insure position accuracy. AOA is to be controlled manually or by loading an

external data file. Variables that affect the degree of movement and other characteristics of the mount will be externally defined to allow mount tuning without software modification. The final AOA position would be displayed on the screen upon the conclusion of the move. Logic sampling of the A/D ports for positioning data will need to provide for transiant voltage signals and line noise, to be filtered within the software.

For the completed design, these items will be supplied and documented:

1. Technical drawings used in the manufacture of the mechanism.

2. Listing of any computer code used in the control hardware.

3. Operation guide to installation and maintenance of the mechanism

4. Electrical schematics and requirements.

REFERENCES

[1]Vinceint, John, "New Technologies for a European Fighter," AEROSPACE AMERICA, 24 (Sept 86), 34.

[2]Wright, Orville, Jr., "Squeezing the Testing Cycle," AEROSPACE AMERICA, 26 (Feb 88), 17-19.

[3]Dietz, W. E., Jr. and Altstatt, M. C., "Experimental Investigation of Support Interface on an Ogive Cylinder at High Incidence," AIAA Paper 78-165, 16th Aerospace Sciences Meeting,

Jan 16-18, 1978.

[4]Mouch, Thomas N. and Nelson, Robert C., "The Influence of Aerodynamic Interference on High Angle of Attack Wind Tunnel Testing," AIAA Paper 78-827, 1978.

[5]Johnson, Joseph L., Grafton, Sue B. and Yip, Long P., "Exploratory Investigation of the Effects cf Vortex Bursting on the High Angle-of-Attack Lateral-Directional Stability Characteristics of Highly-Swept Wings," AIAA Paper 80-0463, March 1980.

[6]Ericsson, Lars E. and Reding, J. P., "Support Interference in Static and Dynamic Tests," ICIASF '81 Record, pp. 213-223.

[7]Rae, William H., Jr., and Pope, Alan, Low-Speed Wind Tunnel Testing (New York: John Wiley & Sons, 1984), p. 175.

[8]Malcolm, Gerald N., "New Rotation-Balance Apparatus for Measuring Airplane Spin Aerodynamics in the Wind Tunnel," AIAA Paper 78-835, 1978.

[9]Ericsson, L. E., "Reflections Regarding Recent Rotary Rig Results," AIAA Paper 86-0123, AIAA 24th Aerospace Sciences Meeting, Jan 6-9, 1986.

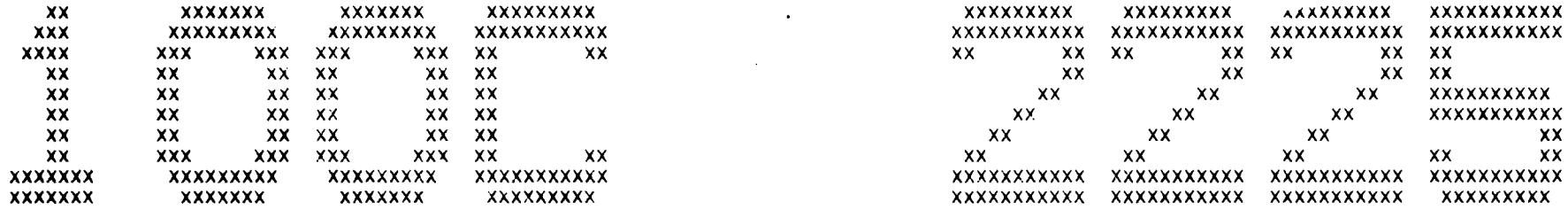

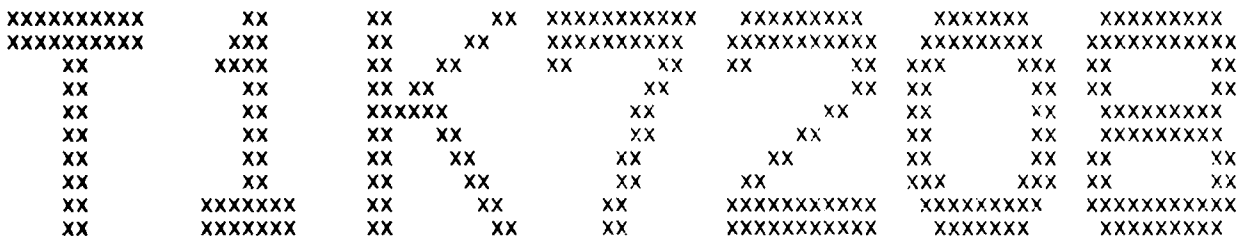

```
********  JES3 JOB SUMMARY  *********
*                                    *
*            0 CARDS READ            *
*                                    *
*            0 LINES SPOOLED         *
*                                    *
*            0 CARDS SPOOLED         *
*                                    *
*                                    *
**************************************
```

```
*****  WRITER CHARACTERISTICS  ******
*                                    *
*  DEVICE= XEROX3    TRAIN= PN       *
*                                    *
*  FORMS=  11B1      FCB=   8        *
*                                    *
*  SYSOUT= A         JDE=   MC110T   *
*                                    *
*                                    *
**************************************
```

```
**************************************
*                                    *
*       TEXAS A&M UNIVERSITY         *
*     COMPUTING SERVICES CENTER      *
*                                    *
*   IBM 3090-200E       MVS/XA/JES3  *
*                                    *
*    15.23.42       29 JUN 89.180    *
*                                    *
**************************************
```

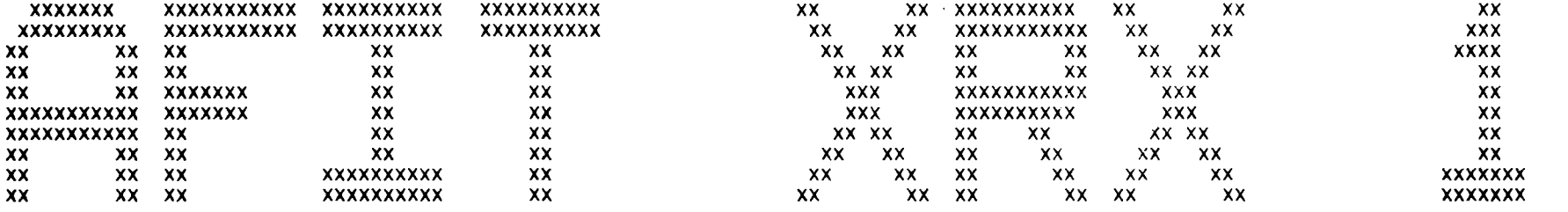

```
//T1K7208  JOB (B191,100C,  ,99,TK),'AFIT.XRX;1                JOB 2225 T1K7208  BOX 100C
```

DESIGN OF A HIGH ANGLE OF ATTACK ROBOTIC STING MOUNT FOR TESTS IN A LOW SPEED WIND TUNNEL

A Thesis

by

TOMMY JACK KUBLER

Submitted to the Office of Graduate Studies of
Texas A&M University
in partial fulfillment of the requirements for the degree of

MASTER OF SCIENCE

August 1989

Major Subject: Aerospace Engineering

DESIGN OF A HIGH ANGLE OF ATTACK ROBOTIC STING MOUNT FOR TESTS IN A LOW SPEED WIND TUNNEL

A Thesis

by

TOMMY JACK KUBLER

Approved as to style and content by:

Thomas C. Pollock
(Chair of Committee)

Donald T. Ward
(Member)

Walter E. Haisler
(Head of Department)

Maurice J. Marongiu
(Member)

August 1989

ABSTRACT

Design of a High Angle of Attack Robotic Sting Mount for

Tests in a Low Speed Wind Tunnel. (August 1989)

Tommy Jack Kubler, B.S., Texas A&M University

Chair of Advisory Committee: Dr. Thomas C. Pollock

A sting mounting system designed for high angle of attack (AOA) testing has been developed for the 7×10 foot low-speed wind tunnel (LSWT) at Texas A&M University (TAMU). The mechanism was able to position the model from -15° to +90° of pitch with accuracy to within 0.2°, while keeping the model near the center of the test section. Compatible with the current turntable apparatus, the high angle of attack robotic sting (HARS) retained the turntable's full range of yaw movement of ±90°. All model positioning was done without shutting the tunnel down to manually alter the sting or mounting apparatus. Pitch adjustment progressed at about 4° per second, with final position tuning taking nearly 15 seconds. The mechanism consisted of two square steel telescoping tube struts that were joined at the ends in the test section by a cross-link that held the existing TAMU LSWT small Langley sting. Wind tunnel blockage and flow irregularities near the model were minimized by mounting drive hardware under the tunnel floor. An IBM/AT compatible microcomputer equipped with an analog-to-digital conversion board provided position control, drive motor signaling, and input signal filtering.

DEDICATION

This is dedicated to my parents, especially my mom, whose support and love kept the ship afloat during the turbulent period which accompanied my time on this project. Without them, and God's will, the completion of this work would not have been possible.

NOMENCLATURE

a	Section width
$a.c.$	Aerodynamic center
A	Area of cross section
AR	Aspect ratio
b	Wing span
c	Aerodynamic chord
c_r	Chord length at wing root
c_t	Chord length at wing tip
C_D	Drag coefficient
C_f	Coefficient of skin friction
C_l	Sectional lift coefficient
C_L	Lift coefficient
C_m	Pitching moment coefficient
C_n	Yawing moment coefficient
ds	Discrete step along cell wall
E	Young's modulus
F	Fineness ratio function
F_c	Column loading
G	Material shear modulus
I	Section moment of inertia
K	Torsional constant
K_p	Potential flow lift constant
K_v	Vortex lift constant
$K_1 - K_2$	Fuselage correction for fineness ratio
l	Column length
$\frac{L}{d}$	Fineness ratio
L	Length of section

M	Bending moment at the end of the strut
MAC	Mean aerodynamic chord
q	Dynamic pressure
R	Lifting surface correlation factor
S	Surface area
x_a	Distance to a.c. of tail in x body axis
z_a	Distance to a.c. of tail in z body axis
t	Wall or section thickness
$\frac{t}{c}$	Maximum chord thickness to length ratio
T	Torsional moment about the section
α	Angle of attack (AOA)
ΔC_{D_0}	Miscellaneous additional drag
ΔC_{D_B}	Parabolic drag curve variation
$\Delta_{\frac{1}{4}}$	Sweep angle
λ	Taper ratio
Λ_{LE}	Leading edge sweep angle
θ	Angle of twist per unit length

Subscripts

b	Base
B	Body
cyl	Cylinder
ac	Aerodynamic center
E	Exposed wing area
i	Induced
f	Friction
fus	Fuselage
L	Lift
max	Maximum
Nac	Nacelle
0	Zero lift

t	Tail
v	Polar
w	Wing
W	Total wing
WB	Wing-body
α	Angle of attack contribution

TABLE OF CONTENTS

APPENDIX Page

LIST OF TABLES

LIST OF FIGURES

INTRODUCTION

Current aerodynamic challenges of design include the development of high angle of attack (AOA) systems capable of sustained, controllable flight at moderate to low air speeds[1]. While controllability is being emphasized, end-users of aircraft are demanding more results from flight tests, namely, demonstrated improvements in reliability and maintainability of the airframe[2]. Unfortunately, the increased demand on flight testing has not been matched with increased budgetary funding. To more efficiently utilize the limited time available to flight test, wind tunnel testing is being relied upon even more in new high AOA systems. Traditional high angle of attack wind tunnel testing was limited to about 30° AOA; evaluation of the current generation of high performance aircraft has required this to be extended to 90° and beyond. Former testing methods have been reexamined for applicability in today's evaluation arena and new techniques are being researched to overcome the liabilities of the past.

Wind tunnel model mounting practices have varied widely, depending upon the testing facility practices and the type of tests performed. Figure 1 shows the two most common types of model support systems, the strut and the sting. Sting supports attach to the model along its longitudinal axis. Strut mounts join the model at an oblique angle, generally with the central axis of the strut passing through the aerodynamic center of the model. Since the mid-1970s, high AOA testing has found substantial differences in stability data derived from the use of these two support

This thesis follows the style and format of AIAA *Journal of Aircraft*.

systems. One important fact has become apparent; the sting arrangement is superior to the strut system, where stability data may vary by up to 30% in AOAs above 65°[3].

Support mounting systems also contribute destabilizing effects, mostly observable at low air speeds[3,4]. Johnson, Grafton, and Yip linked problems in lateral-directional stability characteristics to premature vortex bursting induced by the mount support or other obstacles located downstream of the model[5]. Figure 2 shows the type of struts used in their static force investigations. While wind tunnel wall interference may also contribute to the forementioned deviations, a review of current ground facility testing support systems by Ericsson and Reading in 1981 concluded that for most investigations, the interference was largely from support structure. They went further to state that strut supports caused significantly greater flow variations than other mounting techniques examined. Realisticly, interference can not be eliminated, but it can be minimized[6].

NASA wind tunnel facilities have used several designs in high AOA investigations. For their 30 × 60 ft Langley tunnel, NASA have used a scimitar shaped track (Fig. 3) on which a driver/instrumentation package rode[7]. To maintain the aerodynamic center of the model in the middle of the tunnel, this design placed the drive package within a cord length of the model. Similar to the apparatus used by Johnson, et al. (Fig. 2), the model was not far enough from the test article to provide clean, unimpinged flow about the model.

In 1978, NASA developed a rotation-balance apparatus for measuring airplane spin aerodynamics in their 12-foot pressure tunnel at the Ames Research Center[8]. Capable of testing AOAs up to 100° and angle of sideslip to 30°, the sting/balance assembly utilized an extremely complex articulated mounting system (Fig. 4) and three different struts for high AOA simulations (Fig. 5). The effects of rotating the large apparatus structure behind the model, unfortunately, caused significant support interference with vortex shedding[9]. This system, besides giving undesirable flow impingement, would be prohibitively expensive to construct, present the undesirable use of a strut for model support and cause certain flow problems in smaller, unpressurized wind tunnel facilities.

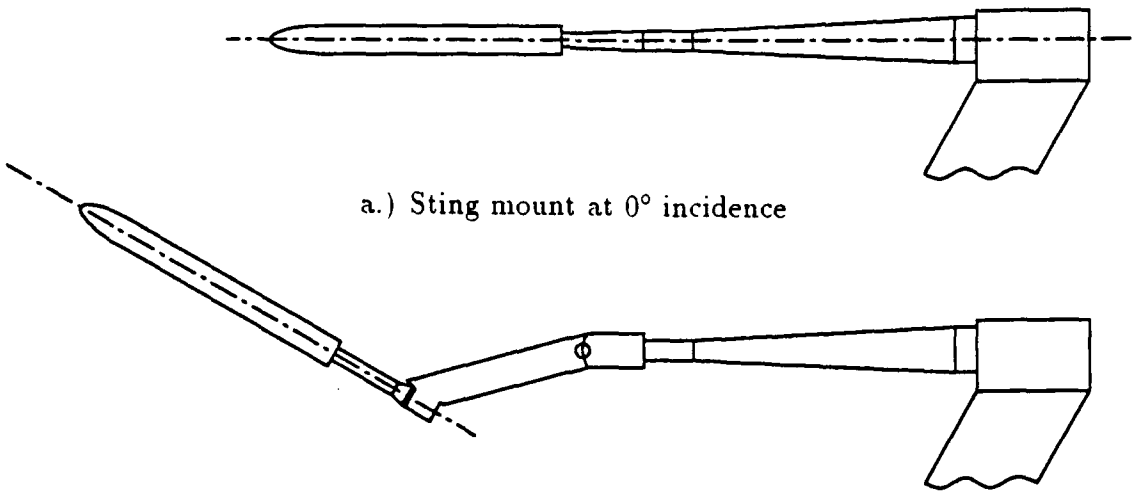

a.) Sting mount at 0° incidence

b.) Sting mount at 30° incidence

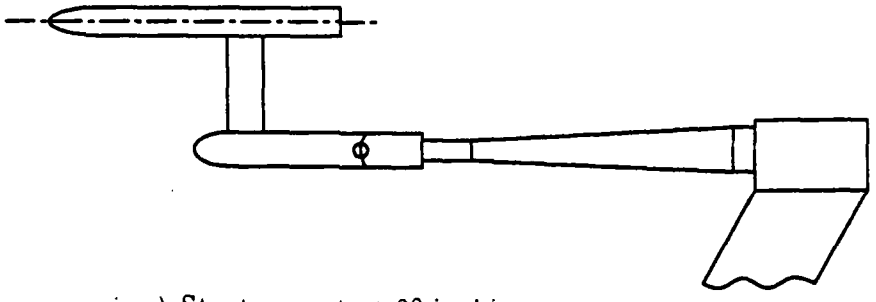

c.) Strut mount at 0° incidence

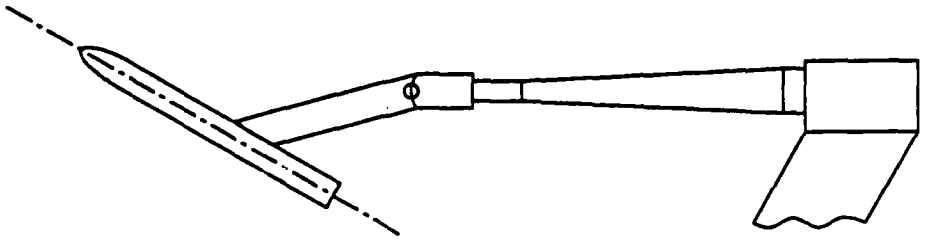

d.) Strut mount at 30° incidence

Fig. 1. Typical High Angle of Attack Support Systems.

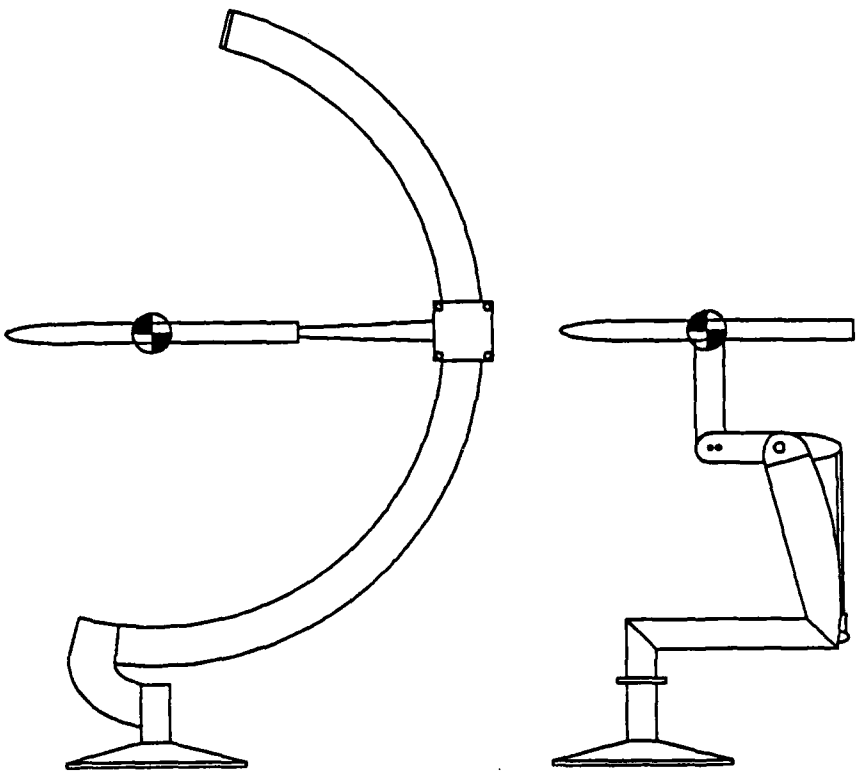

a.) Curved strut b.) Vertical strut

Fig. 2. Static force test mechanisms used by Johnson, et al.

Another type of model mounting system was used in the 3×3m LSWT of the Deutsche Forschungs- und Versuchsanstalt für Luft- und Raumfahrt E. V. Aerodynamische Versuchsanstalt Göttingen Institut für Strömungsmechanik (DFVLR-AVA)[10], Fig. 6. This arrangement used a pair of curved rails supporting a truss structure. The range of motion of the mount was limited to 30°: higher AOA testing required additional stings similar to those of Figure 5a. The amount of structure comprising the truss was not a factor for the DFVLR-AVA LSWT since it had an open circuit tunnel, but the mount could seriously affect flow in closed circuit wind

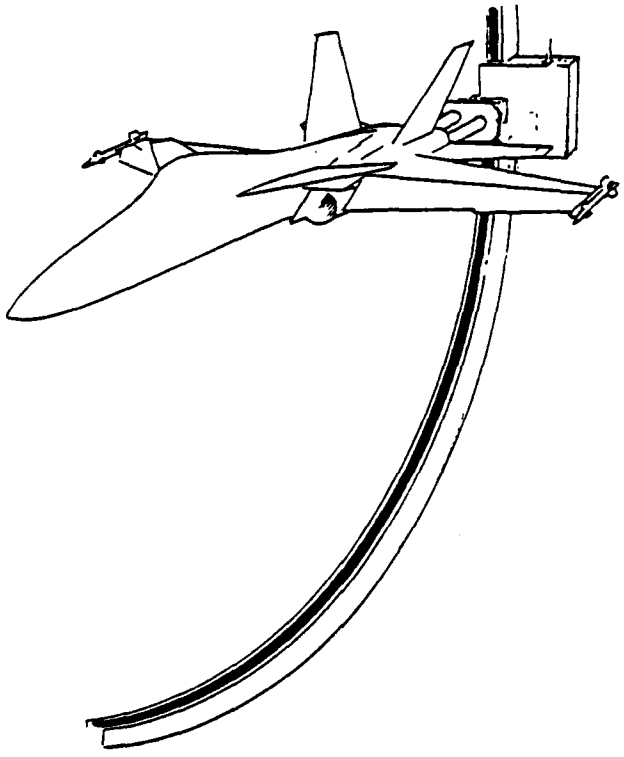

Fig. 3. NASA Langley's quadrant mounted sting.

tunnels where the negative impact of downwind model supports have already been stated. This mounting system was later found to contribute to severe model vibrations at a frequency of 6 Hz which was independent of Reynolds number and, or angle of attack[10]. The problem was solved by adding more structure to mount commercially available shock absorbers to the mount.

At the TAMU LSWT high AOA testing was done by mounting the model with wings vertical, Fig. 7. Pitch was controlled by rotating the test section turntable, and

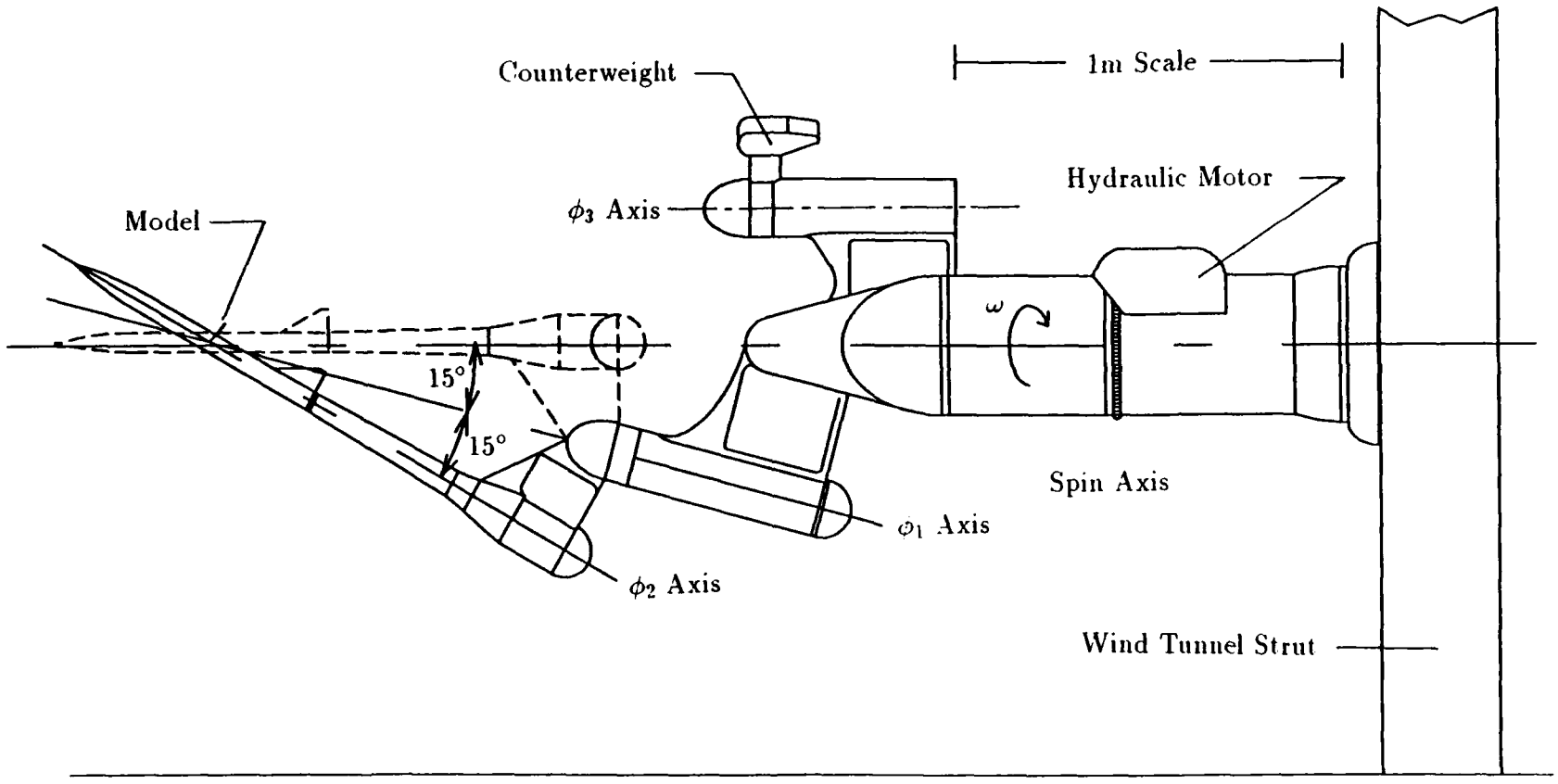

Fig. 4. NASA Ames' rotary-balance apparatus.

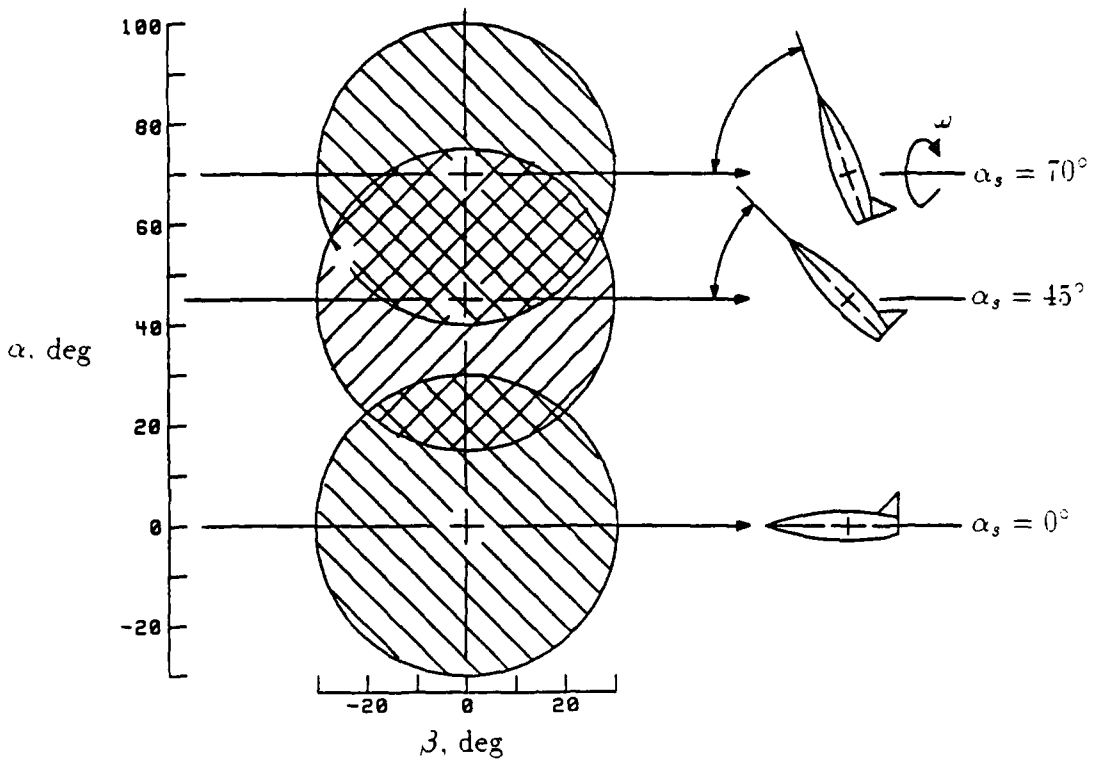

a.) Angle of attack and sideslip envelope

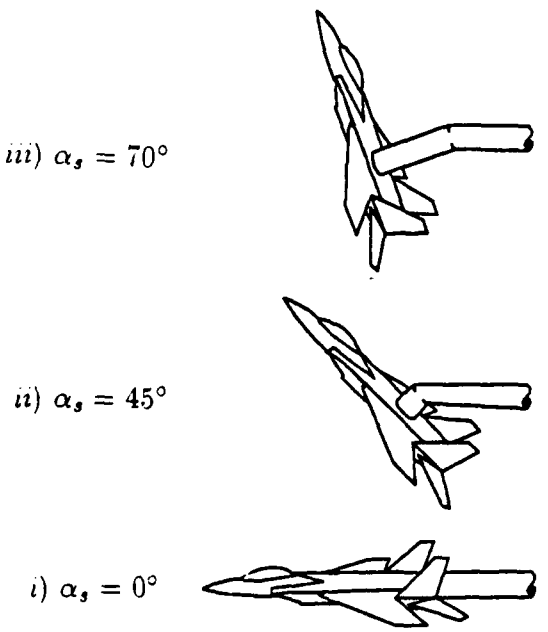

b.) Model mounted using the different stings

Fig. 5. Model mounting methods and attitude spectrum for NASA Ames' rotary-balance.

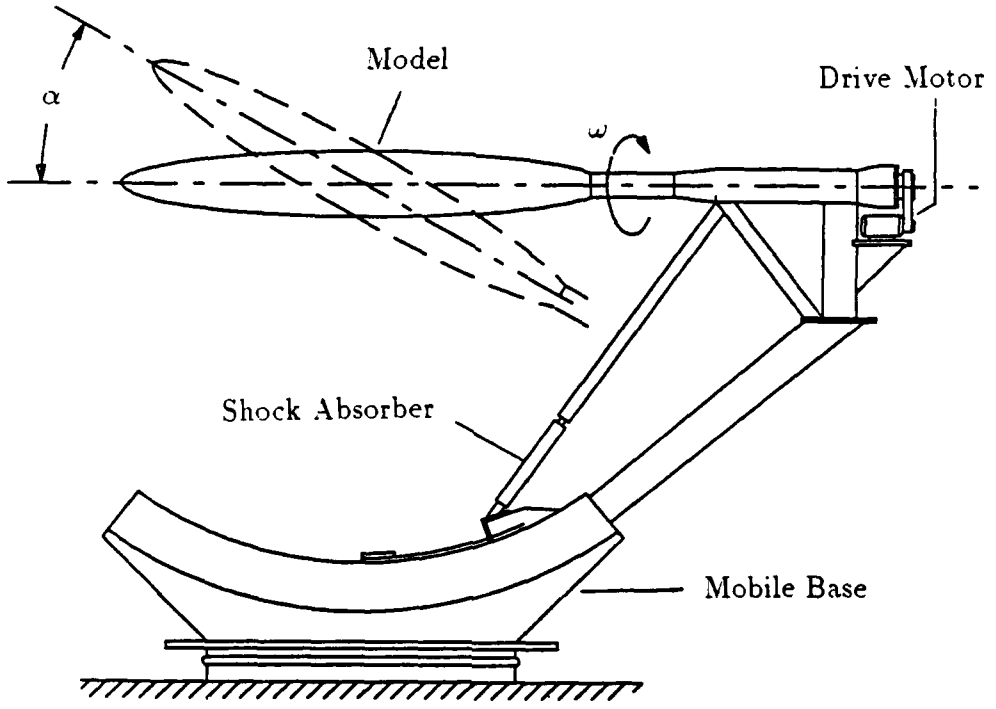

Fig. 6. Mobile balance used at the DFVLR-AVA.

yaw was controlled by an adjustable mounting knuckle. Pitch was restricted to 68° to avoid contacting the tunnel wall with the mounting mechanism. Yaw could be set from -5° to −30° in 5° increments. The adjustment of yaw was done by hand which hampered data collection since each adjustment required shutting down the tunnel to prepare the model for the next data collection set. The asymmetric mounting of the model was recognized as creating lateral-directional stability derivative errors.

and adversely affecting flow quality about the model, but these effects were not quantified[11].

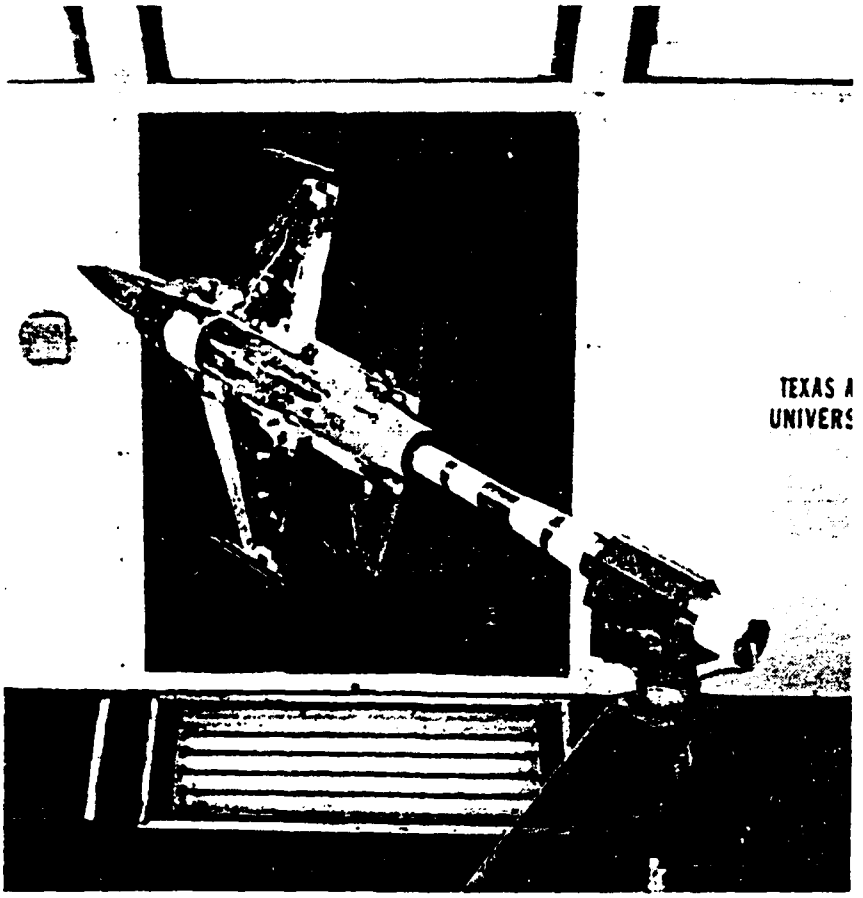

Fig. 7. Previous TAMU mounting method.

An ongoing research program at Texas A&M University required the development of a design to overcome these problems while increasing the range of pitch angle. Seven criteria were defined to be sought within the design; emphasis was placed on the ability to make high AOA testing with less tunnel down time, and minimal support generated flow disturbance, and tunnel blockage. These criteria were:

1. The design must allow a model undergoing high AOA testing to sweep through a series of pitch and yaw angles without shutting down the tunnel to set one of the flow direction angles, pitch to range from 0°

to 90°. This capability will increase test productivity by minimizing tunnel down time used to reposition the model.

2. The design must fit on the present turntable without affecting yaw rotations for up to 50°. This amount of yaw will cover the normal testing range.
3. The model must be mounted wings level in the tunnel to minimize effects on lateral-directional coefficients.
4. A 36 inch long model must be maintained near the center of the tunnel where the dynamic pressure variation does not exceed 0.4%.
5. The mechanical system must be remotely controlled from the operators control room to maintain central control of the wind tunnel and model position.
6. Pitch angle must be positioned to within 0.25°, repeatably, to give repeatable data collection performance.
7. The sting mechanism must support a 200 lb model throughout the envelope described above. This capacity will accomodate the majority of models tested.

DESIGN DEVELOPMENT

Tunnel Environment

The TAMU LSWT has a rectangular test section 7 feet high, 10 feet wide and 12 feet long (Fig. 8). The corners have 12 inch fillets which house fluorescent lamps. Cross sectional area of the test section is 68 square feet. Three inch wide vertical venting slots in the side walls at the test section exit maintain near atmospheric static pressure. The test section sidewalls diverge about 1-inch in 12-feet to account for boundary layer growth.

The floor of the test section of the TAMU LSWT is dominated by a seven foot diameter turntable which rotates with, but isolated from an external pyramidal balance. The balance, located beneath the test section, is a Dynametrics, Incorporated, six component, virtual center, mechanical balance. The range of rotation for the turntable and balance is 180° to either side. While the turntable rotates with the balance, it can also be turned separately to allow the mounting slot of the two pieces to be offset. They can then be locked together in the new relationship, and once again move in unison; however, the resulting range of movement is limited to the range remaining for either component.

Figure 9 shows the structural relationships and open space available for securing the mounting mechanism under the tunnel floor. Figure 9a details orientation for the lower turntable when it is parallel to the longitudinal axis of the test section. In Fig. 9b the lower turntable has been rotated counterclockwise 90°. Shaded areas are solid structure that cannot be removed from a 10 inch swath projected downward from the upper turntable mounting slot. Unshaded, blocked-in areas are structure immediately bordering the projected space.

Dynamic pressure variation within the test section, mapped in Fig. 10, varies by no more than 0.4% of the core velocity when farther than one foot from the wall.

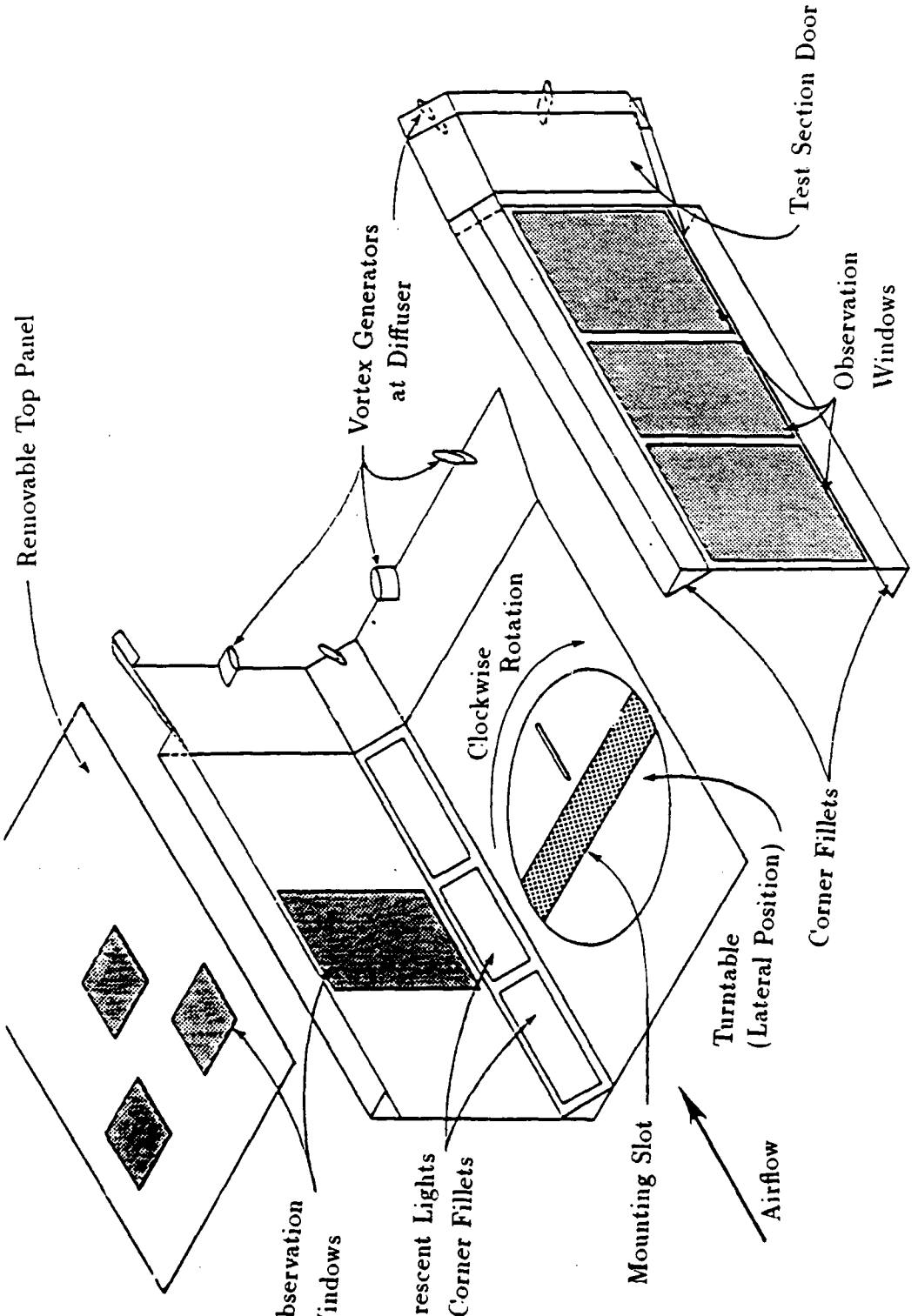

Fig. 8. Wind tunnel test section. An oblique 3-view.[12]

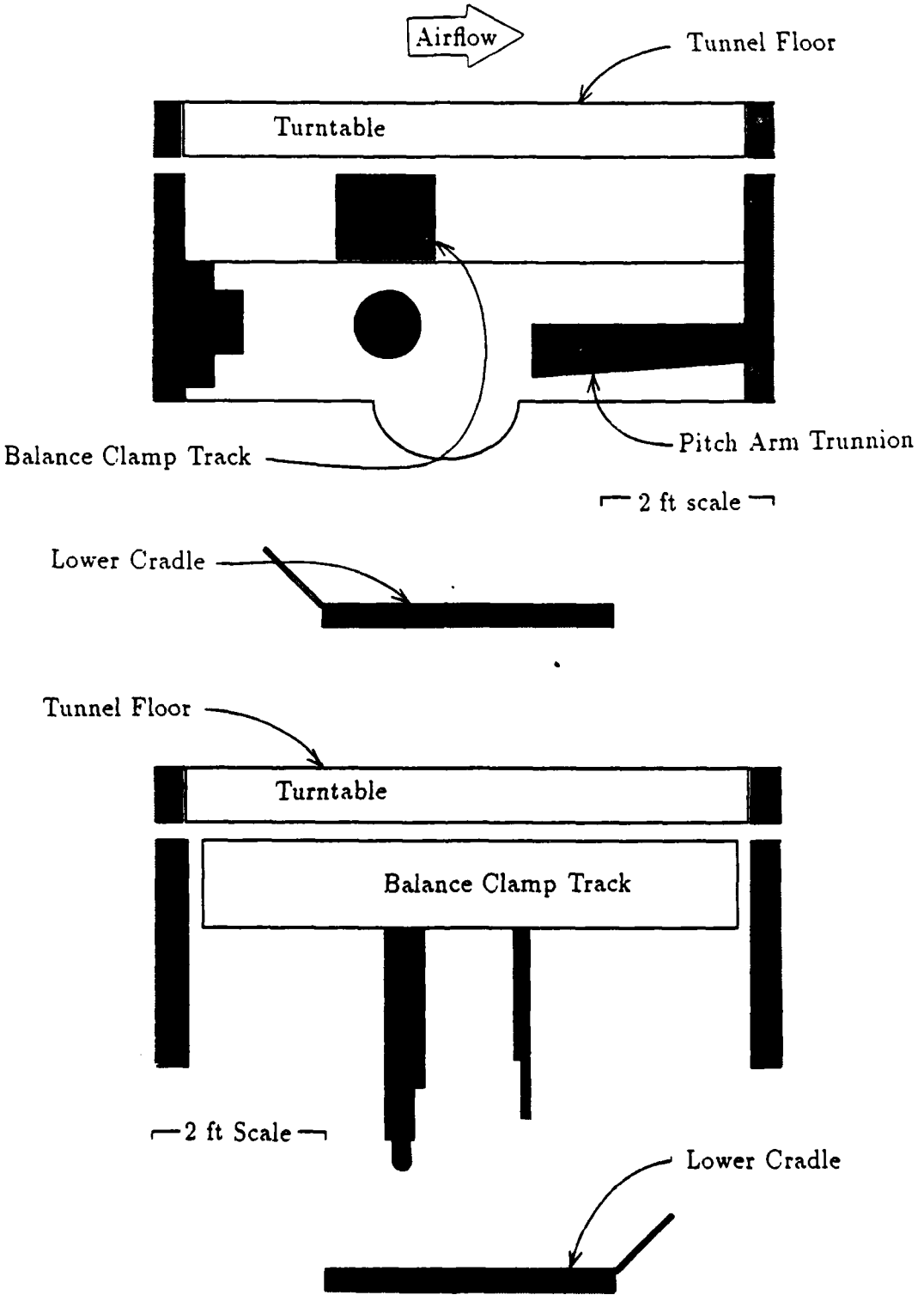

Fig. 9. Turntable structure cross section.

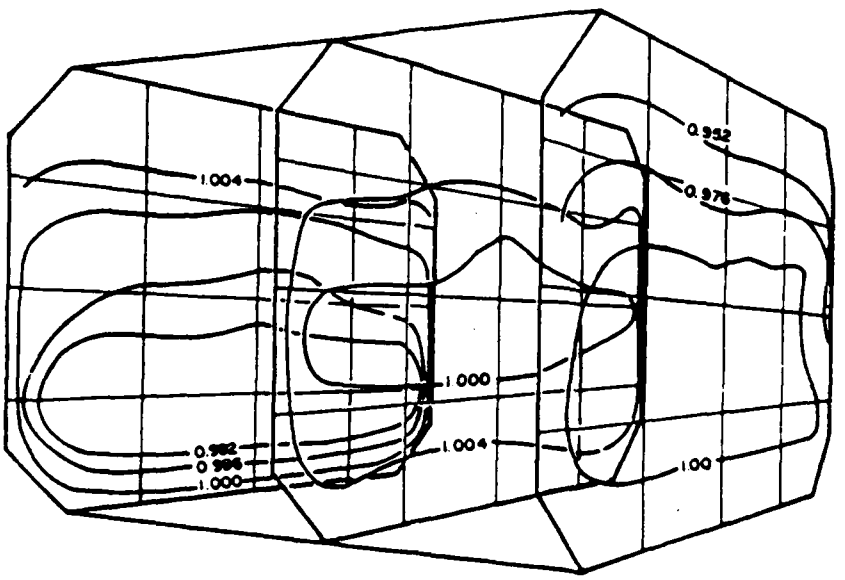

Fig. 10. Mapping of the dynamic pressure variation.[12]

representative of an empty test section's dynamic pressure variations evaluated at 30, 50, 80 and 100 pounds per square foot. To meet the flow quality requirements sought for the design, the mounting mechanism was designed to keep model out of this one foot boundary.

Preliminary Concepts

In addition to the mounting methods of other wind tunnel facilities, a number of alternative concepts were evaluated against previously discussed restrictions. Some of the alternative designs (Fig. 11) included a tripod structure, a single screw mechanism, and a dual screw arrangement. While developing each concept, consideration was given to the possibility of keeping the aerodynamic center of a model confined to the virtual center of the external balance. This capability would have allowed the external balance to be used in the evaluation of the model's aerodynamics. None

of the proposed structures adequately maintained this position, and the traditional mounting systems that could, presented undesirable flow disturbances near the model. Hence, possible use of the pyramidal balance was abandoned in favor of using internal balances for model force and moment data collection.

The tripod concept used three motors and screws. The first screw lengthened the forward support, raising the forward pivot point in relation to the rear. The other two motors spread the rear legs, dropping the mounting fork's rear pivot points. The structure's strongest advantage was rigidity obtained in triangulating the supporting structure. Secondly, being floor mounted, it could be quickly installed and removed. Disadvantages of the concept centered on the undesirable impact upon test section flow characteristics caused by the amount of structure in the vicinity of the model. Also, this concept did not appear to have the ability to maintain the model within the center of the test section over the complete pitch range.

A single screw mechanism, while providing little downwind structure to disturb the flow, had some undesirable characteristics. Lacking rigidity in both torsion and bending, this design could not maintain model position in the test section.

The third concept was able to take advantage of the space below the tunnel. The twin jackscrew arrangement could be fully extended to start the model as close to the center of the tunnel as possible. As pitch angle increased, it could lower the base of the sting toward the floor; hence, the nose of the model could be kept out of the one foot boundary of the tunnel wall. With the jackscrews in tandem, less disturbance to the flow could be achieved than with the tripod concept, as well as a more rigid structure than the single jackscrew idea. The pieces involved were relatively simple, and easy to manufacture. Seeming to have the best attributes of all the mounting systems examined, it was formally developed.

Concept Development

Figure 12 illustrates two possible variations of the developed dual jackscrew concept. The mechanism was composed of two square steel tubing telescoping struts

a.) Tripod

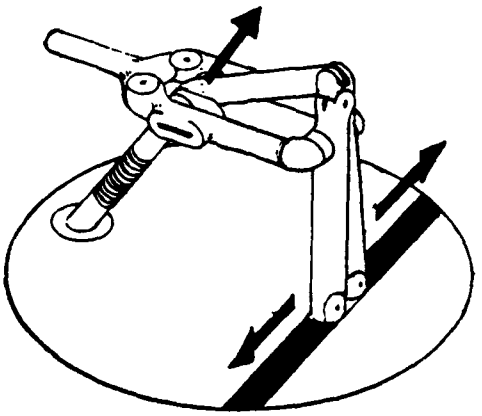

b.) Single Screw

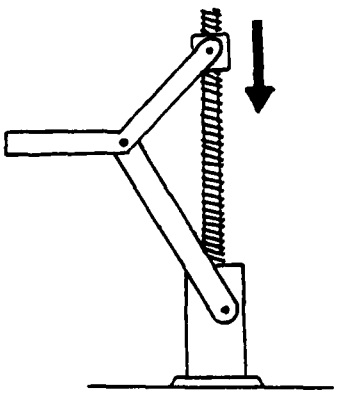

c.) Dual Screw

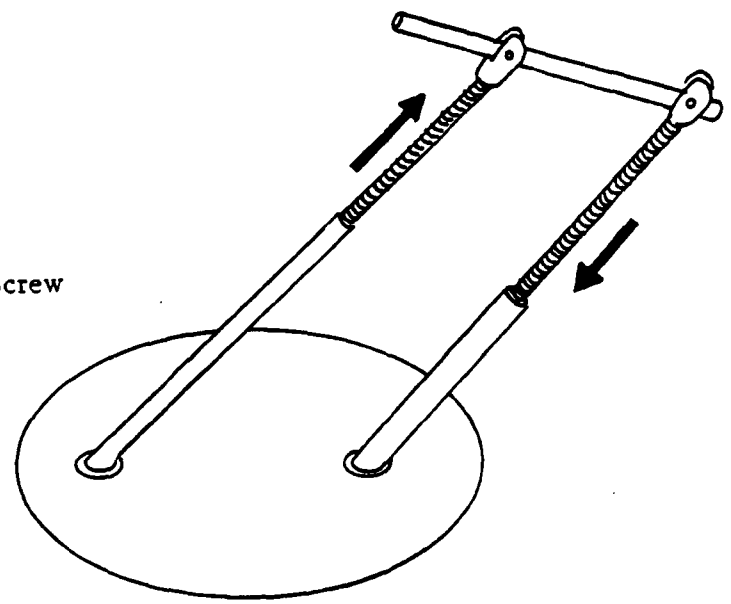

Fig. 11. Some alternative mounting methods considered.

retracting at differing rates,and joined at their upper ends by a cross-link. The cross-link, also referred to as a transverse link, held a small sting. The angular variation between the struts, occurring as the cross-link rotated, was accommodated by joining their lower ends with a pivoting joint. Each strut was powered by an electric motor geared to a drive screw running through the strut center.

The only component difference between the two variations was the adapter attaching the front strut to the mounting plate and an extension bar for the canted installation. These two parts are shaded in Fig. 12 . Mounting the front strut at a 30° angle to vertical, HARS had clearance to sit longitudinally with the balance structure. Mounted vertically, HARS sat laterally to the balance; however, in this configuration a pitch attitude of 90° was not possible. With the pitch limitations of the latter installation, only the 30° mounting angle was fully developed and tested. The 0° installation hardware was, though, still manufactured, and allowance for it made in the controlling software. Figure 13 shows HARS' positions at 0° and 90° of pitch for the 30° mount configuration.

Preliminary Sizing

Among the mounting apparatuses in the LSWT inventory was a small, Langley Mark 10+13 sting (Fig. 14), well suited to use with HARS. Its installed length was approximately 25 inches. This sting was already compatible with a number of internal balances commonly used for testing in the tunnel, and saved the expense of manufacturing a custom sting.

The small sting's installed length contributed to the environmental limitations which defined some of the physical dimensions of HARS. Accounting for the 12 inch clearance of the tunnel ceiling, a 36 inch model, the 33 inch sting length, and 2 inch clearance of the pivot bolt, the forward pivot of the transverse link at 90° of pitch could have been no higher than 1 inch above the tunnel floor.

Strut casing lengths were largely defined by the available space below the turntable, but with allowances for hardware installation. A space, seven inches deep,

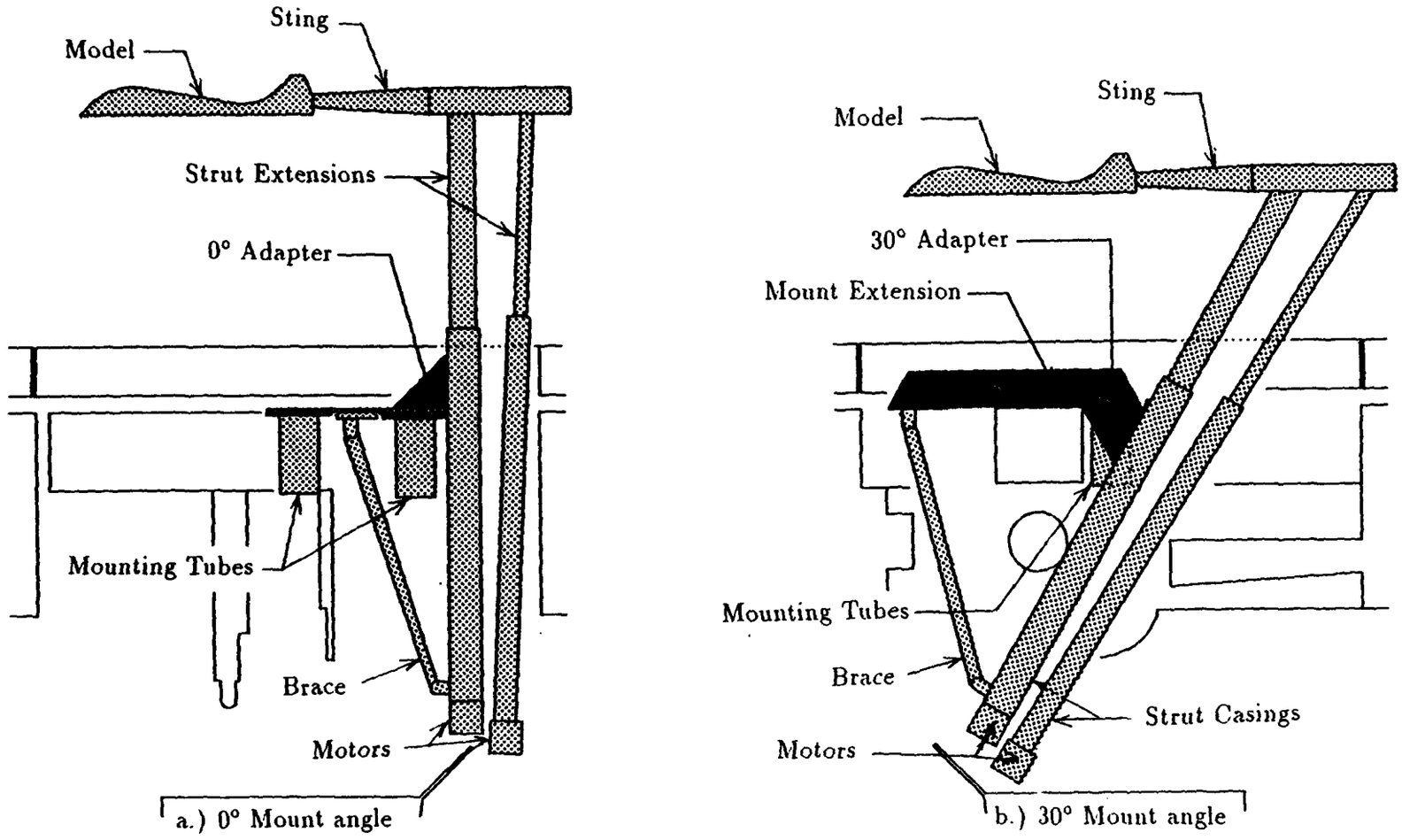

Fig. 12. General characteristics of high angle of attack robotic sting (HARS)

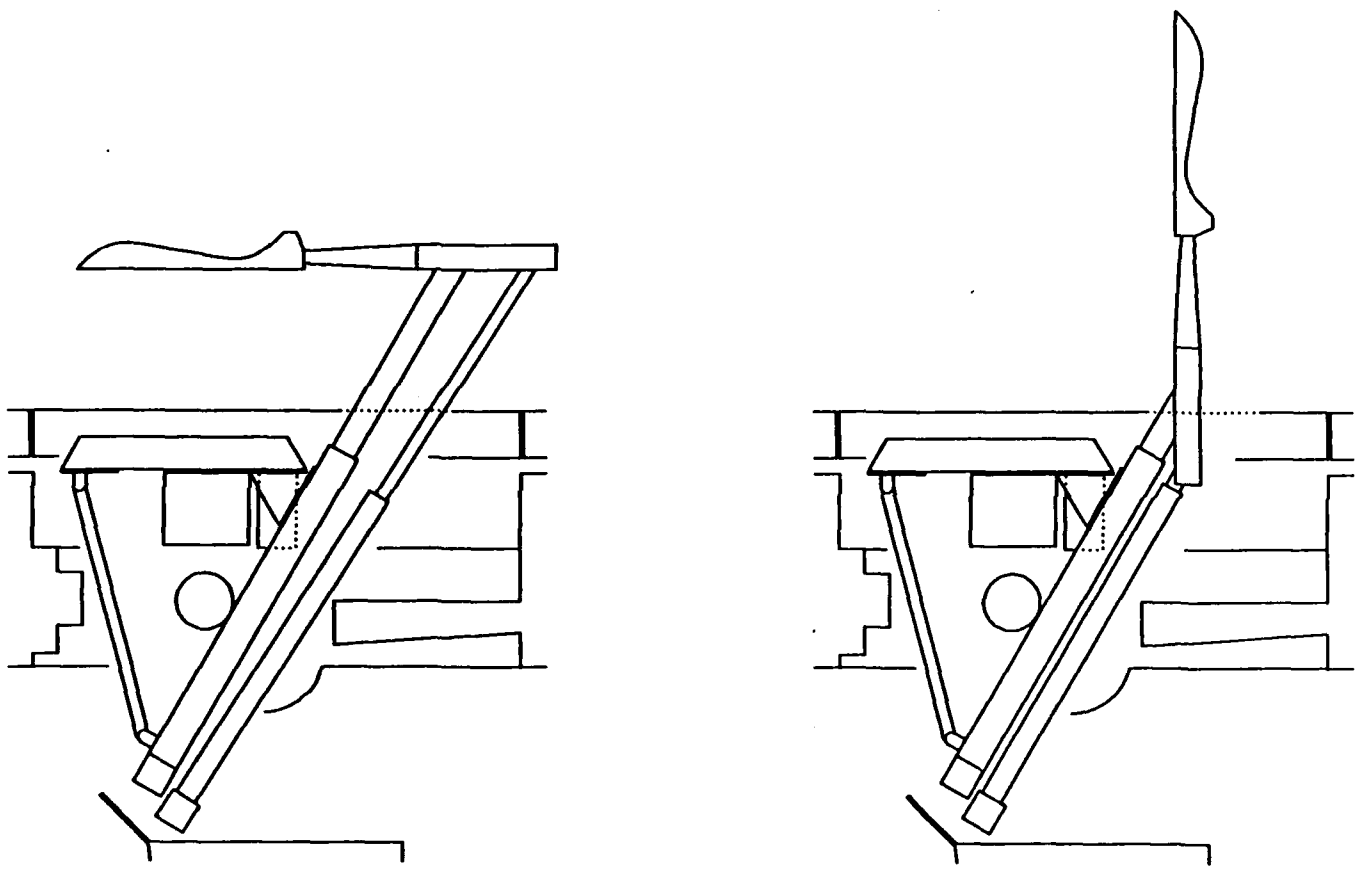

Fig. 13. Representative views of HARS at 0° and 90° AOA.

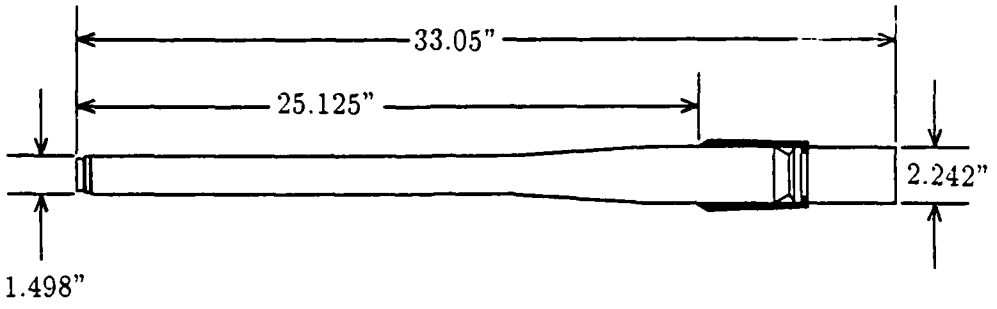

Fig. 14. Dimensional drawing of TAMU LSWT small Langley sting.

was reserved at the bottom of both struts for gearing and motor placement (Fig. 15). Preliminary size estimates of the struts outside dimensions were made to establish the operating space of the mechanism; a five inch square main strut, separated from a three inch rear strut by one inch, was assumed. With the lower extent of the strut casings limited by the pyramidal balance's cradle platform, the upper end of the casings were limited by the cross-link. The cross-link needed to be manufactured from four inch square stock in order to hold the small sting. A six inch area, the extra inch added for casing clearance, was centered on the previously established transverse link forward pivot point and projected downward. Where the projections of the strut casings and cross-link intersected established the upper extent of the installed casings.

Fore and aft rotation of the rear strut was limited to insure clearance of the external balance's pitch arm trunnion and to maintain proper spacing with the front strut casing. Strut rotation angle was minimized by placing the lower pivot point as low as possible, even with the bottom of the main strut casing. To prevent interference between the rear strut drive hardware and front strut's hardware during rotation, the end of the front strut had to be four inches above the rear strut (Fig. 16). The small

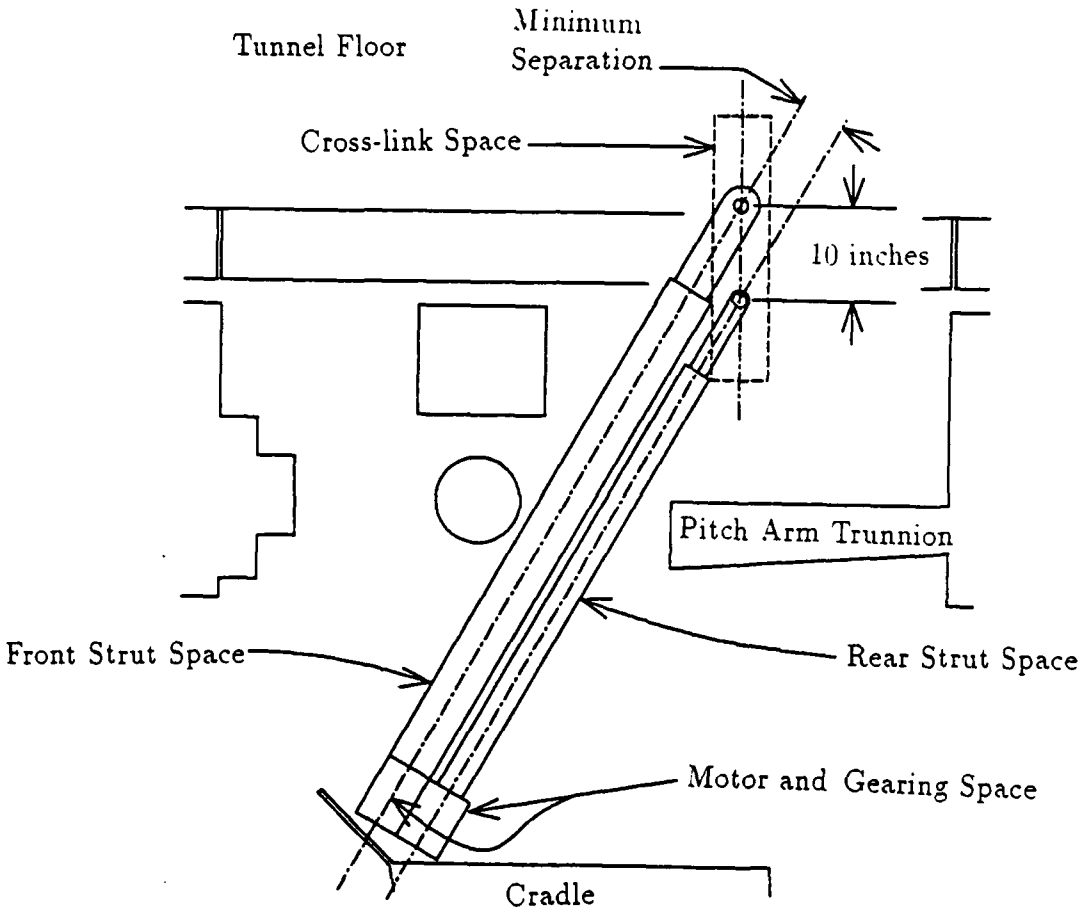

Fig. 15. Strut casing spacial restrictions.

strut was free to rotate to 4.7° (to 34.7° from the vertical) from its position parallel to the front strut.

The maximum lengths of the strut extensions were defined by the available space within the strut casings when at 90° of pitch. This pitch attitude marked the upper extent of the strut extensions, and the lower extent was two inches less than the casing length to account for the thickness of the lower casing cap and some coasting

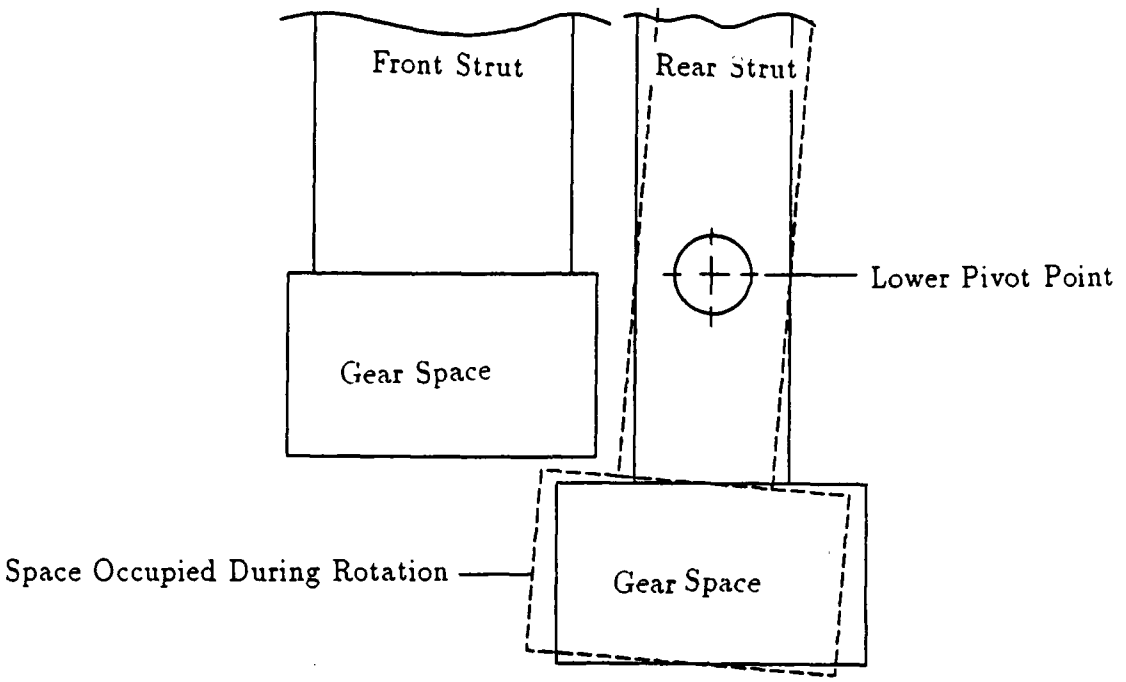

Fig. 16. Lower strut casing-to-casing clearance.

space for the extension. This space was included so that any unforeseen mechanism momentum, that would carry the strut past a commanded stopping point, would be arrested by system friction. This buffer is most important, for if the strut and casing were forcibly drawn together, it would damage the screw and/or splitnut in the strut.

The height if the cross-link above the test section floor at 0° of pitch was partly limited by the length of the rear strut extension that needed to remain captured at full extension. The rear strut capture was estimated at ten inches or 20% of the estimated total length of the rear strut. This amount provided a surface area capable of firmly holding the fully extended strut extension in alignment with the casing, while minimizing the compressive side loads on the casing lining materials.

The other defining dimension for the transverse link height at 0° of pitch was the length of the transverse link; the longer the cross-link, the lower it would reside because of the increasing angular difference between the front and rear strut. The minimum length between the pivot points of the cross-link was 10 inches, obtained when the centerlines of the two struts were parallel and HARS had a pitch angle of 90°. However, a maximum transverse link length was sought to give the rear strut as large a moment arm as possible when at 90° of pitch.

The maximum length of the link was a function of the cross-link's least allowable clearance of the pitch trunnion. The rear strut would pass through the maximum rearward angle (4.7°) when the transverse link became perpendicular to it(at 30 ° of pitch). Establishing where the maximum angle would occur necessitated defining how HARS would logically locate the upper pivot point on the front strut, and hence, one end of the cross-link. HARS retracted the front strut linearly with the absolute value of the commanded pitch attitude. At a pitch angle of 0°, the main strut was at its most extended position. 30° of pitch was known to occur when the front strut was two thirds extended.

The maximum length of the transverse link was then iteratively solved for. The length of the cross-link established the amount of main strut extension; at 0° pitch, the front strut's upper pivot point had to be level with the same point of the fully extended rear strut. With the full length of the front strut at 30° of pitch and transverse link known, the most rearward angle attained by the back strut was known, and then compared to the 4.7° limit. This process resulted in the selection of a 12 inch pivot-to-pivot transverse link length, and a 30 inch height above the tunnel floor at 0° of pitch.

Aerodynamic Load Estimation

To calculate the necessary structure to maintain angular precision within design specifications, forces and moments on the mounting mechanism were estimated. The aerodynamic forces on a simple delta wing model (Fig. 17) at a q of 100 were calculated

for AOA from 0° to 90° (Appendix A). In these computations, a maximum C_L of 1.35 at an AOA of 32° and the maximum C_D, 1.51, occurred at 90° AOA.

A FORTRAN program, **FORCES** (Appendix B), was written to facilitate the transformation of aerodynamic coefficients into forces and moments experienced by HARS. Two operational cycles were analyzed; the normal, linear strut operation, and an abnormal circumstance wherein the front strut would remain fully extended. The abnormal operation was included to insure structural strength under any combined operation possibility. Sideslip angles of 0 and 30° were also examined. The forces translated into the extremes of torsional and bending moments on the front strut of 142.84 ft-lb and 1378.48 ft-lb, respectively. It was advantageous during these calculations to calculate the location of the model's end tip. This tracking indicated that under the abnormal operation where the front strut did not move at all, the model was still out of the foot thick wall boundary up to 40° of pitch. At 55° of pitch, the model contacted the tunnel ceiling.

Strut Sizing

To begin the component sizing phase, some simplifying assumptions were made about the structural characteristics and loads:

1. The main (forward) strut would singularly carry torsional, and bending loads.
2. The rear strut would sustain the full compressive loading generated by moments acting about the pivot point atop the main strut.
3. Forces and moments would act over a 55.4 inch unsupported length of front strut extension (48 inch vertical height at 30° slant).
4. Forces due to lift would not reduced by the weight of the model.
5. A factor of safety of six would be used for all material sizing.
6. All structural materials would be low carbon steel except where a specialized function requires otherwise.

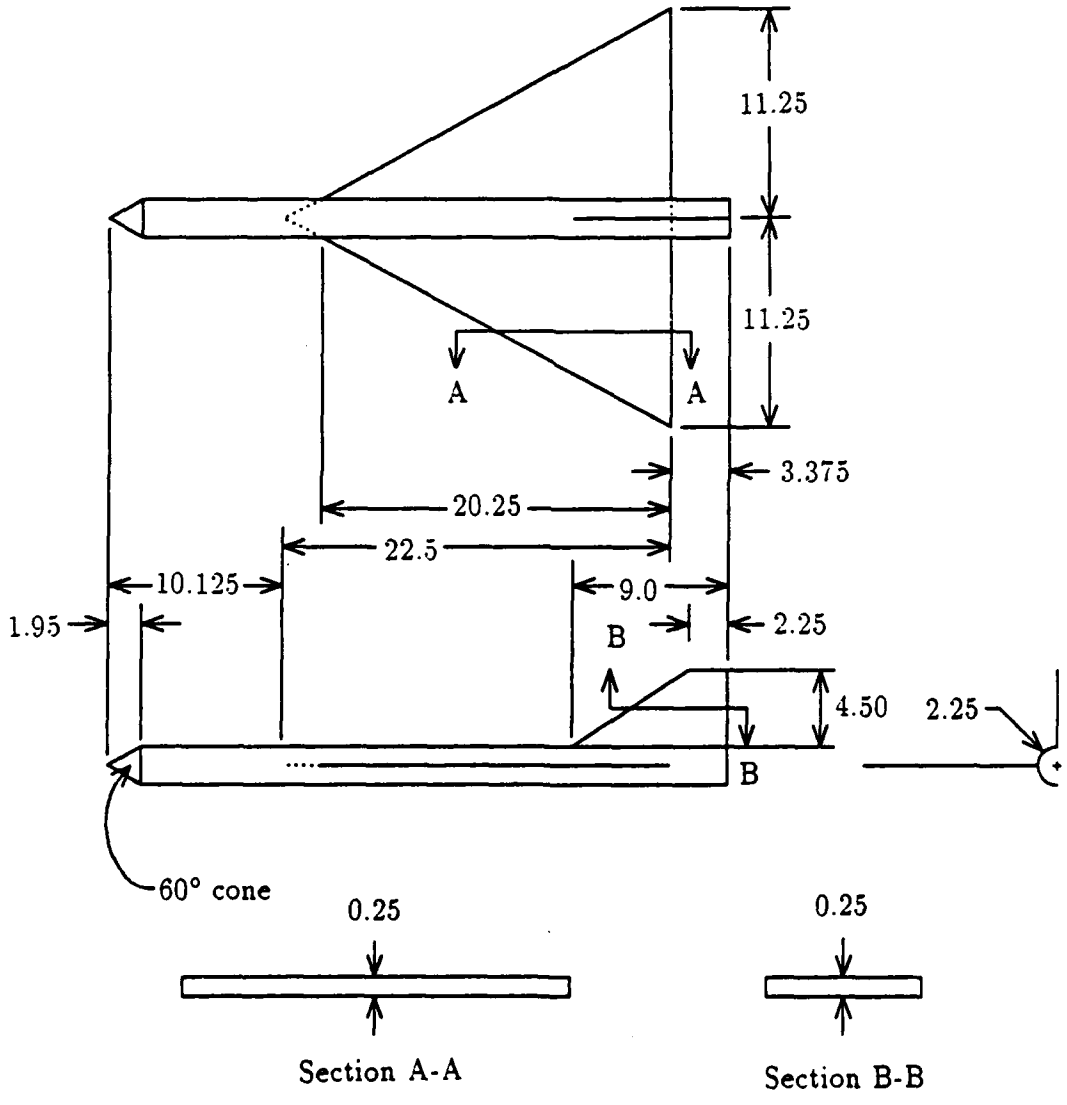

Fig. 17. Simplified aircraft shape.

In practice, bending and torsional loads were shared by the two struts, and the loads were carried by lengths much less than 48 inches.

HARS used a 4×0.25 inch low carbon steel square tube (outside dimensions– 4 inches square; wall thickness– 0.25 inches) for the main strut extension. The tube's resistance to torsion was calculated in accordance with the Bredt theory of torsion[13] using equation 1

$$\theta = \oint \frac{TL}{4A^2Gt} ds \tag{1}$$

Use of this equation predicted a rotation of 0.06° at the end of the main strut extension, assuming no external support over the full 55.4 inch length of the extension. The maximum bending at the end of the extension was calculated using equation 2

$$\delta = \frac{Ml^2}{3EI} \tag{2}$$

This calculation predicted a deflection of 0.20 inches at the upper pivot point, which increased the angle between the strut and cross-link by 0.20°, still assuming the strut to be 55.4 inches long.

Stiffness of the strut was considered inconsequential if the ears (Fig. 18) at the end of the strut, where the cross-link mounted, were not rigid enough to resist the torsional load. Each ear was assumed to equally share the full torque found in the strut. The tolerable angle of twist was 0.50° over the 12 inches that separated the cross-link pivot point and the end of the strut extension tube. From St. Venant's equation,

$$\theta = \frac{T}{KG} \tag{3}$$

was used in the form

$$K = \frac{T}{G\theta} \tag{4}$$

where:

$$K = at^3[\frac{16}{3} - 3.36\frac{t}{a}(1 - \frac{t^4}{12a^4})] \tag{5}$$

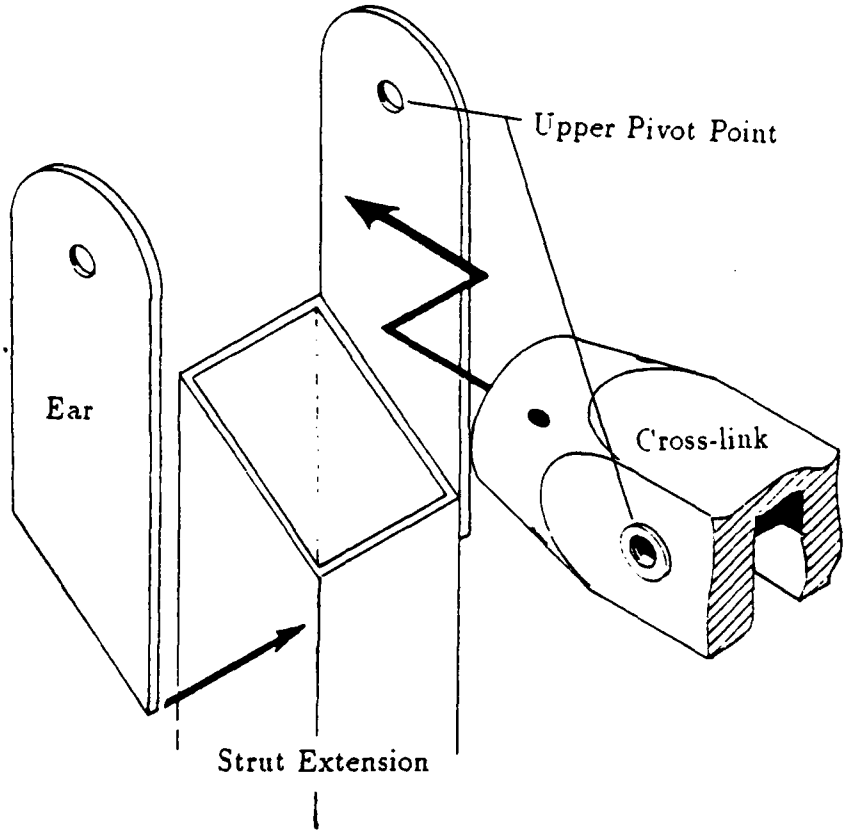

Fig. 18. Oblique view of front strut extension pivot joint.

Iteration of equation (4) for t to the nearest $\frac{1}{16}$ inch, determined that the ears could be no thinner that $\frac{3}{8}$ of an inch to provide adequate torsional resistance. At the thickness used, the predicted angle of twist was 0.24°. Since the ears were not alone in resisting torsion, the actual angle of twist was less, but not calculated.

The rear strut compressive loading calculations was complicated, because it accounted for the decreasing strut length, and increasing air loads from raising angle of pitch. The calculations were completed using a computer program, `RSTRUTLD` (Appendix C). Using Euler's equation for column buckling,

$$F_c = \frac{\pi^2 E I}{l^2} \tag{6}$$

RSTRUTLD computed the compressive loading of the rear strut, its length, and then calculated the minimum sectional I required. The largest moment of inertia encountered was 0.23 in^4 at 30° AOA. While $1\frac{1}{2} \times \frac{3}{16}$ square tubing was adequate for the task, it did not provide sufficient material to house the central drive screw. A larger, thicker square tubing was used, $1\frac{3}{4} \times 11$ gage; its I was 20% higher than the smaller stock, and 50% higher than was required.

The estimates of the strut casings' outside dimensions were accurate enough that the front strut sizing did not require revision, but the rear strut casing was reduced to $2\frac{1}{2}$ inches. For rigidity, their thicknesses were chosen as $\frac{1}{4}$ and $\frac{1}{8}$ inch, respectively. This allowed both extensions to be isolated from the casings by $\frac{1}{4}$ inch thick wear pads.

Wear Pad Design

Figure 19 shows a conceptual view of the wear pads used in HARS. Wear pads were chosen over roller bearings with a number of considerations in mind. Roller bearings, while offering vastly reduced resistance to movement, did not present any simple, compact means of installation and maintenance. They required considerable expense to purchase and fabricate the special adjustable mountings. The wear pads; while more prone to losing clearance adjustment due to wear, more difficult to optimally adjust, and not as friction free as the rollers; offered a much simpler, economic system.

To minimize the drawbacks of wear pads, the properties different plastics were examined to find an economical, long wearing material with a low coefficient of friction. 1 shows some of the plastics considered and their properties.

Delrin had the lowest coefficient of friction, but not much higher than Nylatron which was considerably stronger and less expensive. Nylon, while cheaper still, was too inconsistent in its coefficient of friction, and was not much better than Delrin in strength. Torlon, while possessing impressive strength, was priced too high for

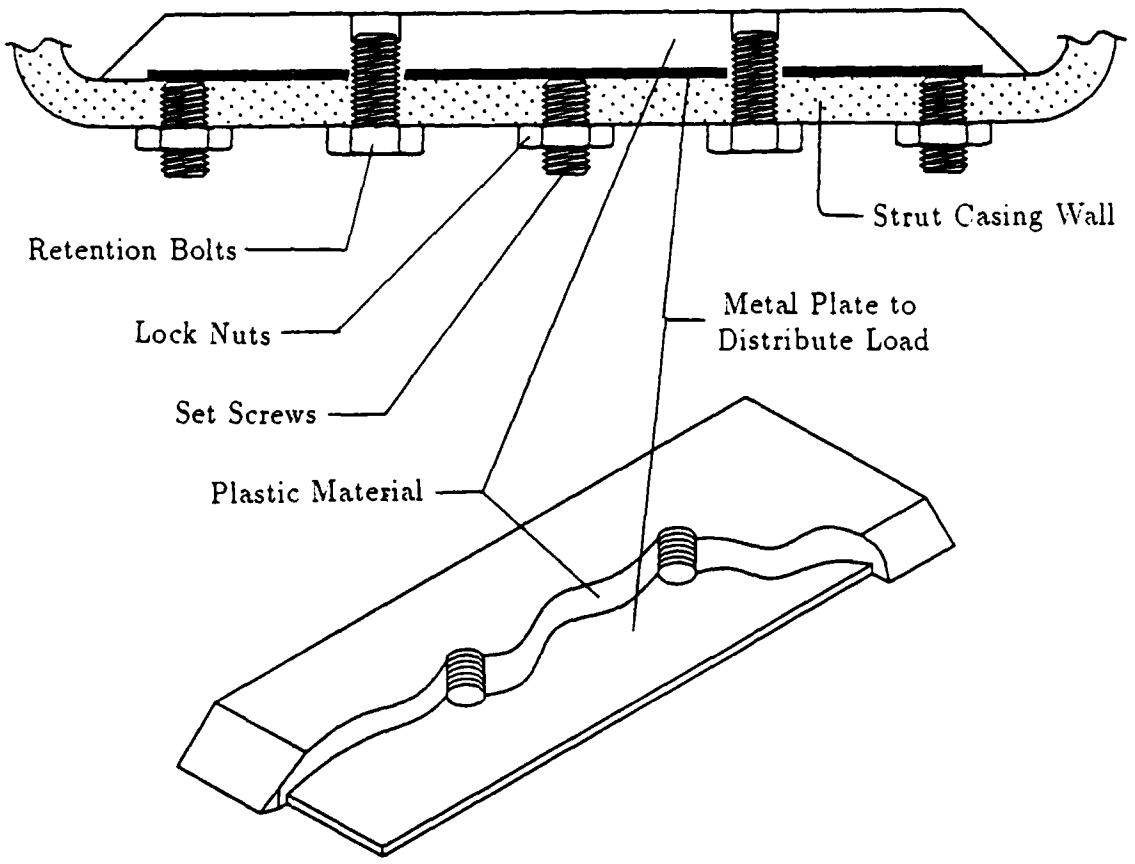

Fig. 19. Typical wear pad design.

consideration in this project. Nylatron NSM was chosen for the bearing material in the wear pads.

Four positioning bolts and five adjusting set screws adjusted the clearance on each wear pad. Positioning bolts threaded into the pad to maintain pad position, and were tightened only after proper clearances are set. Set screws threaded into the casing housing and pushed the pads against the strut extension to remove clearance. Once adjusted, the set screws were held fast by jam nuts.

Fasteners

All fasteners used in HARS, other than those fastening HARS to the turntable, were fine threaded (UNF). This type of bolt offered greater resistance to stripping

Table 1. Wear pad plastic materials considered

PROPERTY	MATERIAL			
	DELRIN AF	NYLATRON NSM	TORLON 4301	NYLON 101
Shear strength(psi)	8000	11500	16000	9600
Compressive strength(psi)	4500	13000	30000	5000
Coef of friction(dynamic)	0.15-0.16	0.13-0.16	0.13-0.25	0.17-0.43
Hardness(D-785)	R118	R120	M120(D676)	R115
Deformation under load[a]	0.6	0.5-1.0	unknown	1.0-3.0
Cost($\frac{1}{2}$" sheet/sq ft)	$171.75	$36.60	$384.48	$32.66
Wear factor(K)[b]	65	21	unknown	unknown

a. 122°F, 2,000 psi

b. $K=\frac{h}{5000T}10^{10}$ where: h = radial wear(in) & T = test duration(hrs)

threads because there is a larger contact area per unit length supporting the load, and hence a lower realized shear strain within the parent material. Most of the screws used were the socket head type (allen head) for two reasons; they generally exceed SAE grade 8 strength, and the smaller handle of an allen wrench would help prevent over torquing fasteners on assembly of HARS.

For bolt spacing, a rule of thumb used throughout this design was to give fasteners one diameter's clearance from other material boundaries. Plots of the stress gradient near a circular hole versus distance from the edge, normalized by the radius of the hole, have shown that stress within the material structure becomes roughly equivalent to a void free material within two radii[14].

Drive Mechanism

Figure 20 is a cut-away drawing of the mechanical drive mechanism used in HARS. The strength and spacing of the bolts used to assemble the various pieces in

this area were critical, as they withstood all aerodynamic loads and the weight of the extension and drive system.

The maximum longitudinal load calculated for the front strut occurred at -30° of pitch. This load was used to analyze required fastener strength of the bolts attaching the lower casing cap. The loads supported by these fasteners are summarized in 2.

This load was divided between eight flush head socket cap screws (FHSCSs), each one required to carry 1,395 lb in shear. For screws with no less than a 35 ksi shear strength, MIL-HDBK-5D, Table 8.15(a), qualified a fastener size of $\frac{1}{4}$ inch. The rear strut casing cap attachment bolts were determined similarly, except that the MA on the strut is 4.5 for an AOA of 30°. The screw, being longer would weighed about 12.35 lb, and the extension weighed only 13.30 lb. The load on the rear strut bolts was then 9,188.34 lb. Divided among four bolts, $\frac{5}{16}$ inch fasteners was required; using eight fasteners, as with the front strut, #12 screws (0.216 inch) sufficed. For consistency, eight $\frac{1}{4}$ inch screws were used on both strut casings.

The bolts holding the transmission plate to the strut were analyzed using the same forces used in sizing bolts of the casing cap. In this case, the bolts were under tension rather than shear. To determine the loads on each bolt, forces and moments were summed about an outside corner of the plate as shown in Fig. 21 . Summing forces and moments about point a provided a solution for A (= 2762.98 lb), and B (= 2863.63 lb). Assuming that the pair of bolts carrying each of these loads were SAE grade 8, MIL-HDBK-5D, Table 8.15 qualified the use of $\frac{1}{4}$ inch bolts.

In similar fashion, the loads on the bolts for the adapter holding the strut to the mounting plate were estimated. The 8271. lb bending moment calculated earlier was used as the load, with the moment arms as shown in Fig. 22. Bolts A were under a 2678.09 lb tensile load; bolts B, a 251.31 lb load. While this junction could be fastened with as little as a $\frac{5}{16}$ inch bolt[15], a $\frac{9}{16}$ inch bolt, which is three and a half times larger was selected to better cope with the repeated large torques experienced during HARS' installation. Since a prediction of the person's strength performing this the installation was impractical, as was assessing of a load cycle history of the screw, the increase in fastener size was prudent.

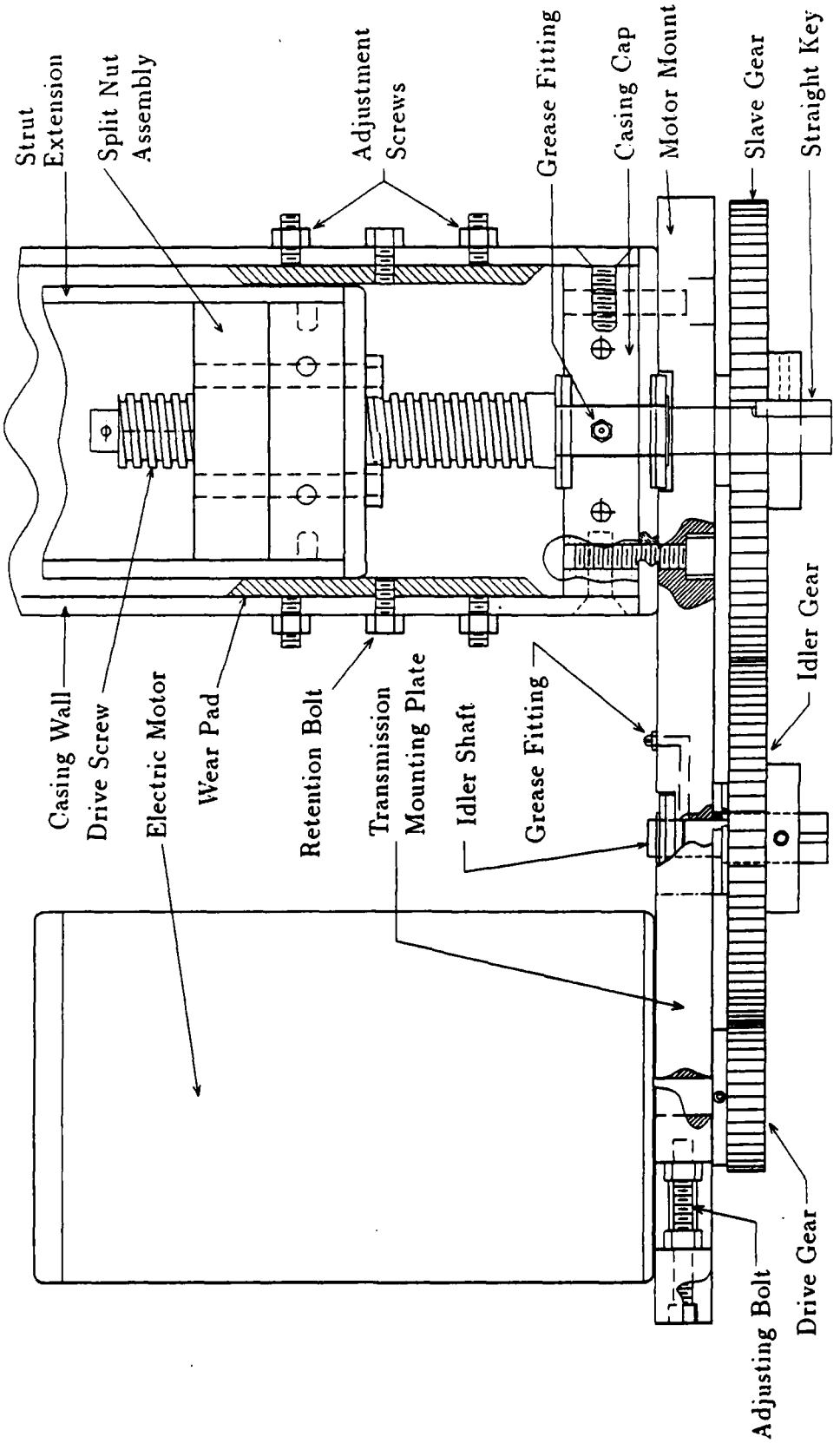

Fig. 20. General construction of drive mechanism.

Table 2. Maximum predicted longitudinal loads on front strut

ITEM	LOAD (lb)
motor	12.00
transmission	2.00
drive screw	9.23
extension	70.21
transverse link	75.00
sting	29.24
model	150.00
airloads	1512.50 - 275 @ 5.5 mechanical advantage (MA)
$\sum$	1860.18 $\times$ factor of safety (FS) of 6
=	11,161.08 – Total front strut longitudinal load

Drive Screws

The minimum required sectional moment of inertia, I, of the drive screws was predicted by Euler's buckling formula. The largest compressive load calculated from the casing cap bolt analysis was used for the front strut. A factor of safety of three was applied, the force distributed over the longest free length of drive screw, 29 inches. This safety margin required an I of 0.0164. Assuming that the threads of the drive screw did not contribute to its over all stiffness, the minimum root diameter of the screw was derived from the moment of inertia equation for a circular area, equation 7.

$$I_{\text{circle}} = \frac{\pi \times r^4}{4} \tag{7}$$

This equation predicted a minimum required root diameter of 0.571 inch. The maximum screw diameter was limited by the proximity of the bore through the strut extension split nut to surrounding fasteners. There was enough material in the rear strut's split nut for a one inch diameter drive screw to be used without encroaching to within a bolt diameter of the fasteners used therein. This load level served as a maximum limiting factor.

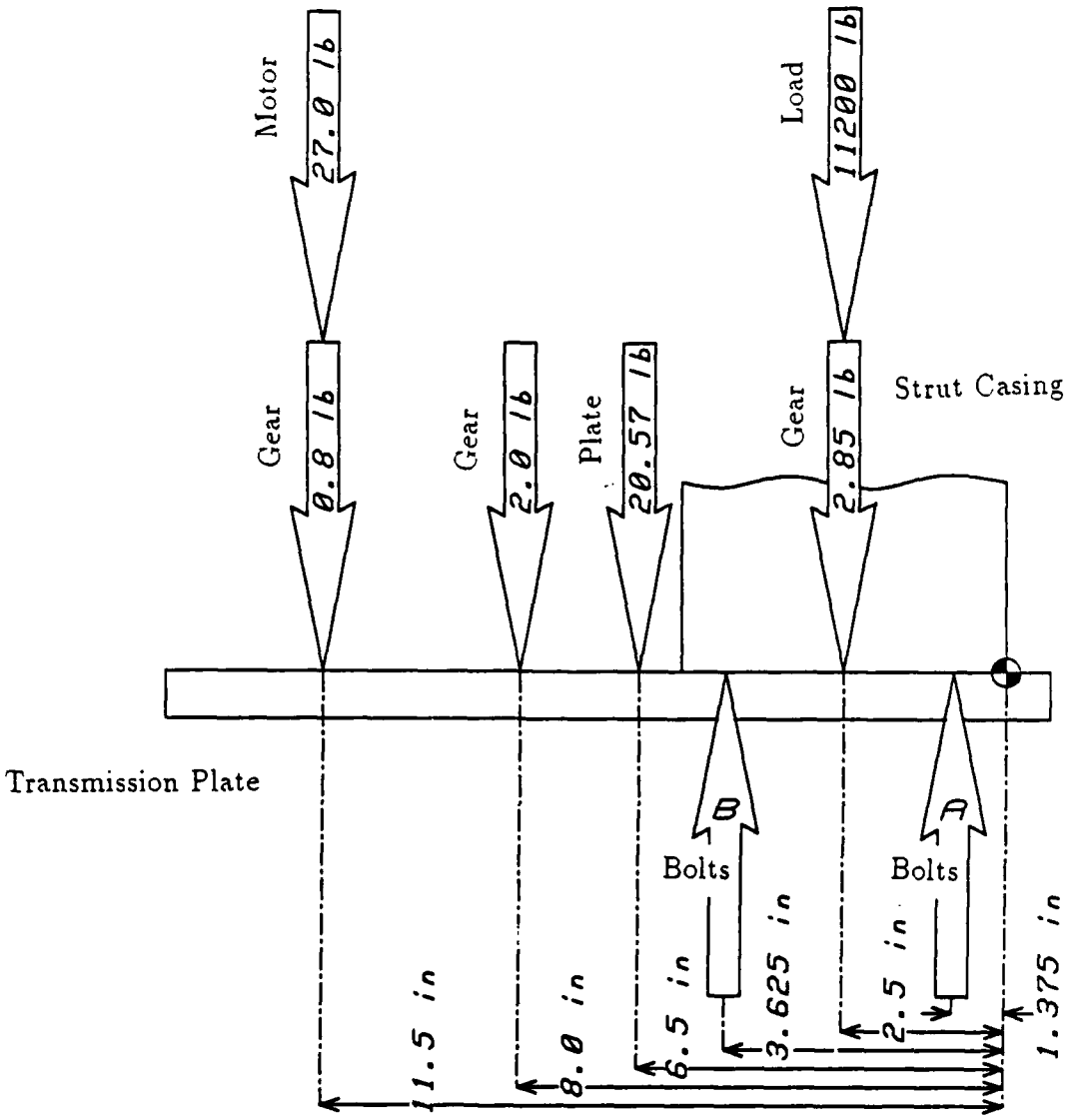

Fig. 21. Transmission to strut bolt force diagram.

A representative stepper motor was selected to determine the optimum motor to drive screw gear ratio and drive screw pitch. The holding torque needed to maintain strut position under load was calculated to screen for a representative motor, from which a torque versus rpm curve could be obtained. Using a factor of safety of 1.5 and neglecting friction, a supportive force of 558.34 lb was required to maintain position under the maximum load found in the front strut. A torque of 174.5 in-lb applied

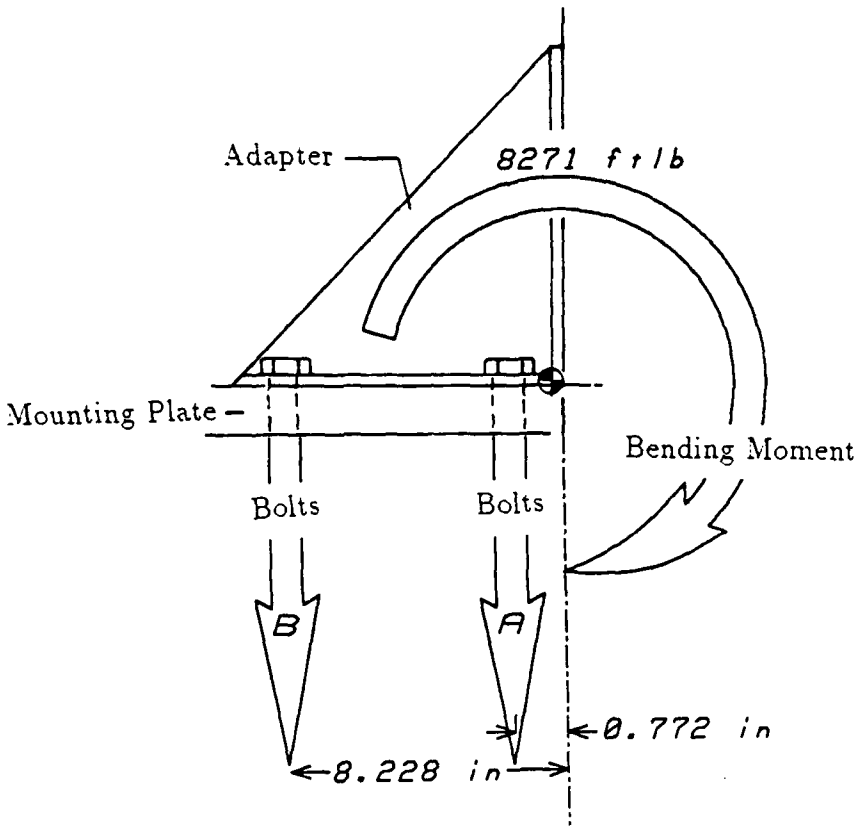

Fig. 22. Strut adapter bolt force diagram.

at the pitch diameter (PD) of 0.625 inches (pitch diameter of the standard screw) would then be required to maintain the main strut position, a smaller torque for the rear strut. Sigma Corporation's catalog listed a dozen stepper motors that met the requirement for holding torque. Of them, The most powerful was characterized, and used in a computer program, **SCREW** (Appendix D), to determine the optimum screw pitch and diameter.

SCREW varied three input variables to determine the maximum extension speed of the front strut under maximum loading conditions. The gear ratio between the motor and the screw varied from 1:1 to 30:1 by 1 per step. The outside diameter of the screw varied from $\frac{10}{16}$ to $\frac{16}{16}$ths of an inch, in $\frac{1}{16}$th inch increments. The number of threads per inch varied from 1 to 32 in steps of 1. For each outside diameter and pitch combination, the program calculated and displayed root diameter, pitch diameter, diametrical pitch, helix angle, and the torque available from the motor. **SCREW** went on to predict the strut extension speed for the given torque versus rpm curve of the sample motor. A maximum extension speed (for a one inch screw at 0.2657 inches per second) was predicted for gear ratio/ threads per inch combinations 6:1/5 and 5:1/6. The deciding factor between these two was the amount of linear contact area per inch of shaft length, a determining factor in the calculation of friction. This length was calculated as 1.9996, and 3.1780, respectively. Hence, a one inch, five threads per inch acme thread was chosen for the drive screws. Of economic benefit, the chosen thread was standard screw stock, saving time and expense in fabrication.

Motor to Drive Screw Gearing

Spur gears, to makeup the gear train between the motor and drive screw, were selected with close attention to the horsepower rating of the gears. The needed horsepower calculations were made with the equation

$$HP = \frac{F \times Pitch\ radius \times RPM}{63025}. \tag{8}$$

The force would be reduced by a factor of the mechanical advantage derived from the screw, a factor of 13 71 for this case. Therefore, to move the front strut at the rate calculated in **SCREW** would be

$$\frac{407.1 \times 0.43635 \times (0.2657 \times 5 \times 60)}{63025} = 0.23\ HP.$$

Other factors limited the spur gears used in the transmission. The largest outside diameter was limited to 6.25 inches to avoid interference with the operation of the other strut mechanisms. Three standard diametrical pitches (DPs) were possible, 12, 16, and 20. Gear ratios ranging from 8:1 to 2:1 were explored in each DP for the broadest versatility. DP 20 gears were not strong enough to supply any of the high gear ratios. DP 12 gears could not supply a ratio 8:1 and still remain within the outside diameter restriction. The DP 16 gears offered the full range of gear ratios. The smallest inside diameter (ID) gears capable of handling 0.23 horsepower and fitting the motor shaft limited the final ratio to a ratio no higher than 6:1.

Drive Mechanism Lash Adjustment

Gear train clearance adjustment was simplified by placing the drive screw mounted gear and the idler gear at a fixed center-to-center distance. With the fixed separation distance, the two gears, one with 80 teeth and the other with 96 teeth, were freely swapped to change the gear ratio between the motor and the drive screw. The third gear attached to the electric motor, and could be one of three sizes; a 16, 24, or 32 tooth. This made six gear ratios possible: 2.5, 3.0, 3.33, 4.0, 5.0, and 6.0. To make the center-to-center distance of the drive gear adjustable, the motor was mounted on a sliding plate that locked into position for proper gear engagement. Each gear was given a $\frac{1}{8}$ inch straight keyway and setscrew to maintain a positive grip on the end of its respective shaft. The gear train is shown in Fig. 23 as it would be installed on the main strut.

A split nut was designed for the drive screw to provide zero lash on the drive screw. Conventional split nuts used in this application are typically split longitudinally, and the two sides offset to provide positive contact on the opposing halves of the screw face. A more practical, simplified solution in HARS was to split the nut laterally, separating the halves by shim stock. The upper half of the nut rode along the bottom face of the screw and the lower half along the top face to provide zero backlash. Longitudinal play in the drive screws within the lower casing cap was

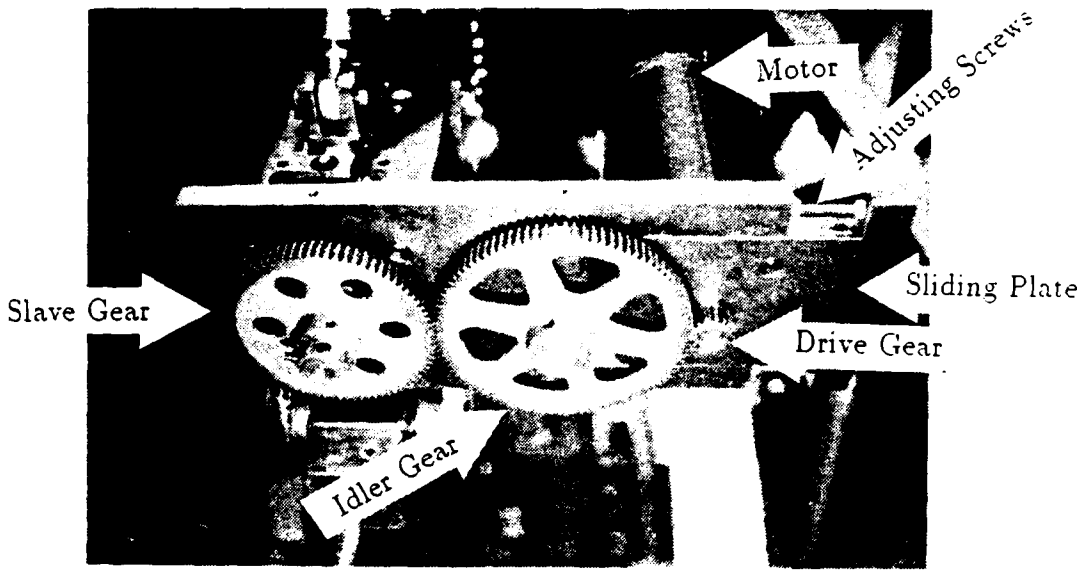

Fig. 23. Power transmission gears. Typical installation

removed by installing a proper thickness thrust washer between the spur gear that rotated the drive screw, and the mounting plate which carried the electric motors and other spur gears. The unavoidable backlash in the spur gears allowed less than a 0.001 inch variance in the strut length. This difference was undetectable when measured using the linear potentiometers.

Electrical System Design Overview

Strut movement and position was controlled by an IBM AT compatible microcomputer through an analog to digital (A/D) board. Linear potentiometers were used to feedback position. A control signal from the digital to analog (D/A) port, too weak to run the motors alone, was amplified to supply power to the motors. In

the event of a malfunction, a master disable switch was used to shut off power to the system.

Figure 24 is a basic schematic of HARS' electrical system and controls loop. For illustrative purposes, the control loop for only one of the struts is shown. Three power sources were required; one heavy duty unit to supply 28 VDC to the electric motors, a small unit for a voltage across the linear pots, and another small unit for the 'panic' switch. Permanent magnet electric motors manufactured by American Bosch powered the struts. These motors were rebuilt surplus items and able to handle up to 36 VDC. HARS utilized them at 28 VDC to insure longer service life, and to avoid supplying excessive power to the lower gear train.

Linear Potentiometers

Linear potentiometers were used to determine the amount of strut extension by measuring the voltage drop across the potentiometer (pot) and lead voltage to the pot. The linear pots were manufactured by Waters Manufacturing and advertised to be linearly accurate to within 1%; however, a characterization procedure demonstrated that one of the pots had an error exceeding 1.7%.

The characterization procedure plotted the percent of total voltage error versus percent of poteniometer extension. The resulting curve was then included in the controlling computer code. Using a 10 volt filtered power supply, voltage was applied across the potentiometer as illustrated in Fig. 25. A small tape measure was secured to the side of the pot, the tape's tongue extended and fastened to the position rod by clamping the the tongue between a pair of large diameter washers. With the pot's position rod fully seated, a stationary pointer was secured to the pot housing marking a convenient tic mark on the tape, i.e. 1 inch precisely. Voltage across the resistor and wiper was measured using a digital voltmeter to obtain a greater resolution and repeatability of readings than could be obtained using typical analog voltmeters. The pot's position rod was extended in one inch increments to full extension, and the wiper voltage recorded.

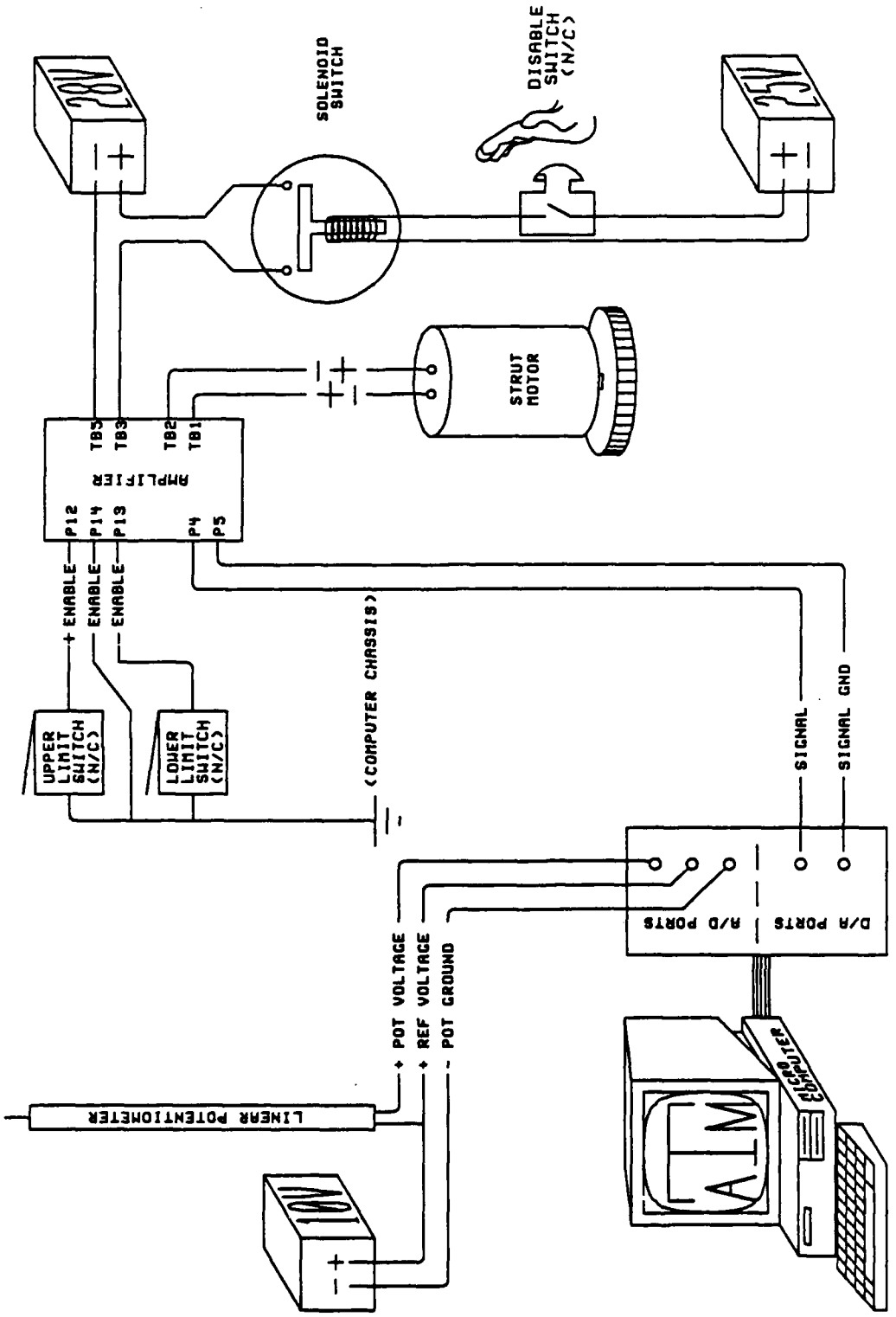

Fig. 24. HARS electrical and controls loop diagram

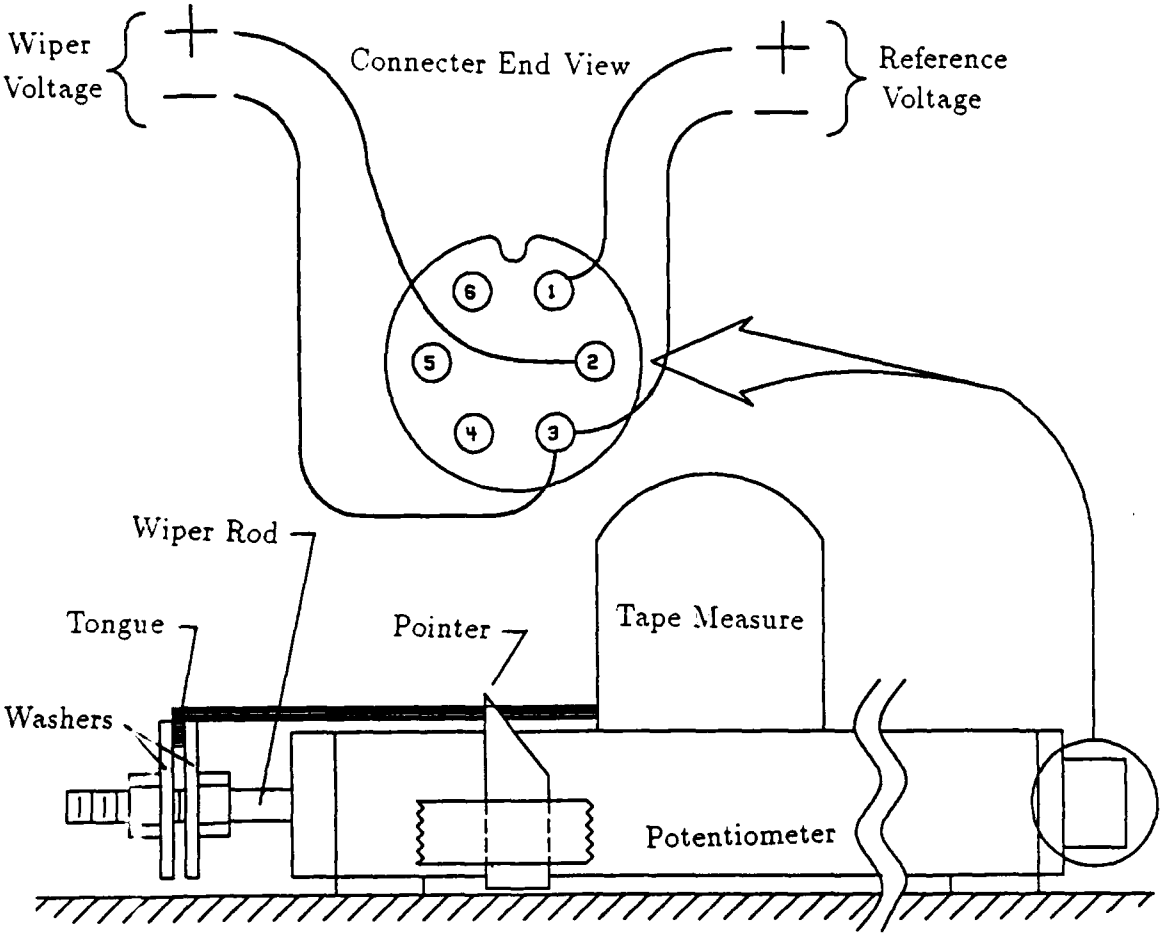

Fig. 25. Illustration of linear potentiometer characterization procedure.

Reference voltage was recorded at the beginning and end of each test to detect any drift of the power supply setting. Out of six calibration tests, four had some variance of reference voltage. Except for one case where the voltage varied by 0.35%, each data set's reference voltage varied by less than 0.15%. The reference voltage change was compensated for by linearly adjusting the reference voltage value used to calculate the percentage of voltage drop across the pot.

Hysteresis was examined by repeating the test in reverse immediately after finishing the forward collection. Hysteresis was not observable within the visual ability to resolve the rod position. The difference between the percent of pot extension and

the percent of reference voltage is shown in Fig. 26. These data curves were used later within the controlling software.

Signal Processing

The analog signal from the pots and the signal to the electric motors was handled through a Data Translation, Inc. A/D board in a Hewlett-Packard ES-512 microcomputer, an IBM/AT compatible. The board, a DT2821-F-16SE subsystem, was factory configured for 16 single ended analog inputs, 16 digital input/output (I/O) lines, and 2 D/A channels out. Dynamic performance was listed as a maximum A/D acquisition-to-memory speed of 150kHz and a D/A channel change of 20 volts in 5 microseconds. The board used 12 bits to represent the digital translation of analog input. With a limit on analog input being 10 volts, digital resolution was to within 0.0024 volts. Specifications for this hardware are included in Appendix E.

The D/A ports were used to supply a control signal to the Copley Controls Corp., Model 240, servo amplifiers. These amplifiers were very compact, measuring only 4.63 $\times$ 7 $\times$ 2.40 inches and offered failsafe circuitry to protect against output overload, excessive temperature, and improper supply connection. Operation was enabled by connecting the *enable* remote shutdown switch to the earth ground of the signal source (the computer chassis). Positive and negative output voltages were identically enabled. All three switches- *enable*, *positive enable*, and *negative enable*- required grounded connections to operate HARS; the switches were an integral part of hardware protection against over extension/retraction of the struts.

These amplifiers are designed to amplify signal current rather than signal voltage. With no current control in the D/A channels, strut velocity and motor torque control was not possible by simple channel signaling. The current limit adjustment pot was set at maximum to insure adequate power would be available to the motors. Bench testing of the amplifiers discovered that a minimum signal of 2.3 volts must be supplied to the amplifier for it to supply power to the motors. Factory specifications and configuration for the amplifiers are detailed in Appendix F.

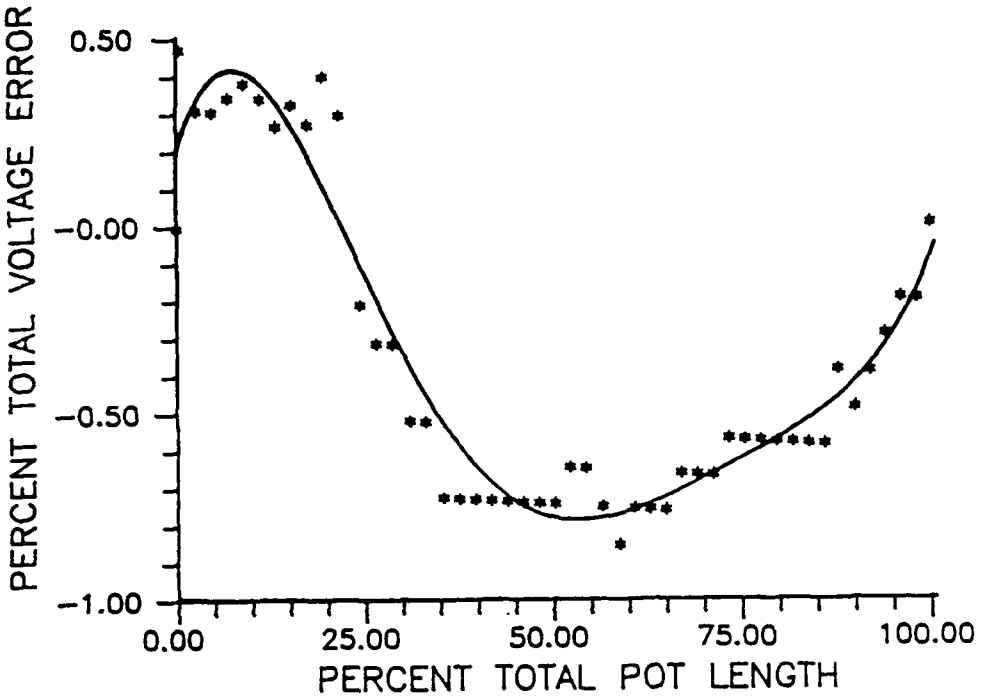

a. Front strut

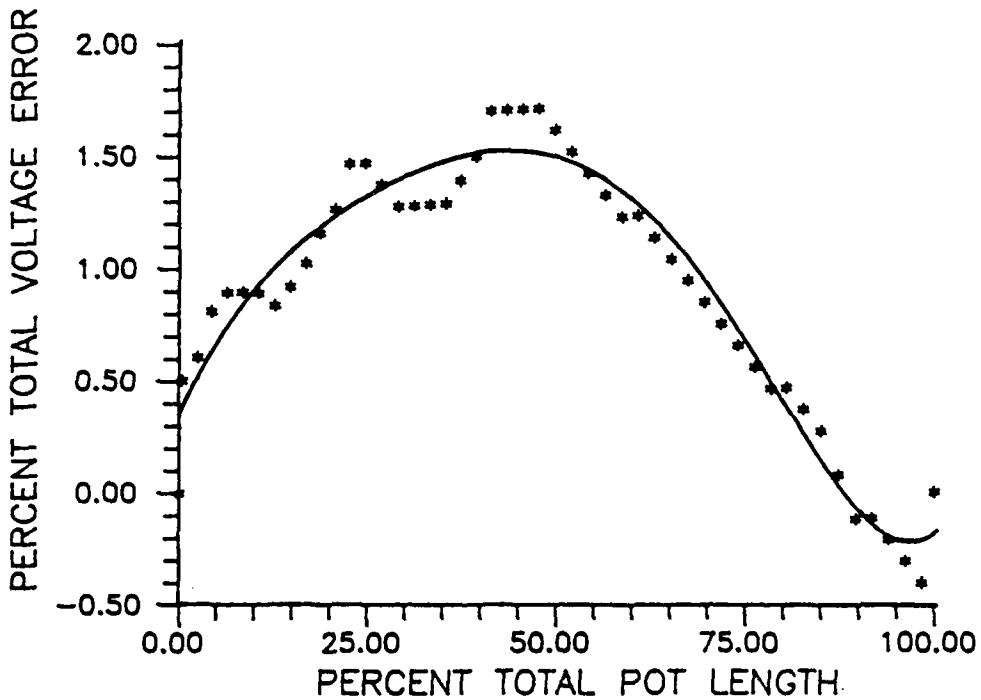

b. Rear strut

Fig. 26. Plot of results of linear pot characterization.

Hardware Protective Circuitry

A pair of microswitches on each strut protected against movement past physical limits that would damage the sting or model (Fig. 27). The ground connection for the amplifier's *positive enable* switch was directed to a microswitch which opened when the strut reached its upper limit of travel. The *negative enable* switch was similarly connected. The microswitch's roller tip contacted the outside surface of the strut extension and opened when slots milled into the surface of the strut extensions passed the switch. The amplifiers supplied the feed voltage (28 VDC) to the motors only when there was a control signal and the protective microswitches were closed.

The microswitches were protection for only a limited number of circumstances; to provide more universal operation protection, a disabling solenoid switch was placed between the motor's 28 volt power source and the amplifiers. The switch was closed only when a 20-28 volt, low current signal was supplied to it. The signal passed through a 'panic' button connected to a small power supply. The switch was an aircraft surplus item manufactured by Guardian Electric, Model 11400037. It had three heavy duty contacts rated at 460 V at 10 A, 60 Hz and a pair of light duty auxiliary connections. Appendix H contains details of installation of the solenoid switch on page 6 of the hardware installation schematics.

Hardware to Software Interface

A software interface package, **ATLAB**, was supplied with the A/D board. **ATLAB** subroutine libraries were compatible with three languages: C, FORTRAN, and PASCAL. Though not all were needed for this application, the subroutines were able to perform these tasks:

1. Direct Memory Access (DMA) A/D and D/A transfers to and from memory.
2. Single-value, non-DMA A/D, D/A, and DIO transfers.

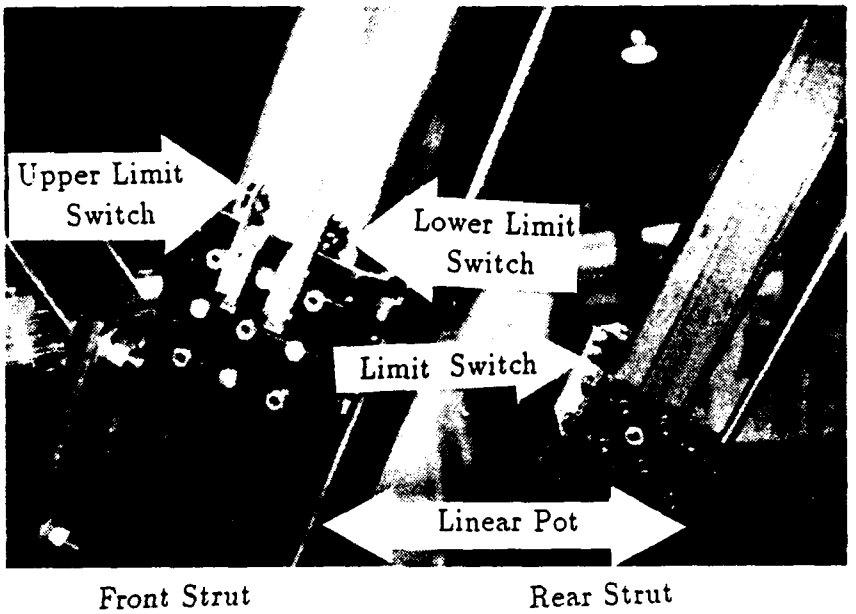

Fig. 27. Hardware protection microswitches.

3. Multiple-value, non-DMA A/D and D/A transfers to and from memory.
4. Allocation and management of the IBM AT extended memory space.
5. Data buffer management.
6. On-board clock setup.
7. Error handling.

ATLAB needed the operating system PC-DOS v3.0 or later, and at least one high-density floppy drive and a hard drive. The minimum memory required was 256K KBytes. In the control software for HARS, continuous DMA was avoided because it

involved buffered operations. Directly accessing the few needed A/D channels was more efficient, and provided more timely information.

Control Software

HIALST, for HIgh ALpha STing, was a FORTRAN program written to control HARS; a general logic flowchart is included in Appendix G. It began with internal data structuring; initializing **ATLAB**, reading an external ASCII data file, and setting the pitch correction due to installation variations. The external data file, **HIALST.DAT**, contained information about the physical configuration of HARS, position error correction data, and a number of user variable parameters used to control HARS' performance characteristics.

As **HIALST** read the data file it scanned the first character of each record for an alphabetic character indicating how the following record(s) was to be processed. Only one record set was optional; if an **A** appeared in the first column (for alpha list), HARS automaticly adjusted the angle of pitch in the order listed on the following read; otherwise, the user interactively directed pitch attitude. All other record sets were required for HARS to operate properly. Provisions were not included to insure all required data sets were present, so care had to be taken to have all data available for **HIALST**. One of the data records allowed the user to change logic parameters HARS used to seek a new position and filter noise in the linear pot readings. Another record contained the coefficients of a sixth order polynomial used to correct for the pot nonlinearity (curve plotted in Fig. 26). Also included in the data file was a list of the error of pitch at 10° increments obtained during the setup qualification tests.

The physical information read in from the data file included lengths of the struts at these important operation points:

1. Physical length, excluding any extended length.
2. Maximum and minimum length of the extension when the strut's protective microswitch stops the motor.
3. Maximum and minimum length for the strut's position at 0° and 90°

of pitch.

4. Extendible length of the linear pots.
5. Lengths separating the front and rear strut pivot locations.
6. The angle from vertical at which the front strut is mounted.

Pitch Attitude Logic

HARS calculated the pitch angle of the cross-link through simple geometric relationships illustrated by the simple linkage drawing of Fig. 28. The structure is not an irregular trapezoid, but two triangles joined at two vertices.

HARS sampled the linear pots for the strut lengths; the length of all four sides of the outer scribed trapezoid were then known – the cross-link was a fixed distance, as was the separation distance at the rear strut's lower pivot point. One of the angles in the triangle formed by the front strut was always fixed at 90°. A known angle with adjacent sides of known length fully describe a triangle, the three included angles, and the lengths of the three sides. The third side of the rearward triangle was then known, and hence its three included angles. The angular relationship between the front strut and the cross-link was then given by adding the calculated angles of iota, ι, and kappa, κ. A similar process was used to predict the strut lengths needed to obtain a requested angle of attack; only in this case the rear strut length was unknown at the beginning. The front strut length was known because of the linear motion assumption made earlier. The rearward triangle was then described by subtracting the computed value of ι from the desired angle. Within HARS these two procedures were done by the subroutine **TRGTL**. The mounting angle was included in this calculation; hence, the procedure was valid for both standard installations, as well as any future mounting geometries.

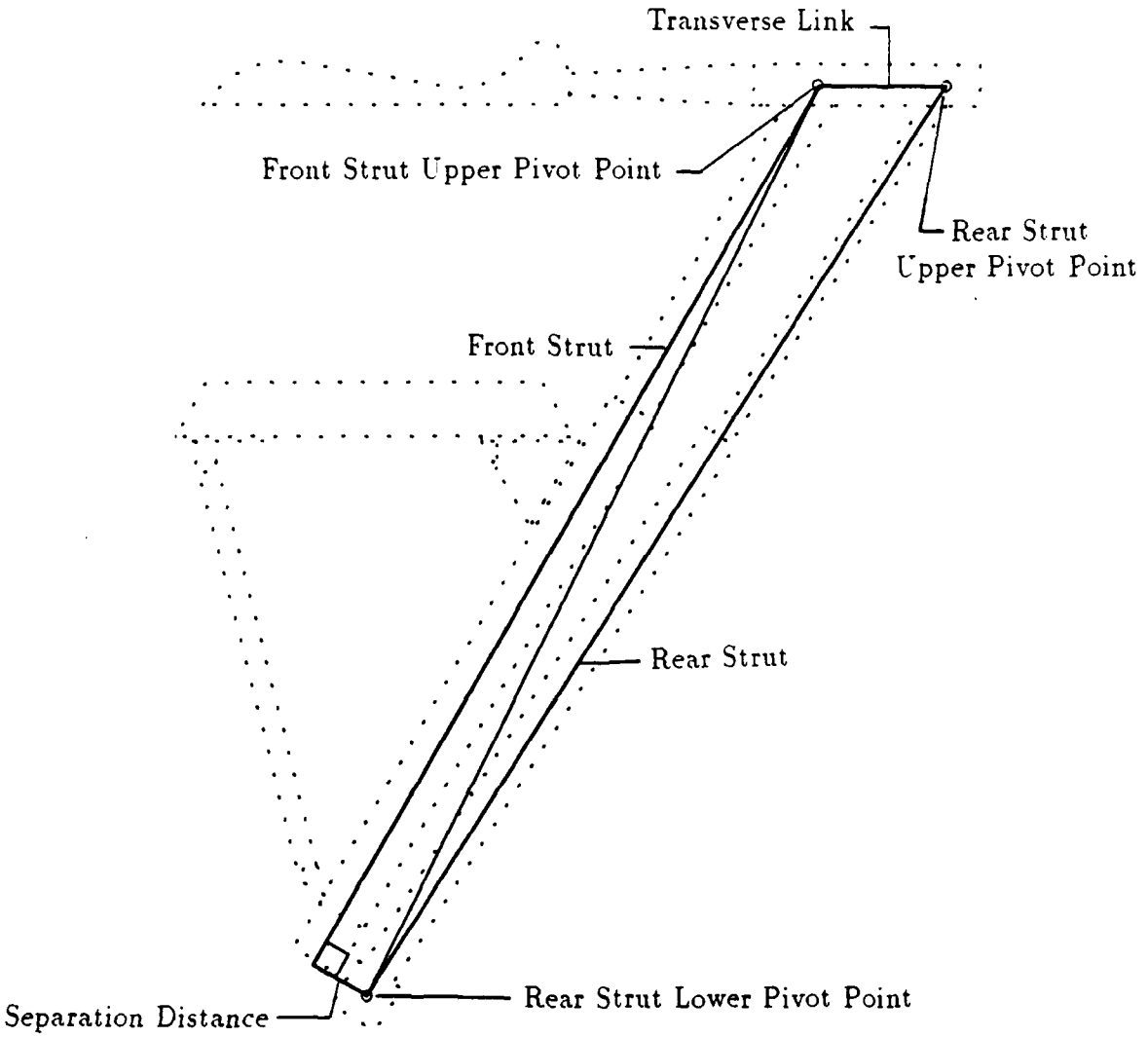

Fig. 28. Simplified HARS geometry.

Software Operation

After initialization procedures, **HIALST** offered to calibrate the mechanism's angle of attack setting to account for misalignment of HARS due to variances in installation. To measure this offset, HARS positioned itself at zero degrees of pitch, and waited for the user to measure the true angle using an inclinometer across the

top face of the cross-link. Since the skewedness of this position was present in all as, this position measurement of HARS had to be precise. The operator had the option of entering the angular error measured, or bypassing this operation by entering the error known from an earlier calibration check.

The software was then ready to begin position commands. Subroutine **FINDL** told the driver program the current position of the struts. Subroutine **TRGTL** found the lengths of the struts and the window of length for the struts to be moved to that satisfy the pitch request. The strut motors were then powered in the direction of the target position. Strut position was sampled in an continuous loop while the struts moved. When the struts passed to within a defined distance of the final location, power to the motors was cut. After both strut's movement had been terminated, **HIALST** began a station keeping mode to fine tune the position before displaying the final pitch attitude to the operator and seeking further instructions. While software apparently waited for instructions, it continually monitored HARS' position, taking appropriate steps to maintain position.

The operator's console requested current position information without affecting the on going process by entering an [A]. However, other commands, such as a [<cr>] or an [I], caused temporary suspension of operation while entering the new pitch angle. [I] interrupted table-directed pitch control. The ability of the console to change operating modes during tunnel testing allowed the insertion of pitch settings left off the list, or selective positioning of the model. Automatic pitch positioning was resumed, beginning where terminated, at the operators instruction([C]). Program execution was terminated at any time after entering the positioning section of code by entering a [Q].

RESULTS AND DISCUSSION

Design Revision

Some of the design specifications changed during the manufacture of HARS for a variety of reasons. The wear pad material, nylatron, was not readily available, so common nylon was substituted to avoid slipping the fabrication schedule. Few stepping motors had the power available to comply with that requirement indicated during the force analysis phase of the HARS design. Those which could qualify were too costly for the limited budget of this project; therefore, they were replaced with permanent magnet d.c. motors. The effect of the first of these changes cannot be quantified, the second had significant impact on the control design. Stepping motors were originally desired because of the precision in which they can be driven to position. Using a d.c. electric motor for power, the refinement of movement became a responsibility of the control software. The options available in the construction of control logic were further restricted when the amplifier's inability to proportionally amplify signal voltage was discovered.

Static Evaluation

Preliminary tests of the integration of software and hardware were done with the assembled HARS on a test stand (Fig. 29) where all systems were accessible. In

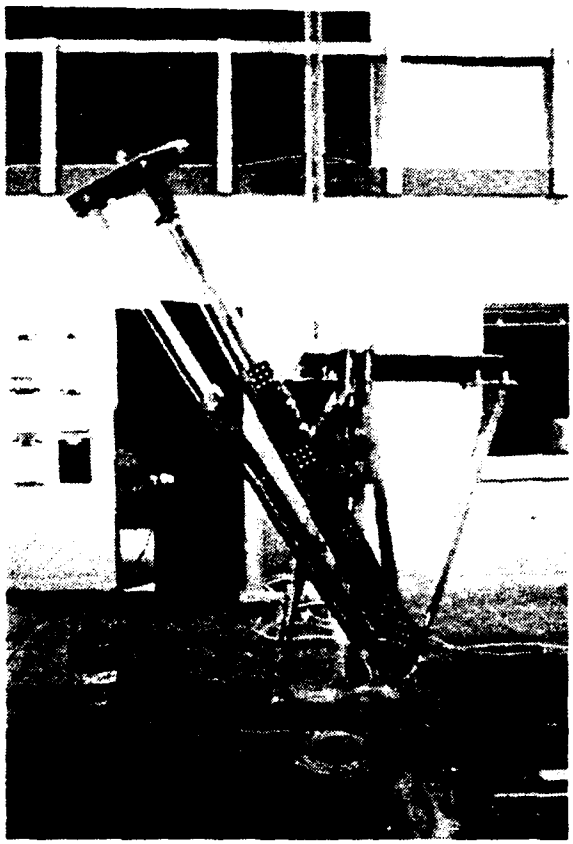

Fig. 29. Assembled HARS on a test stand.

this figure. HARS' true size is evident. The wind tunnel floor would be inches above the mount extension bar which is extending horizontally to the right.

When voltages applied to the A/D board changed, the digital translation was not instantly reflected. When continuously monitored, digital values were observed to scroll toward the new value, overshoot, and oscillate slightly before stabilizing. Even stable input values were observed to float as external noise affected the lines or when

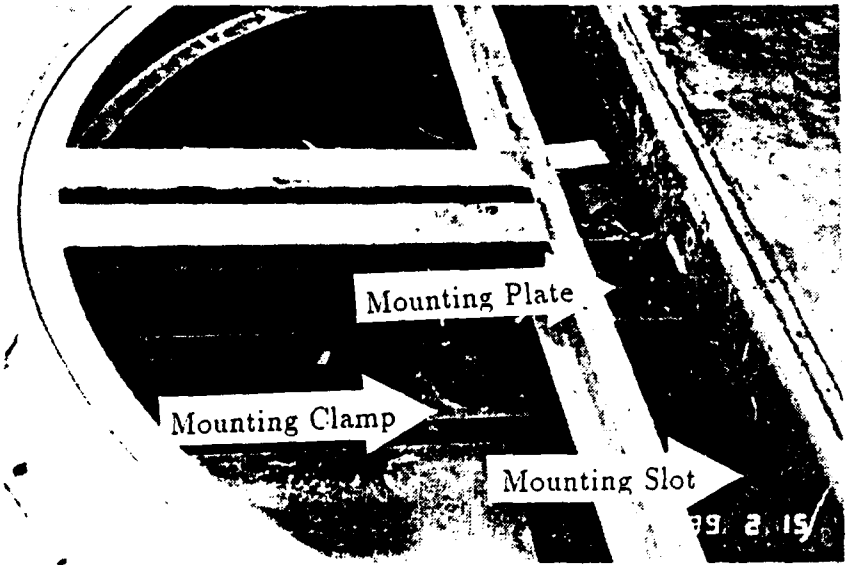

Fig. 30. HARS mounting plate installation for 30° configuration.

voltages straddled a value too fine for a digital translation . To filter this, subroutine **FINDL** made a number of inquiries– an externally defined number– and calculated a mathematical mean before returning the strut length. The mean stabilized with between 30 and 40 reads of the A/D board.

Installation of HARS into the TAMU LSWT using the procedures outlined in Appendix I required six hours. Most work was accomplished with two people; however, three people were the minimum needed for some tasks. Figure 30 shows the mounting plate installed transversely to the tunnel centerline. Part of the tunnel flooring has been removed to better see the upper balance structure. The lower extremities of HARS are shown in Fig. 31. When the turntable is rotated for yaw, the cradle-like structure, which is about four inches below the transmission gears, remains stationary. During yaw angle sweeps, HARS hardware approached no closer than three inches to any permanent structure.

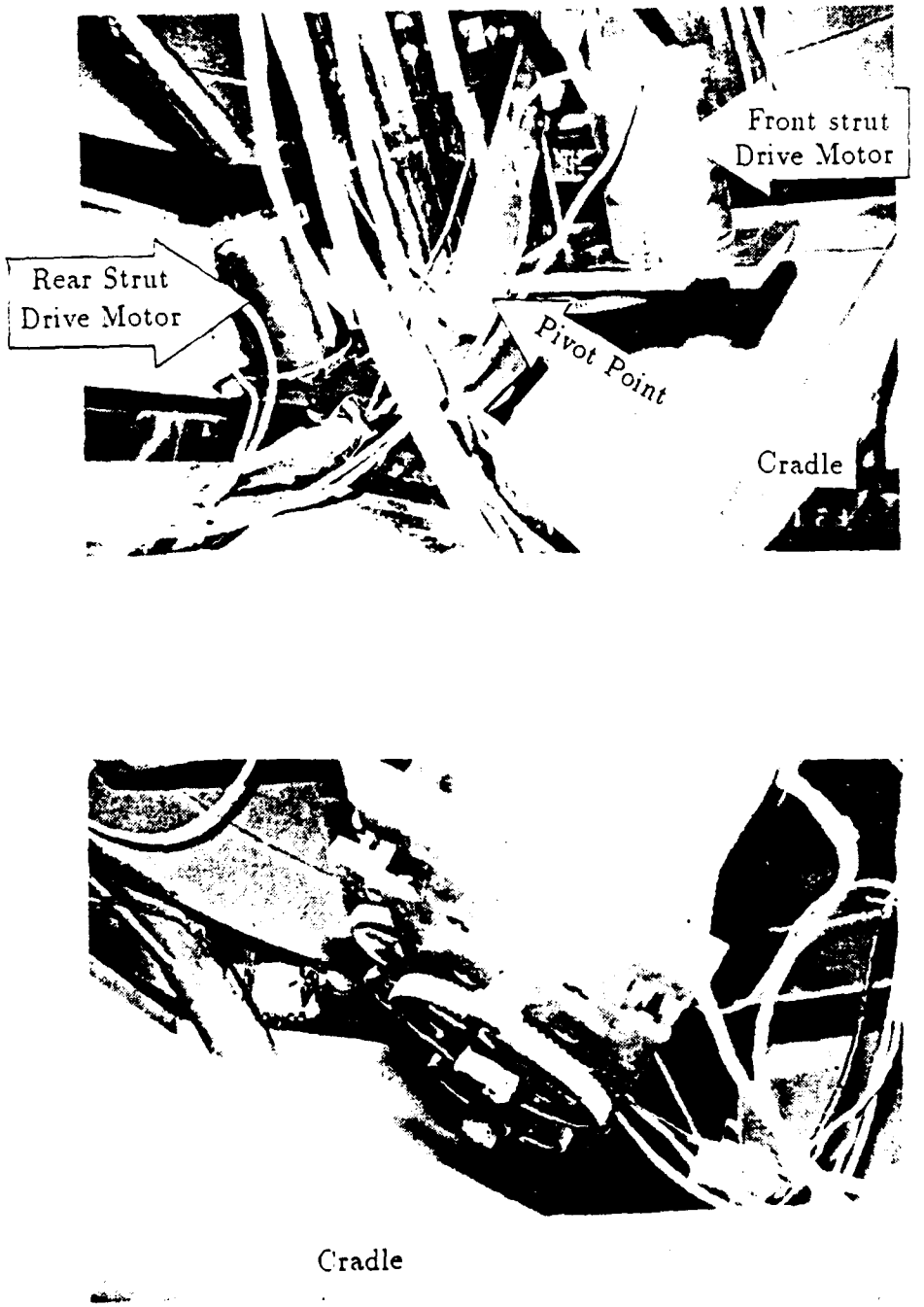

Fig. 31. HARS drive system detail.

Once installed, HARS was positioned repeatedly from 0 to 90° of pitch without using the angular correction inputs mentioned earlier. HARS' attitude was always measured statically, without operating the wind tunnel, using a vernier inclinometer. Differences between the calculated HARS position and the actual pitch attitude ranged from 4.70° for a requested 0° to a maximum error of 6.89° for 40° before dropping to a minimum error of 0.75° for the requested pitch of 90°. Certainly some of the error was due to installation misalignment, but this error would have been constant through the range of movement. The remainder was assumed to be due to irregularities in the physical lengths supplied to **HIALST** through it's external data file. A series of tests where each of the physical parameters were varied were inconclusive in isolating the error.

To correct for this error another subroutine was added to **HIALST**, and additional data was added to the external data file. The new subroutine interpolated a correction from the additional data which was the error in pitch attitude as measured at 10° increments. This method required the mechanism to be run through the full range of pitch angles, with all correction factors set to zero, recording the variance between HARS' calculation of pitch and it's true position in 10° increments. When complete, this information is entered into the external data file for pitch angle correction during operation.

With this later correction included, HARS was repeatedly commanded to position at random pitch attitudes. Figure 32 shows HARS installed in the TAMU LSWT with the small sting and a model attached. Each position was compared to a measurement of the transverse link's attitude taken with the inclinometer. The inclinometer was accurate to one minute of angular measure. With the external data file directing **HIALST** to maintain a ± 20° accuracy, HARS' pitch attitude was within the desired accuracy in over 100 separate commands. Remaining position error was not correlative to the desired pitch attitude, or the direction the commanded pitch

angle was approached from. No means to measure HARS' attitude with the wind tunnel in operation was in place during operational tests.

The operation speed of HARS varied with the beginning and ending positions. An average of 4° per second, with 15 seconds to finely adjust the pitch attitude was observed.

Operational Evaluation

HARS was operationally tested through out the design envelope using a YF-16 model at dynamic pressures up to 80 psf. Use of the sting mounting system spanned a three week period, during which four problems arose. The first one was minor; HARS was only able to achieve a maximum of 88° of pitch. This limit was acceptable during the test so no measures were taken to allow a full 90° of pitch.

By the end of the second day of testing, HARS had lost clearance adjustment on the main strut. This clearance maladjustment allowed as much as half a degree of pitch attitude error, determined by measuring the change in mounting angle of the transverse link while an assistant manually forced the sting to move up and down. Excessive clearances were eliminated by adjusting those pads which could be accessed with HARS installed in the LSWT. The current drawn by the motors increased from 15 amps, for properly adjusted clearances, to 23 amps following tightening the pads, emphasizing the important affects of proper maintenance relating to power required to run the mount. A look at the close tolerances of HARS' installation can be found in Fig. 33. In this figure HARS was sitting at 30° of pitch where the front to rear strut clearance is maximized, and the close quarters of the balance structure is obvious. Less than three and typically less than two inches of clearance separate HARS from the pyramidal balance's lower turntable structure.

The third problem arose with high q testing. While testing at a q equal to 80 psf, the electric motors did not have enough power to position the m del against the wind. In this situation, as HARS started to move to a higher angle of attack, the model was blown back to a full 88° of pitch. Once in this position, HARS could be

a.) -15° α

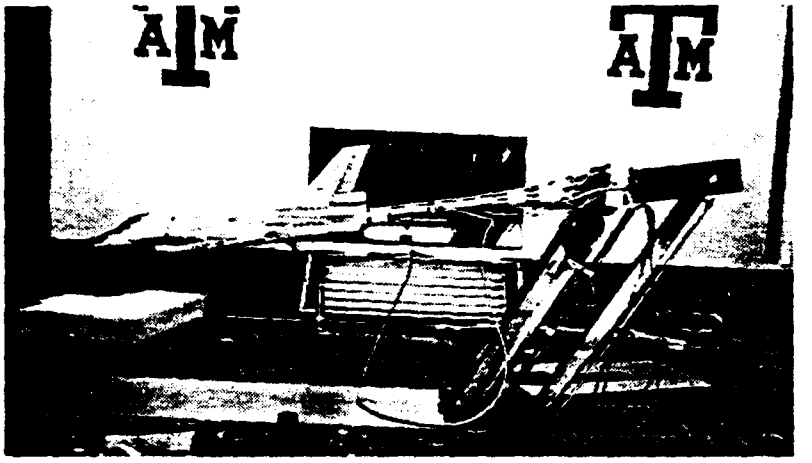

b.) 0° α

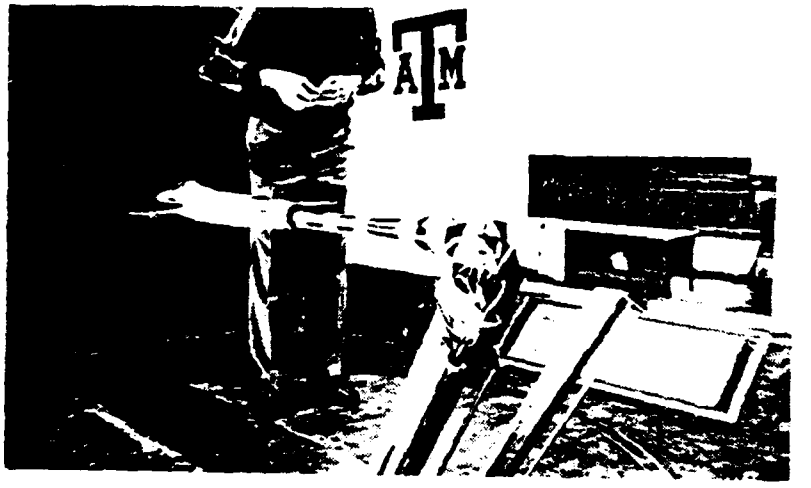

c.) 90° α

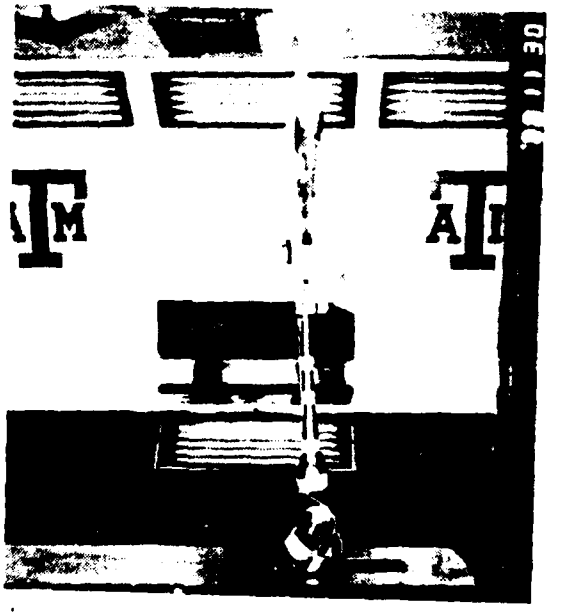

Fig. 32. Installed HARS mechanism at various angles of attack.

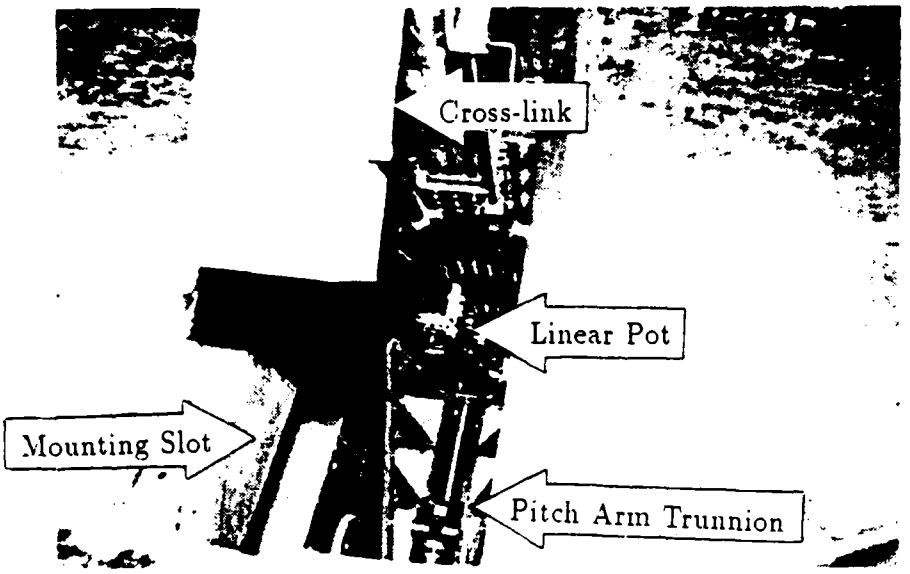

Fig. 33. Rear strut to pitch trunnion clearance. Looking down from the test section.

seen attempting to correct the pitch attitude, but the sting could not draw down against the wind. The problem was dealt with by dropping q to 60 psf or lower, waiting for the pitch attitude to stabilize, and then bringing the tunnel back up to speed. HARS held and maintained the new position, but could not cope with the initial mo ment toward a higher pitch angle.

The last item occurred at the conclusion of a series of pitch examinations, when HARS was extending both struts to return to 0° of pitch. Occasionally, the front strut would quit extending without reaching the proper height. Since the rear strut was still extending, this caused the model to dip dangerously close to the tunnel floor. Before contact was made, the 'panic' button cut power to the motors. The front strut began operating normally after restoring power. This problem was later traced to a faulty upper limit micro switch.

CONCLUSIONS AND RECOMMENDATIONS

Conclusions

1. HARS was able to position the model successfully from 0° to 90° of pitch, with up to 90° of yaw under most conditions. No movement restrictions were noted below a pitch angle of 60°; however, for dynamic pressures at and above 80 psf, the tunnel wind velocity had to be dropped to a lower q for HARS to position itself. The tunnel velocity could then be raised and data taken from the model.
2. HARS attached to the present turntable without requiring any modification to the later hardware.
3. Model was positioned wings level for testing from 0° to 90° of pitch, with up to 90° of yaw.
4. A 36 inch long model remained in the center of the tunnel test section (which has less than a 0.4% q variation).
5. A microcomputer fully controled the position of HARS from the operators console.
6. Pitch attitude at the model was consistently measured within an error of 0.2°, although it was only staticly measurable. There was no mechanism to measure the actual pitch angle during the course of tunnel operation.
7. The combination of the strut potentiometer's linearity error, the limited resolution of the A/D board, and the unknown operational physical displacement limited HARS' current accuracy capabilities.
8. There may have been very low frequency noise within the model data due to vibration of HARS structure.

9. Dynamic testing using HARS, in its current configuration, is not possible due to the limited strength of the gears, and the liabilities of the amplifier-motor combination.

Recommendations

1. Measures to overcome the positioning problem during high q operation need exploration. Possibilities would include larger motors, a different transverse link for high pitch angle/high q testing, or software refinement for critical position adjustment.
2. An additional bracket needs to be constructed to attach the forward edge of the mount extension bar to the tunnel edge to decrease the chance of mount vibration during operation.
3. Clearance problems experienced by the end of the second day of operations can be minimized in any one or a combination of ways, which include:
   A. Machine the surface of the struts to obtain a less abrasive surface.
   B. Coat the extensions with a durable dry film lubricant, such as, graphite impregnated epoxies.
   C. Install pads of greater durability and lubrication qualities.
4. A mechanism to measure the actual angle of pitch during the course of tunnel operation needs to be included. The instrumentation of the sting to provide this information could document operational errors as well as be channeled back to the computer for position tracking.
5. An upgrade to the electronics of HARS should include a revision of the controlling software and hardware. The 'on-off' control of the electric motors might be overcome by designing an oscillating output signal from the computer which would, in effect, permit running the motors at a controlled, variable rate. This modification would increase operation response to commanded changes to pitch settings. A change of amplifiers might also be a solution to this problem. The computer signal could then

vary operation speed by varying the signal voltage strength. This latter method would be preferable since it would be less prone to variation of the computer's operation speed as the programming logic used to generate an oscillating signal would be.

6. HARS' impact on flow within the tunnel should be documented. While the basic guidelines for insuring a low degree of flow restriction and flow effects about the model were followed, the effects of high AOA testing on flow quality within the test section are not known. Nor is there quantification of flow behavior as compared to other model mounting systems.
7. Dynamic testing should consider a modified version of the single jackscrew concept. The necessary modification would be an addition of a second screw for lowering and raising the primary mechanism. The mechanism could be plunged without changing pitch attitude, and would mathematically modeled using modern robotic techniques. Such modeling would allow torque and force requirements to be calculated, and a greater degree of control of model velocity during position changes.

REFERENCES

[1] Vinceint, J., "New Technologies for a European Fighter," *Aerospace America*, Vol. 24, Sept. 1986, p. 34.

[2] Wright, O., Jr., "Squeezing the Testing Cycle," *Aerospace America*, Vol. 26, Feb. 1988, pp. 17-19.

[3] Dietz, W.E., Jr. and Altstatt, M.C., "Experimental Investigation of Support Interference on an Ogive Cylinder at High Incidence," AIAA Paper 78-165, 16th Aerospace Sciences Meeting, Jan. 16-18, 1978.

[4] Mouch, T.N., and Nelson, R.C., "The Influence of Aerodynamic Interference on High Angle of Attack Wind Tunnel Testing," AIAA Paper 78-827, 1978.

[5] Johnson, J.L., Grafton, S.B., and Yip, L.P., "Exploratory Investigation of the Effects of Vortex Bursting on the High Angle-of-Attack Lateral-Directional Stability Characteristics of Highly-Swept Wings," AIAA Paper 80-0463, Mar. 1980.

[6] Ericsson, L.E., and Reding, J.P., "Support Interference in Static and Dynamic Tests," *ICIASF 1981 Record*, pp. 213-223.

[7] Rae, W.H., Jr., and Pope, A., *Low-Speed Wind Tunnel Testing*, Wiley and Sons, New York, 1984, p. 175.

[8] Malcolm, G.N., "New Rotation-Balance Apparatus for Measuring Airplane Spin Aerodynamics in the Wind Tunnel," AIAA Paper 78-835, 1978.

[9] Ericsson, L.E., "Reflections Regarding Recent Rotary Rig Results," AIAA Paper 86-0123, AIAA 24th Aerospace Sciences Meeting, Jan. 6-9, 1986.

[10] Kreplin, H.P., Meier, H.U., and Maier, A., "Wind Tunnel Model and Measuring Techniques for the Investigation of Three-dimensional Boundary Layers," AIAA Paper 78-781, 1978.

[11] Erb, R.E., *Evaluation of the Use of Hinged Strakes on a High Performance Fighter Aircraft*, thesis, Texas A&M University, May 1985.

[12] *Low Speed Wind Tunnel Facility Handbook*, Texas Engineering Experiment Station, The Texas A&M University System, Jan. 1985.

[13] Bruhn, E.F., *Analysis and Design of Flight Vehicle Structures*, Jacobs Publishing, Carmel, Indiana, 1973, pp. A6.3-A6.6.

[14] Polakowski, N.H., and Ripling, E.J., *Strength and Structure of Engineering Materials*, Prentice-Hall, Inc., Englewood Cliffs, New Jersey, 1966, p. 401.

[15] DOD Publication FSC 1560, *Military Standardization Handbook - Metallic Materials and Elements for Aerospace Vehicle Structures*, Department of Defense, 1 Jun. 1983.

[16] Bertin, J.J., and Smith, M.L., *Aerodynamics for Engineers* , Wiley and Sons, New York, 1981, pp. 208-214.

[17] Nicolai, L.M., *Fundamentals of Aircraft Design*, Mets Inc., San Jose, Calif., 1975, pp. 11-5–11-23.

[18] Hoerner, S.F., *Fluid Dynamic Drag*, published by the author, Midland Park, New Jersey, 1958, p. 92.

[19] Perkins, C.D., and Hage, R.E., *Airplane Performance Stability and Control*, Wiley and Sons, New York, 1967, pp. 216-229.

Supplementary Sources Consulted

[1] *Plastics Reference Handbook* Regal Plastics Supply Company, National Association, 1987, pp. 183-196, (Private collection, T. Kubler).

APPENDIX A

AERODYNAMIC CALCULATIONS

Aerodynamic calculations will be done on the following simple aircraft shape:

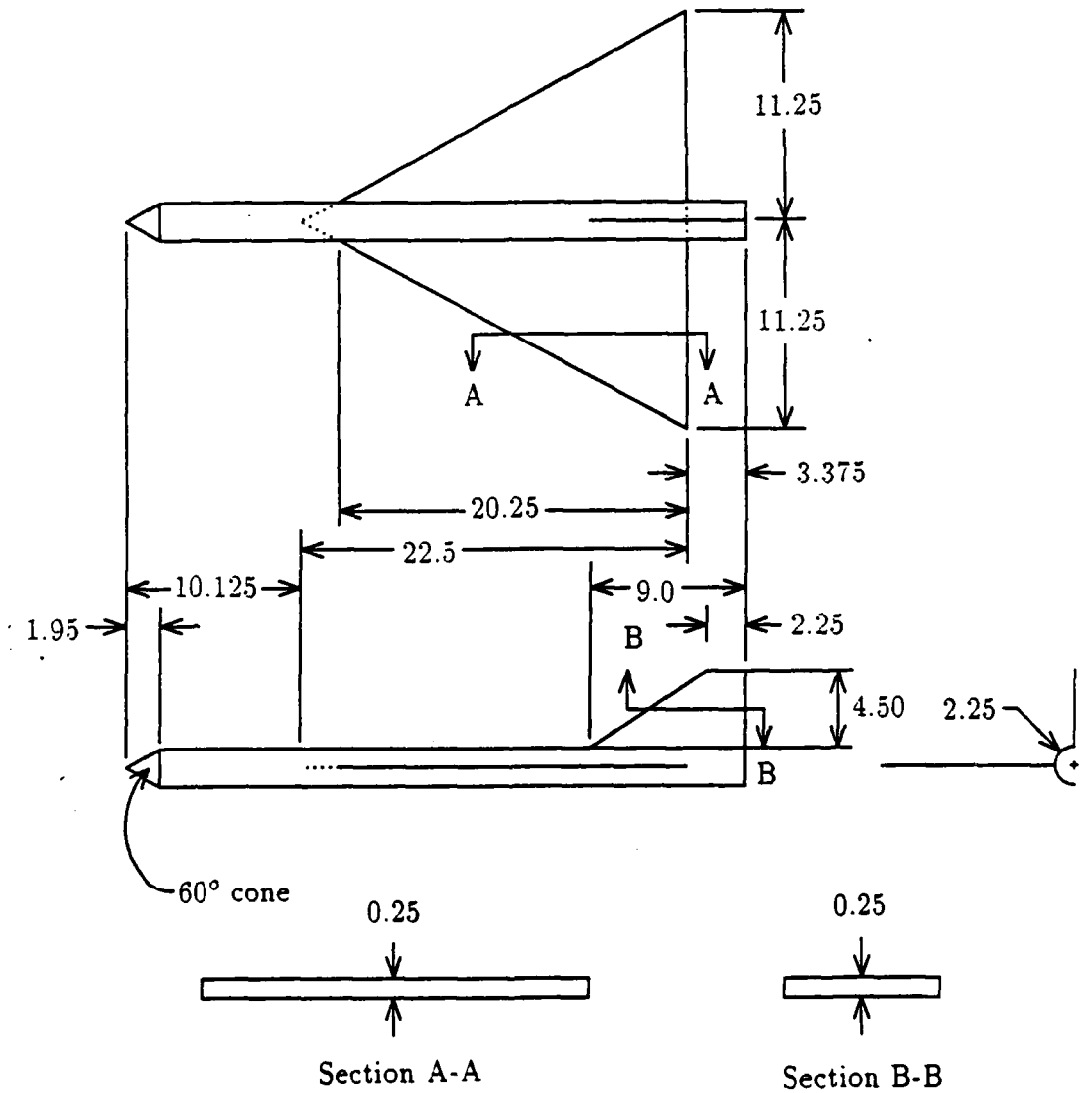

Wing parameters: MAC = 15" t/c = 1.67% a.c. @ fs 22.4250

Vertical tail parameters: MAC = 6.3" t/c = 1.98%

Aircraft data:

$$\text{Aspect Ratio}(AR) = \frac{b^2}{S}$$
$$= \frac{22.5^2}{\frac{1}{2}(22.5)(22.5)}$$
$$= 2$$

$$\text{Taper Ratio} = \lambda$$
$$= \frac{c_t}{c_r}$$
$$= 0$$

$$\text{Sweep angle} = \Delta_{\frac{1}{4}}$$
$$= tan^{-1}\left(\frac{\frac{3}{4}(c_r)}{\frac{1}{2}(b)}\right)$$
$$= tan^{-1}\left(\frac{\frac{3}{4}(22.5)}{\frac{1}{2}(22.5)}\right)$$
$$= 56.31^\circ$$

1.LIFT CALCULATIONS

1.A. LIFT CURVE SLOPE[16]

$$C_l = K_p \sin\alpha \cos^2\alpha + K_v \sin^2\alpha \cos\alpha \qquad (6.58)$$

where: K_p is given by Fig. 6-32[16]

$$K_p = f(\text{AR},\ \Lambda_{LE},\ \frac{a}{c})$$

$$K_p = 2.3030(2.3535)$$

K_v is given by Fig. 6-33[16]

$$K_v = 2.8586(3.2449)$$

NOTE: Since $\frac{a}{c}$ versus Λ_{LE} gave different values than AR versus Λ_{LE}, both are shown; AR versus Λ_{LE} is the first value. In Fig. 6-34[16], this equation correlated well with experiment for an $\alpha = 15^\circ$ up to $R_e = 6.0 \times 10^6$; after which, the lack

of reattachment caused error. With our $R_e = 2.9 \times 10^6$, assume correspondence for another 10°, to an α of 25°.

α	-5	0	5	10	15	20	25
C_L	-.1776	0.000	.2208	.4727	.7411	1.0098	1.2622
(C_L)	-.1790	0.000	.2281	.4927	.7783	1.0675	1.3422
%diff	0.8	0.000	3.3	4.2	5.0	5.7	6.3

The larger values will be used hence forth.

To extend the range of C_L, Fig. 6-36[16] , "Lift coefficeints for Delta Wings of Various Aspect Ratios"; $t = 0.12c, R_e \cong 7 \times 10^5$ is used on the chart information for $AR = 2.38$; beyond 35° the data is extrapolated along a curve of similar form found for $AR = 1.61$. Data for $AR = 2$ are linearly interpolated.

From fig 6-36[16]:

	—	—	—	—	C_L	—	—	—	—	—
$AR\backslash\alpha$	-5	0	5	10	15	20	25	30	35	40	45
1.61	-.170	0.00	.168	.340	.500	.700	.900	1.05	1.15	1.15	1.07
2.00	-.195	0.00	.191	.395	.563	.785	.925	.985	.985	.880	.705
2.38	-.220	0.00	.213	.450	.626	.870	.950	.920	.820	.610	.340

Comparing to earlier values, the trends of this range of data will be extrapolated

to predict thin airfoil lift characteristics

α	C_L (6-36)	$\%\Delta C_L$	C_L (6.58)	$\%\Delta C_L$
5	0.191		0.2208	
		1.068		1.141
10	0.395		0.4727	
		0.425		0.568
15	0.563		0.7411	
		0.394		0.363
20	0.785		1.0098	
		0.178		0.250
25	0.925		1.2622	
		0.065		—
30	0.985		1.3442	
		0.000		—
35	0.985		1.3442	
		-.107		—
40	0.880		1.2004	
		-.199		—
45	0.705		0.9615	
		-.4(est)		—
50	—		0.5769	

1.B. WING-BODY $C_{L\alpha}$[17]

$$\left(C_{L\alpha}\right)_{WB} = F\left(C_{L\alpha}\right)_{W}$$

where:

$$F = f\left(\frac{d}{b} = \frac{\text{body diameter}}{\text{wing span}}\right)$$

$$F = f\left(\frac{2.25}{22.5}\right)$$
$$= f(\frac{1}{10})$$
$$= 1.1712$$

NOTE: This is referenced to exposed wing area (S_E), not total wing area (S_w)!

$$C_{L_E} q S_E = C_{L_W} q S_w \Rightarrow C_{L_E} = C_{L_W}(\frac{S_w}{S_E})$$

finding $\frac{S_w}{S_E}$: $\quad \frac{S_w}{S_E} = \frac{\frac{1}{2}(22.5)^2}{2(\frac{1}{2})(20.25)(10.125)}$

$$= 1.2346$$

$$\left(C_{L_\alpha}\right)_{WB} = 1.1712(1.2346 C_{L_W})$$
$$= 1.4459 C_{L_{\alpha_W}}$$

1.C. CURVE FIT OF RESULTS OF 1.A. TO 90° USING FRENCH CURVE

α	C_L
50	0.5769
55	0.2742
60	0.1738
65	0.1133
70	0.0684
75	0.0371
80	0.0195
85	0.0070

1.D. TOTAL C_L

A	B	C	D	E	F
α	C_{L_W}	$C_{L_{\alpha_W}}$ $\frac{B_n - B_{n-1}}{A_n - A_{n-1}}$	$C_{L_{\alpha_E}}$ $1.4459B$	C_{L_E} $\frac{E_{n-1}+}{D(A_n - A_{n-1})}$	$C_{L_{TOTAL_W}}$ $\frac{E}{1.2346}$
-5	-.1776	—	—	-0.2565	-0.2078
0	0.0000	0.0355	0.0513	0.0000	0.0000
5	0.2208	0.0442	0.0639	0.3195	0.2588
10	0.4727	0.0504	0.0729	0.6840	0.5540
15	0.7411	0.0537	0.0776	1.0720	0.8683
20	1.0098	0.0537	0.0776	1.4600	1.1826
25	1.2622	0.0505	0.0730	1.8350	1.4864
30	1.3442	0.0164	0.0237	1.9435	1.5742
35	1.3442	0.0000	0.0000	1.9435	1.5742
40	1.2004	-.0288	-.0416	1.7355	1.4058
45	0.9615	-.0478	-.0691	1.3900	1.1259
50	0.5769	-.0769	-.1112	0.8340	0.6755
55	0.2742	-.0605	-.0875	0.3965	0.3212
60	0.1738	-.0201	-.0291	0.2510	0.2033
65	0.1133	-.0121	-.0175	0.1635	0.1324
70	0.0684	-.0090	-.0130	0.0985	0.0798
75	0.0371	-.0063	-.0091	0.0530	0.0429
80	0.0195	-.0035	-.0051	0.0275	0.0223
85	0.0070	-.0025	-.0036	0.0095	0.0077
90	0.0000	-.0014	-.0020	0.0000	0.0000

2. DRAG CALCULATIONS

2.A. TOTAL DRAG COEFFICIENT FOR WING DUE TO LIFT

$$C_{D_L} = C_{D_0} + C_{D_v} + \Delta C_{D_B}$$

where:

$$C_{D_0} = 0.0040$$

$$C_{D_v} = \frac{C_L{}^2}{\pi e AR}$$

$$= C_L{}^2\left(\frac{1}{\pi(.85)2}\right)$$

$$= 0.1872 C_L{}^2$$

ΔC_{D_B} = parabolic curve variation

$$C_{D_L} = 0.0040 + 0.1872 C_L{}^2 + \Delta C_{D_B}$$

α	C_{D_0}	C_{D_v}	$\%C_{L_{max}}$	$\%\Delta\%C_L$	$\%\Delta C_D$	ΔC_{D_B}	C_{D_L}
-5	0.0040	0.0081	—	—	—	0.0000	0.0121
0	↓	0.0000	—	—	—	0.0000	0.0040
5	↓	0.0125	—	—	—	0.0000	0.0165
10	↓	0.0575	—	—	—	0.0000	0.0615
15	↓	0.1412	—	—	—	0.0000	0.1452
20	↓	0.2619	—	—	—	0.0000	0.2659
25	↓	0.4137	93.77	58.47	17.66	0.0731	0.4908
30	↓	0.4640	99.31	95.40	64.84	0.3009	0.7689

2.B. ZERO LIFT DRAG OF BODY

$$(C_{D_0})_{WB} = \left(C_{D_0}\right)_W + \left(C_{D_0}\right)_B + \Delta C_{D_0} + C_{D_L}$$

where:

$$\left(C_{D_0}\right)_W = \frac{C_f\left[1 + L\frac{t}{c} + 100\frac{t}{c}^4\right] RS_w}{S_{ref}}$$

where[17]:

$$L = 2.0 \text{ for } \left(\frac{t}{c}\right)_{max} \leq 0.3c$$

$$\frac{t}{c} = 0.02$$

$$S_w = 2S_e$$

$$= 2(410.0625)$$

$$= 820.1250$$

$$= S_{ref}$$

$$R = 0.8483(\text{ from Fig.11.8})$$

$$C_f = 3.9 \times 10^{-3}(\text{ turbulent })$$

C'_f based on natural metal $-K = 0.16 \times 10^{-3}$

$$\left(C_{D_0}\right)_W = 3.9 \times 10^{-3}\left[1 + 2.0(0.02) + 100(0.02)^4\right]0.8483(0.81)$$

$$= 0.0028$$

2.C. BODY DRAG[17]

$$\left(C_{D_0}\right)_B = \left(C_{D_f}\right)_B + C_{D_b}$$

where:

$$\left(C_{D_f}\right)_B = \frac{C_f\left[1 + \frac{60}{l_{B_d}^3} + .0025l_{B_d}\right]S_s}{S_B}$$

where:

$C_f = 0.16 \times 10^{-3}$ – based n natural metal $-K$

$S_s = 2\pi(1.125)(33.75) + 2\pi(2.25)(0.375)$

$= 243.8661$

$S_B = \pi(1.125)^2$

$= 3.9761$

$$= 3.3 \times 10^{-3}\left[1 + \frac{60}{4096} + 0.04\right]\frac{243.8661}{3.9761}$$
$$= 0.2135$$

$C_{D_b} = 0$, assuming the sting fills the base

$\left(C_{D_0}\right)_B = 0.2135$

2.D. MISC DRAG, ΔC_{D_0}

zero; no stores, canopies, etc.

2.E. WING-BODY DRAG

$$\left(C_{D_0}\right)_{WB} = \left(C_{D_0}\right)_W + \left(C_{D_0}\right)_{\frac{S_b}{S_{ref}}} + \Delta C_{D_0}$$
$$= 0.0028 + \left[0.2135 + \frac{\pi(1.125)^2}{253.1250}\right]$$
$$= 0.0062$$

2.F. TOTAL DRAG COEFFICIENT FOR -5 TO 30° α

$$C_D = \text{2.A.} + \text{2.E.}$$

α	C_{D_L}	C_{D_0}	C_D
-5	0.0121	0.0062	0.0183
0	0.0040	↓	0.0102
5	0.0165	↓	0.0227
10	0.0615	↓	0.0677
15	0.1452	↓	0.1514
20	0.2659	↓	0.2721
25	0.4908	↓	0.4970
30	0.7689	↓	0.7751

2.G. POST 30° DRAG

$$C_D = C_{D_0} + C_{D_i} + C_{D_f}$$

where:

$C_{D_0} = 0.0040$

C_{D_i} = (assume flat plate past 30 degrees AOA)

$= (1.1805 - 0.0040)\sin\alpha$

$= 1.17655\sin\alpha$

C_{D_f} = fuselage drag when modeled as circular cylinder

$= f(\ L,\ d,\ \sin\alpha\ )$

where: L = exposed cylindrical fuselage length

= cylindical portion + $\frac{2}{3}$ conical portion

= 14.4510

$\frac{L}{d}$ used to obtain C_d[18]

$\frac{L}{d}$	C_d
1	0.63
5	0.80
10	0.83

but this is for the projected characteristic area of the cylinder, it is reduced by multiplying by the projected area of an equivalent circumferential cylinder and characterized by dividing by wing area (253.125)

α	$C_{D_{0,w}}$	C_{D_L}	$\frac{L}{d}$	$C_{D_{cyl}}$	a_{circ}	S_{cyl}	$C_{D_{fus}}$	C_D
35	0.0040	0.6748	3.6839	0.7441	1.9614	83.2686	0.2448	0.9236
40	↓	0.7562	4.1284	0.7630	1.7502	85.8646	0.2588	1.0190
45	↓	0.8319	4.5415	0.7805	1.5910	88.4630	0.2728	1.1087
50	↓	0.9013	4.9200	0.7966	1.4686	90.9868	0.2863	1.1916
55	↓	0.9637	5.2611	0.8016	1.3734	93.3699	0.2957	1.2634
60	↓	1.0189	5.5622	0.8034	1.2990	95.5493	0.3033	1.3262

α	$C_{D_{0,w}}$	C_{D_L}	$\frac{L}{d}$	$C_{D_{cyl}}$	a_{circ}	S_{cyl}	$C_{D_{fus}}$	C_D
65	0.0040	1.0663	5.8209	0.8049	1.2413	97.4802	0.3100	1.3803
70	↓	1.1055	6.0353	0.8062	1.1972	99.1153	0.3157	1.4252
75	↓	1.1364	6.2038	0.8072	1.1647	100.4232	0.3202	1.4606
80	↓	1.1586	6.3251	0.8080	1.1424	101.3773	0.3236	1.4862
85	↓	1.1720	6.3982	0.8084	1.1293	101.9536	0.3256	1.5016
90	↓	1.1765	6.4226	0.8085	1.1250	102.1470	0.3263	1.5068

3. PITCHING MOMENT

In general from eqn 5-4[19]

$$C_m = \frac{C_n x_a}{c} + \frac{C_c z_a}{c} + C_{m_{ac}} + C_{m_{fus,Nac}} - C_{n_t}\frac{S_t}{S_w}\frac{l_t}{c}\nu_t$$

3.A. FUSELAGE[19]

$$\frac{dM}{d\alpha} = \frac{\text{volume}}{28.7} g(K_2 - K_1)$$

where:

$$\begin{aligned} K_2 - K_1 &= f\left(\frac{L}{D}\right) \\ &= f(16) \\ &= 0.97 \end{aligned}$$

$$\begin{aligned} \text{volume} &= \pi(1.125)^2(36 - 1.95) + \text{ (nosecone volume)} \\ &= 135.3855 + \frac{1}{2}(1.125(1.95)(0.375)(2\pi)) \\ &= 137.9700\text{in}^3 \\ &= 0.0798\text{ft}^3 \end{aligned}$$

therefore:

$$\frac{dM}{d\alpha} = 100\left(\frac{0.0798}{28.7}\right)0.97$$

$$\frac{dM}{d\alpha} = 0.2698\frac{\text{ft} - \text{lb}}{\text{rad}}$$

3.B. WING CONTRIBUTION[19]

$$C_{m_w} = C_n\left(\frac{x_a}{c}\right) + C_c\left(\frac{z_a}{c}\right) + C_{mac}$$

where:

$$C_n = C_L\cos(\alpha - i_w) + C_D\sin(\alpha - i_w)$$

$$= C_L\cos\alpha + C_D\sin\alpha, \text{ since} i_w = 0$$

$$C_c = C_D\cos(\alpha - i_w) - C_L\sin(\alpha - i_w)$$

$$= C_D\cos\alpha - C_L\sin\alpha$$

$$\frac{x_a}{c} = \frac{20.8006 - 22.425}{15}$$

$$= -0.1083$$

$$\frac{z_a}{c} = \frac{-0.0481}{15}$$

$$= -0.0032$$

$$C_{mac} = 0$$

therefore :$C_{m_w} = -0.1083(C_L\cos\alpha + C_D\sin\alpha) - 0.0032(C_D\cos\alpha - C_L\sin\alpha)$

APPENDIX B

FORTRAN SOURCE LISTING: FORCES

```
      PROGRAM FORCES

      REAL LIFT, LOFRCL, LOFRCD, LAFRCL, LAFRCD, LAFORC, LOFORC, MAC,
     &     MCGLO, MCGLA, MCGFUS, MCG, MNTING, LENGTH
      CHARACTER*1 ANSWER

      DIMENSION AOA(20), CL(20), CD(20), CDV(7)

      DATA AOA/ -5.0,  0.0,  5.0, 10.0, 15., 20., 25.,
     & 30., 35., 40., 45., 50., 55., 60.,
     & 65., 70., 75., 80., 85., 90./
      DATA CL/-.2078, 0.0000, 0.2588, 0.5540, 0.8683, 1.1826, 1.4864,
     &       1.5742, 1.5742, 1.4058, 1.1259, 0.6755, 0.3212, 0.2033,
     &       0.1324, 0.0798, 0.0429, 0.0223, 0.0077, 0.0000/
      DATA CD/0.0183, 0.0102, 0.0227, 0.0227, 0.1514, 0.2721, 0.4970,
     &       0.7751, 0.9236, 1.0190, 1.1087, 1.1916, 1.2634, 1.3262,
     &       1.3803, 1.4252, 1.4606, 1.4862, 1.5016, 1.5068/
      DATA CDV/0.0000, 0.0004, 0.0017, 0.0062, 0.0145, 0.0266, 0.0412/

      XCG    = 20.8006 / 12.
      S      = 253.1250 / 144.
      Q      = 100.
      DGTORD = 1. / ( 180. / 3.141593 )
      XA     = -1.6244 / 12.
      ZA     = -0.0481 / 12.
```

```
      DCMDAL = 0.2698
      LENGTH = 36. / 12.
      MNTING = 30. * DGTORD
      STING  = 30. / 12.
      SDSLIP = 0.
      RETRAC = 0.
      HSINK  = 8. / 12.

      WRITE(*,*)' ENTER DESIRED SIDE SLIP ANGLE>'
      READ(*,*)SDSLIP
      BETA    = SDSLIP * DGTORD

      WRITE(*,*)' ENTER INITIAL MOUNT HEIGHT IN INCHES>'
      READ(*,*)H
      H      = H / 12.
      HPRIME = H + HSINK

      WRITE(*,*) ' RETRACT THE PIVOT POINT?>'
      READ(*,*)RETRAC
      IF( RETRAC .EQ. 0) THEN
  DELTAH = 0.
  ELSE
      DELTAH = H / 18.
ENDIF

      WRITE(*,901)

      DO 10 I = 1,20

      IF( TIPZ .GE. 7.0 ) GOTO 10
```

```
      ALPHA    = AOA(I) * DGTORD
      IF( AOA(I) .GT. 0. ) THEN
  H  = H - DELTAH
  HPRIME = HPRIME - DELTAH
ENDIF
      ICDV     = INT( SDSLIP / 5. ) + 1
      IF( AOA(I) .NE. 90. ) THEN
  CDVERT  = CDV(ICDV) * SQRT( COS( ALPHA ) )
  ELSE
      CDVERT = 0
ENDIF

C*****   WIND AXIS
      LIFT     = CL(I) * Q * S
      DRAG     = ( CD(I) + CDVERT ) * Q * S
      DRAG     = CD(I) * Q * S

C*****   BODY AXIS
      LOFRCL   = LIFT * SIN( ALPHA )
      LAFRCL   = LIFT * COS( ALPHA )
      LOFRCD   = DRAG * COS( ALPHA )
      LAFRCD   = DRAG * SIN( ALPHA )
C*****   FORCES
      LOFORC   = LOFRCL + LOFRCD
      LAFORC   = LAFRCL + LAFRCD
C*****   MOMENTS ABOUT AC
      MAC      = 0.
C*****   MOMENTS ABOUT CG
      MCGLO    = LOFORC * ZA
```

```
      MCGLA    = LAFORC * XA
      MCGFUS   = DCMDAL * ALPHA
      MCG      = MCGLO + MCGLA + MCGFUS + MAC
C*****   MOMENTS ABOUT STING BASE
      TMOMNT   = DRAG * SIN(BETA) * ( ( ( STING + LENGTH - XCG + XA )
     & * COS(ALPHA) ) - ( HPRIME * TAN(MNTING) ) )
      BMOMNT   = LIFT * ( ( STING + LENGTH - XCG + XA ) * COS(ALPHA) -
     & ( HPRIME * TAN(MNTING) ) )
     & + DRAG * COS(BETA) * ( ( STING + LENGTH - XCG + XA )
     & * SIN(ALPHA) + HPRIME )
     & + MCGFUS
C*****   LOCATION OF MODEL TIP
      TIPX     = ( ( ( STING + LENGTH ) * COS( ALPHA ) ) -
     &   ( H * TAN( MNTING ) ) ) * COS( BETA )
      TIPY     = ( ( ( STING + LENGTH ) * COS( ALPHA ) ) -
     &   ( H * TAN( MNTING ) ) ) * SIN( BETA )
      TIPZ     = H + ( ( STING + LENGTH ) * SIN( ALPHA ) )
C*****   LOCATION OF MODEL CENTER OF GRAVITY
      CGX      = ( ( ( STING + LENGTH - XCG ) * COS( ALPHA ) ) -
     &   ( H * TAN( MNTING ) ) ) * COS( BETA )
      CGY      = ( ( ( STING + LENGTH - XCG ) * COS( ALPHA ) ) -
     &   ( H * TAN( MNTING ) ) ) * SIN( BETA )
      CGZ      = H + ( ( STING + LENGTH - XCG ) * SIN( ALPHA ) )
C*****   RECORD HIGHEST VALUES
      IF( TMOMNT .GT. TMAX ) TMAX = TMOMNT
      IF( BMOMNT .GT. BMAX ) BMAX = BMOMNT


C*****   DUMP DATA
      WRITE(*,902) AOA(I), LIFT, DRAG, TMOMNT, BMOMNT, TIPX, TIPY,
     &    TIPZ,   CGX, CGY, CGZ
```

```
10    CONTINUE

      WRITE(*,903) TMAX,BMAX

901   FORMAT(' ALPHA    LIFT      DRAG     TORSIONAL    BENDING '
     &      '  TIP X  TIP Y  TIP Z   CG X   CG Y   CG Z',/,
     &      '                                  MOMENT     MOMENT')
     &      '  COORD  COORD  COORD  COORD  COORD  COORD',/,
902   FORMAT(1X,F5.1,2X,2(F8.2,2X),2(F10.2,2X),6(F5.2,2X))
903   FORMAT(/,' MAXIMUM TORSIONAL MOMENT ENCOUNTERED WAS: Mt =',F10.2,
     &      /,' MAXIMUM BENDING MOMENT ENCOUNTERED WAS:   Mb =',F10.2)
      STOP
      END
```

APPENDIX C

FORTRAN SOURCE LISTING: RSTRUTLD

```
      PROGRAM RSTRUTLD

      REAL LIFT, MNTMAX, LEN, LENATR
      CHARACTER*1 ANSWER

      DIMENSION AOA(20), CL(20), CD(20), CDV(7)

      DATA AOA/ -5.0,  0.0,  5.0, 10.0, 15., 20., 25.,
     & 30., 35., 40., 45., 50., 55., 60.,
     & 65., 70., 75., 80., 85., 90./
      DATA CL/-.2078, 0.0000, 0.2588, 0.5540, 0.8683, 1.1826, 1.4864,
     &       1.5742, 1.5742, 1.4058, 1.1259, 0.6755, 0.3212, 0.2033,
     &       0.1324, 0.0798, 0.0429, 0.0223, 0.0077, 0.0000/
      DATA CD/0.0183, 0.0102, 0.0227, 0.0227, 0.1514, 0.2721, 0.4970,
     &       0.7751, 0.9236, 1.0190, 1.1087, 1.1916, 1.2634, 1.3262,
     &       1.3803, 1.4252, 1.4606, 1.4862, 1.5016, 1.5068/
      DATA CDV/0.0000, 0.0004, 0.0017, 0.0062, 0.0145, 0.0266, 0.0412/

      XCG    = 20.8006 / 12.
      S      = 253.1250 / 144.
      Q      = 100.
      PI     = 3.141593
      DGTORD = 1. / ( 180. / PI )
      SDSLIP = 0.
      FS     = 6.
```

```
      E      = 29.0E6

5     WRITE(*,*)' ENTER DESIRED SIDE SLIP ANGLE>'
      READ(*,*)SDSLIP
      BETA    = SDSLIP * DGTORD

      WRITE(*,901)

      DO 10 I = 1,20

      ALPHA   = AOA(I) * DGTORD
      ICDV    = INT( SDSLIP / 5. ) + 1
      IF( AOA(I) .NE. 90. ) THEN
  CDVERT  = CDV(ICDV) * SQRT( COS( ALPHA ) )
  ELSE
      CDVERT = 0
ENDIF

C*****   WIND AXIS
      LIFT    = CL(I) * Q * S
      DRAG    = ( CD(I) + CDVERT ) * Q * S
      DRAG    = CD(I) * Q * S
C*****   FROCE ON REAR STRUT ABOUT FRONT STRUT PIVOT POINT
      FPRIME  = ( LIFT + DRAG * SIN(ALPHA) * COS(BETA) ) * 3.9020
C*****   ANGLE BETWEEN STING CENTERLINE AND REAR STRUT
      DEL     = ATAN (
     & ( 12. * SIN( ( 120. * DGTORD ) - ALPHA ) - 5. ) /
     &       (
     &        101. -
     &        ( 68. * ALPHA / PI ) -
```

```
     &         ( 12. * COS( ( 120. * DGTORD) - ALPHA ) )
     &        )
     &       )
      DELDEG = DEL / DGTORD
C*****   REQUIRED REACTANT FORCE
      R        = FPRIME / COS( ( 30. * DGTORD ) + DEL - ALPHA )
C*****   UNREENFORCED LENGTH
      LEN      = 44. - ( 68. * ALPHA / PI ) -
     & ( 12. * COS( ( 120. * DGTORD ) - ALPHA ) )
C*****   TOTAL LENGTH OF REAR STRUT
      TOTLEN = ( 101. - ( 68. * ALPHA / PI) - ( 12 *
     & ( COS( ( 120. * DGTORD ) - ALPHA ) ) ) ) / COS ( DEL )
C*****   DETERMINE SECTIONAL MOMENT OF INERTIA FOR STRUT BUCKLING
C*****   ASSUMING TOTAL LENGTH OF REAR STRUT AND A SINGLE BUCKLE NODE
      RWTHFS   = R * FS
      SECMNT   = ( RWTHFS * TOTLEN * TOTLEN ) / ( PI * PI * E )
C*****   RECORD HIGHEST VALUES
      IF( SECMNT .GT. MNTMAX ) THEN
  MNTMAX = SECMNT
  RMAX   = R
  F4RMAX = FPRIME
  LENATR = LEN
ENDIF
      IF( DELDEG .GT. DELMAX ) DELMAX = DELDEG

C*****   DUMP DATA
      WRITE(*,902) AOA(I), LIFT, DRAG, FPRIME, R, DELDEG, LEN,
     &    TOTLEN, SECMNT
10    CONTINUE
```

```
      WRITE(*,903) MNTMAX, RMAX, F4RMAX, LENATR, DELMAX

901   FORMAT(' ALPHA  LIFT    DRAG    INDUCED  REACTANT  '
     &      'STRUT  FREE    TOTAL   MINIMUM',/,
     &      ' (DEG)  (LB)    (LB)    FORCE F  FORCE R   '
     &      'ANGLE  LENGTH  LENGTH  STRUT I',/)
902   FORMAT(1X,F5.1,2(2X,F6.2),2(2X,F7.2),2X,F4.2,3X,2(F6.2,2X),F5.2)
903   FORMAT(/,' MAXIMUM SECTIONAL MOMENT OF INERTIA WAS: I =',F8.2,/,
     &        '   OCCURING FOR R = ',F8.2,',  F = ',F8.2,',  WITH'
     &        ' AN UNSUPPORTED LENGTH OF ',F6.2,' INCHES',
     &      /,' MAXIMUM ANGLE BETWEEN THE FRONT AND REAR STRUT WAS ',
     &        F6.2,' DEGREES')
      STOP
      END
```

APPENDIX D

FORTRAN SOURCE LISTING: SCREW

```
      PROGRAM SCREW
C*****    PROGRAM TO COMPUTE DATA ON ALL POSSIBLE SCREW THREAD DESIGNS
C*****       FOR RESEARCH PROJECT FOR GEAR RATIOS FROM 10 TO 1/10.
      REAL MTRTRQ
      DIMENSION OD(7), PITCH(31), SPS(13), MTRTRQ(13), GEARNG(30),
     & RD(7,31), DP(7,31), PD(7,31), WD(7,31), A(7,31),
     & ADVANT(7,31), FORCE(7,31), TORQUE(7,31),
     & HLXANG(7,31), SPEED(7,31), VFLAG(7,21), EXTSPD(7,31,30)
      DATA SPS/10000., 4000., 2000., 1000., 800., 400., 200., 100.,
     &        70., 50., 30., 10., 0./,
     & MTRTRQ/ 0., 253., 693., 1320., 1440., 1747., 1973., 2147.,
     &        2227., 2267., 2333., 2373., 2630./
      GEARNG(01) = 1.
      GEARNG(02) = 1./2.
      GEARNG(03) = 1./3.
      GEARNG(04) = 1./4.
      GEARNG(05) = 1./5.
      GEARNG(06) = 1./6.
      GEARNG(07) = 1./7.
      GEARNG(08) = 1./8.
      GEARNG(09) = 1./9.
      GEARNG(10) = 1./10.
      GEARNG(11) = 1./11.
      GEARNG(12) = 1./12.
      GEARNG(13) = 1./13.
```

```
GEARNG(14) = 1./14.
GEARNG(15) = 1./15.
GEARNG(16) = 1./16.
GEARNG(17) = 1./17.
GEARNG(18) = 1./18.
GEARNG(19) = 1./19.
GEARNG(20) = 1./20.
GEARNG(21) = 1./21.
GEARNG(22) = 1./22.
GEARNG(23) = 1./23.
GEARNG(24) = 1./24.
GEARNG(25) = 1./25.
GEARNG(26) = 1./26.
GEARNG(27) = 1./27.
GEARNG(28) = 1./28.
GEARNG(29) = 1./29.
GEARNG(30) = 1./30.
OD(1) = 10./16.
OD(2) = 11./16.
OD(3) = 12./16.
OD(4) = 13./16.
OD(5) = 14./16.
OD(6) = 15./16.
OD(7) = 16./16.
PITCH(01) =1./2.
PITCH(02) =1./3.
PITCH(03) =1./4.
PITCH(04) =1./5.
PITCH(05) =1./6.
PITCH(06) =1./7.
```

```
      PITCH(07) =1./8.
      PITCH(08) =1./9.
      PITCH(09) =1./10.
      PITCH(10) =1./11.
      PITCH(11) =1./12.
      PITCH(12) =1./13.
      PITCH(13) =1./14.
      PITCH(14) =1./15.
      PITCH(15) =1./16.
      PITCH(16) =1./17.
      PITCH(17) =1./18.
      PITCH(18) =1./19.
      PITCH(19) =1./20.
      PITCH(20) =1./21.
      PITCH(21) =1./22.
      PITCH(22) =1./23.
      PITCH(23) =1./24.
      PITCH(24) =1./25.
      PITCH(25) =1./26.
      PITCH(26) =1./27.
      PITCH(27) =1./28.
      PITCH(28) =1./29.
      PITCH(29) =1./30.
      PITCH(30) =1./31.
      PITCH(31) =1./32.
      PSTLIM = 9.0E10
      PI     = 3.14159265
      LOAD   = 5580.
C*****    COMPUTE THE MINIMUM SHAFT DIAMETER FOR A GIVEN SHAFT OD AND
C*****       AND PITCH. MINIMUM DIAMETER MUST BE > .5710 AS DONE IN
```

```
C*****       HAND CALCULATIONS ON SCREW SIZING. FLAG ANY SHAFTS FOUND
C*****       TO BE TOO SMALL TO BE PASSED OVER IN FURTHER CALCULATIONS.
C*****  DP - DIAMETRICAL PITCH
C*****  PITCH - DISTANCE BETWEEN INDIVIDUAL TEETH
C*****  WD - WHOLE DEPTH, TICE THE ADDENDUM AND CLEARANCE
C*****  RD - ROOT DIAMETER
C*****  A  - ADDENDUM
C*****  PD - PITCH DIAMETER
C*****  ADVANT - MECHANICAL ADVANTAGE OF THE SCREW
C*****  FORCE - FORCE REQ TO HOLD LOAD IN PLACE
C*****  TORQUE - REQUIRED TORQUE TO SYSTEM TO FURNISH FORCE AT
C*****   THE PITCH DIAMETER
C*****  EXTSPD - SPEED AT WHICH THE EXTENSION CAN BE EXTENDED AT
C*****   LOAD APPLIED. ACTUAL EXTENSION SPEEDS WILL BE
C*****   EXPECTED TO BE HIGHER. ONLY EXPERIMENTAL RESULTS
C*****   WILL BE ABLE TO DETERMINE ACTUAL SPEEDS.
      WRITE(*,901)
      WRITE(*,902) (OD(I),I=1,7)
      DO 20 J = 1,31
      DO 10 I = 1,7
      DP(I,J) = PI / PITCH(J)
      WD(I,J) = 2.157 / DP(I,J)
      RD(I,J) = OD(I) - ( 2. * WD(I,J) )
      IF( RD(I,J) .LT. 0.5710 ) THEN
  VFLAG(I,J) = 1.
  DP(I,J) = 0.
  WD(I,J) = 0.
  RD(I,J) = 0.
  A(I,J) = 0.
  PD(I,J) = 0.
```

```
      ADVANT(I,J) = 0.
      FORCE(I,J) = 0.
      TORQUE(I,J) = 0.
      HLXANG(I,J) = 0.
      EXTSPD(I,J,1) = 0.
      SPEED(I,J) = 0.
      GOTO 10
    ENDIF
          A(I,J)  = 1. / DP(I,J)
          PD(I,J) = OD(I) - ( 2. * A(I,J) )
          ADVANT(I,J) = ( PI * PD(I,J) ) / PITCH (J)
          HLXTAN = PITCH(J) / ( PI * PD(I,J) )
          HLXANG(I,J) = ATAN( HLXTAN ) * 180. / PI
          FORCE(I,J)  = LOAD / ADVANT(I,J)
          TORQUE(I,J) = FORCE(I,J) * PD(I,J) * 16.
10        CONTINUE
          WRITE(*,903) PITCH(J),(RD(I,J),I=1,7)
20        CONTINUE
          WRITE(*,904)
          WRITE(*,902) (OD(I),I=1,7)
          DO 100 J = 1, 31
          WRITE(*,903) PITCH(J),(PD(I,J),I=1,7)
100       CONTINUE
          WRITE(*,905)
          WRITE(*,902) (OD(I),I=1,7)
          DO 110 J = 1, 31
          WRITE(*,903) PITCH(J),(DP(I,J),I=1,7)
110       CONTINUE
          WRITE(*,906)
          WRITE(*,902) (OD(I),I=1,7)
```

```
      DO 120 J = 1, 31
      WRITE(*,903) PITCH(J),(HLXANG(I,J),I=1,7)
120   CONTINUE
      WRITE(*,907)
      WRITE(*,902) (OD(I),I=1,7)
      DO 140 J = 1, 31
      WRITE(*,908) PITCH(J),(TORQUE(I,J),I=1,7)
140   CONTINUE
      WRITE(*,910)
      DO 180 M = 1,3
      NDXBEG = 1 + ( ( M - 1 ) * 10 )
      NDXEND = NDXBEG + 9
      WRITE(*,911) (GEARNG(K),K=NDXBEG,NDXEND)
      DO 160 J = 1,31
      DO 170 L = 1,10
      N = L + ( M - 1 ) * 10
      IF( VFLAG(7,J) .EQ. 1 ) GOTO 160
C*****   COMPARE TORQUE WITH MAXIMUM HOLDING TORQUE, OF STEPPING MOTOR
C*****      SIGMA-24-4296D200-7034-K, OF 2630 in-lb. BYPASS FUTURE
C*****      CALCULATIONS.
      AVLTRQ = 2630. / GEARNG(N)
      IF( TORQUE(7,J) .GT. AVLTRQ ) THEN
  EXTSPD(7,J,N) = PSTLIM
  SPEED(7,J) = PSTLIM
  GOTO 170
ENDIF
C*****    COMPUTE ROTATION RATE AT MAXLOAD
      K = 0
      TRQOUT = TORQUE(7,J) * GEARNG(N)
      IF(TRQOUT .GT. 2630.) WRITE(*,*)'PROGRAM LOGIC ERROR'
```

```
1     K = K + 1
      IF( TRQOUT .GT. MTRTRQ(K) ) GOTO 1
      SPEED(7,J) = ( SPS(K-1) - ( ( TRQOUT - MTRTRQ(K-1) )
     &               / ( MTRTRQ(K) - MTRTRQ(K-1) )
     &             * ( SPS(K-1) - SPS(K) ) ) )* GEARNG(N)
C*****    COMPUTE EXTENSION RATE FOR THE PITCH OF THE SCREW. THE SPEED
C*****      IS THE NUMBER OF STEPS PER SECOND. 200 STEPS TO MAKE
C*****      A COMPLETE REVOLUTION.
      RPS = SPEED(7,J) / 200.
      EXTSPD(7,J,N) = RPS * PITCH(J)
170   CONTINUE
      WRITE(*,912) PITCH(J),(EXTSPD(7,J,K),K=NDXBEG,NDXEND)
160   CONTINUE
180   CONTINUE
901   FORMAT(////
     &     /,' DRIVE SCREW ANALYSIS FOR THE MODIFIED STING MOUNT',
     &    /,' ************************************************',///,
     &       ' R O O T   D I A M E T E R   O F   S C R E W',/)
902   FORMAT(' SCREW                    O U T S I D E   D I',
     &      ' A M E T E R',/,
     &      ' PITCH     ----------------------------------',
     &      '-------------------------',/,
     &      '-------    ',7(F7.4,2X))
903   FORMAT(' ',F6.4,4X,7(F7.4,2X))
904   FORMAT(/////,' P I T C H   D I A M E T E R   O F   S C R E W',/,
     &    ' ******************************************',/)
905   FORMAT(/////,' D I A M E T R I C A L   P I T C H   O F  ',
     &    ' S C R E W',/,
     &     '**************************************************',/)
906   FORMAT(/////,' H E L I X   A N G L E   O F   S C R E W',/,
```

```
     &    ' ************************************',/)
907   FORMAT(/////,' T O R Q U E   R E Q U I R E M E N T   O N ',
     &    ' S C R E W',/,
     &     '****************************************************',/)
908   FORMAT(' ',F6.4,4X,7(F7.0,2X))
910   FORMAT(/////,
     &     ' MAXIMUM EXTENSION SPEED OF FRONT STRUT UNDER MAXIMUM ',/,
     &     ' LOADING CONDITIONS IN INCHES/SECOND FOR VARYING GEAR ',/,
     &     ' RATIOS. THE GEAR RATIOS ARE THE RATIO OF SCREW SPEED ',/,
     &     ' TO STEPPING MOTOR SPEED',/,
     &     ' ************************************************** ',)
911   FORMAT(//,' SCREW                          G E A R   R A T I O',
     &     '   ( S C R E W : M O T O R )',/,
     &     ' PITCH     ----------------------------------',
     &     '----------------------------------------------------',/,
     &     '-------    ',10(F7.4,2X))
912   FORMAT(' ',F6.4,4X,10(F7.4,2X))
      END
```

APPENDIX E

A/D BOARD SPECIFICATIONS

DT2821-F-16SE ANALOG AND DIGITAL I/O BOARD

A/D SUBSYSTEM

ANALOG INPUTS	
Number of Analog Inputs	16SE
Input Ranges	0 to +10V (unipolar) ±10V (bipolar)
Output Data Codes	Straight binary (unipolar), offset binary, or two's complement (bipolar)
Gain Range	1, 2, 4, 8
Input Impedance	Off Channel: 100 megaohms, 10pF On Channel: 100 megaohms, 50pF
Bias Current	±10nA
Common Mode Input Voltage,Maximum	±10.5V
Common Mode Rejection Ratio (CMRR), Gain = 1	80dB at 60Hz, 1 kilohm unbalanced
Maximum Input Voltage without Damage, Power On	±27V
Maximum Input Voltage without Damage, Power Off	±12V
Amplifier Input Noise	0.2 LSB rms

Channel-to-channel Input	
Voltage Error	± 0.1mV
ACCURACY	
Resolution	12 bits
Nonlinearity	Less than $\pm\frac{1}{2}$ LSB
Differential Nonlinearity	Less than $\pm\frac{1}{2}$ LSB
Inherent Quantizing Error	$\pm\frac{1}{2}$ LSB
System Accuracy	
Gain = 1	To within $\pm 0.03\%$ FSR
Gain = 2	To within $\pm 0.04\%$ FSR
Gain = 4	To within $\pm 0.05\%$ FSR
Gain = 8	To within $\pm 0.07\%$ FSR
Channel Crosstalk	-100dB at 1kHz
Gain Error	Adjustable to 0
Zero Error	Adjustable to 0
DYNAMIC PERFORMANCE	
Channel Aquisition Time	
to within $\frac{1}{2}$ LSB	7.65μs
A/D Conversion Time	4μs
A/D Converter Throughput	150kHz
A/D Throughput to System Memory	150,000 samples per second
Sample & Hold Aperture Uncertainty	0.5ns
Sample & Hold Aperture Delay	100ns
Sample & Hold Droop Rate	50mV/ms
Sample & Hold Feedthrough	
Attenuation	80dB at 1kHz

THERMAL CHARACTERISTICS

A/D Zero Drift	$\pm$10 ppm of FSR/°C
Amplifier Zero Drift	$\pm 25\mu$V/°C
Gain Drift	$\pm$30 ppm of FSR/°C
Differential Linearity Drift	$\pm$3 ppm of FSR/°C
Monotonicity	$\pm$0 to +70°C

D/A SUBSYSTEM

ANALOG OUTPUTS

Number of Channels	2, deglitched
Output Ranges (jumper-selectable)	0 to 5V (unipolar) 0 to 10V (unipolar) $\pm$2.5V, $\pm$5V, $\pm$10V (bipolar)
Output Data Coding (jumper-selectable)	Straight binary (unipolar) or offset binary (bipolar)
Throughput	130kHz max, single channel 260kHz max, aggregate
Current Output	$\pm$5mA max
Output Impedance	0.1 ohms max
Capacitive Drive Capability	0.004μF
Protection Against	Short circuit to analog common
Glitch energy	15mV-μs

ACCURACY

Resolution	12 bits
Nonlinearity	To within $\pm\frac{1}{2}$ LSB
Differential Nonlinearity	To within $\pm\frac{1}{2}$ LSB
Gain Error	Adjustable to 0

Zero Error	Adjustable to 0
DYNAMIC PERFORMANCE	
Settling Time to 0.01% of FSR	5μs, 20V step
	1μs, 100mV step
Slew Rate	10V/μs
THERMAL CHARACTERISTICS	
D/A Zero Drift	$\pm$10 ppm of FSR/°C
Gain Drift	$\pm$30 ppm of FSR/°C
Monotonicity	0 to 70°C
DIGITAL I/O SUBSYSTEM	
Number of Lines	16
Number of Ports	2, 8-bit each
DIGITAL INPUTS	
Input Type	Level sensitive
Logic Family	LSTTL
Logic Sense	Positive true
Logic Load	1 LSTTL load
Logic High Input Voltage	2.0V minimum
Logic Low Input Voltage	0.8V maximum
Logic High Input Current	20μA maximum
Logic Low Input Current	-0.4mA maximum
Termination	None; unused inputs float
DIGITAL OUTPUTS	
Output	30 LSTTL loads
Logic Family	LSTTL
Logic High Output Voltage	2.5V minimum
Logic Low Output Voltage	0.4V maximum

Logic High Output Current	-15mA maximum
Logic Low Output Current	24mA maximum
Throughput	As fast as programmed I/O allows (200kHz benchmark)

APPENDIX F

AMPLIFIER SPECIFICATIONS

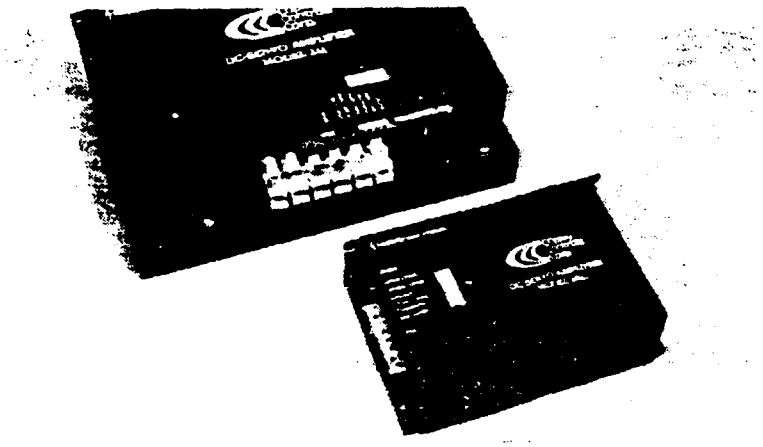

MODEL 240, 241
SERVO AMPLIFIERS

Model 240
± 150 volts at ± 30 amps peak
± 15 amps continuous

Model 241
± 150 volts at ± 60 amps peak
± 30 amps continuous

FEATURES

- *Four Quadrant operation.*
- **Main power supply can vary from 24V to 165V.**
- **22 kHz switching frequency eliminates audible noise.**
- **Small size.**
- **Low cost.**
- **Designed for convenient NEMA rack or surface mounting.**
- **Pulse Width Modulation for maximum efficiency.**
- **No external heat sink required for most duty cycles. Mating heat sink available.**
- **Internal D.C. to D.C. converter allows for operation from one supply.**
- **Failsafe circuitry protects against output overload, excessive temperature and improper supplies.**
- **Variable Current Limiting adjustable from 5 to 100% of rated peak current.**

PRODUCT DESCRIPTION

The Models 240/241 are high power high frequency switching amplifiers having a bridge type output to drive D.C. motors and other high current inductive loads. These amplifiers are functionally complete having all the support circuitry to operate with a D.C. tachometer in a stabilized rate loop for rate control or as an inner loop in a position control system. Each amplifier contains a unity gain input differential amplifier and a high gain servo preamplifier that can be configured with a wide range of user selected compensation values to stabilize most servo loops. The output of the preamplifier drives a PWM current source with a bridge type output. This output bridge is implemented using MOSFET devices switching at 22 kHz. The user can optimize the current feedback for various load inductances. These small size amplifiers are packaged to allow for convenient NEMA, rack, or surface mounting.

These amplifiers operating at 22 kHz are above the audible range and at that frequency allow operation with low inductance motors without having to add any external series inductance which could effect loop response. For rapid motor reversals, the Model 241 amplifier provides 60 amps for up to 4 sec. after which the current is limited to 30 amps. The Models 240/241 operate from a single high voltage power source from 24 to 155 volts. An internal wide range dc-dc converter provides the amplifier with all low level voltages required internally. Additional features of this amplifier include protection for overcurrent, overtemperature, and short circuit across outputs (or to ground). The amplifier can be shut down by an external switch closure as a positive/negative drive disable or completely disabled as might be the case during a power-up routine.

APPLICATIONS

Models 240/241 are designed to drive high power D.C. torque motors and linear actuators in machine control, robotic, material handling, and military applications. The small size of these amplifiers make them suitable for NEMA, rack, or surface mounting where space is at a premium. While many machine tool and other operator controlled equipment applications are concerned about audible noise these amplifiers operating at 22 kHz will not generate this unwanted noise. The high switching frequency makes it possible to operate low inductance high power motors without an external inductor or choke.

The Models 240/241 have been designed with many user features to allow for fast installation and maintainance. The user can by DIP switches change current feedback for various load inductances, tachometer scaling, and loop compensation. This is important in many power applications where motor and load characteristics vary.

As a result of these amplifiers having a combination of high power rating and wide operating voltage range, they are currently being designed into a number of AVG (Automatic Guided Vehicle) applications.

Finally, the Models 240/241 dissipate very low power due to the high efficiency switching technique used; for example, the Model 240 dissipates only 40 watts while delivering 15 amps continuous to the load and the Model 241 dissipates 77 watts at 30 amps continuous output. These power ratings make these amplifiers an ideal choice for those systems where minimum cooling is available.

Copley Controls Corp.
375 Elliot Street ■ Newton, Mass. 02164
Tel. 617-965-2410 ■ Telex: 285957

MODELS 240/241 SERVO AMPLIFIERS
PRELIMINARY SPECIFICATIONS

[redacted]

Typical specifications @ 25°C ambient. Load: 5.0 ohms (240), 2.5 ohms (241) in series with 300 μH (240), 150 μH (241). Voltage: ± 150V.

MODEL	240	241
PEAK POWER OUTPUT	± 150V @ ± 30A, 4.5 kW	± 150V @ ± 60A, 9 kW
Unidirectional current change	2s	"
Bidirectional current change	4s	"
MAXIMUM CONTINUOUS CURRENT		
Heat sink mount @70°C	± 15A	± 30A
Forced air, 400 fpm @50°C	± 7A	± 14A
Forced air, 400 fpm @60°C	± 15A (240H)	± 30A (241H)
Ambient @45°C	± 15A (240H)	± 30A (241H)
OUTPUT VOLTAGE	$V_{OUT} = V_H - (0.12)(I_o)$	$V_{OUT} = V_H - (0.06)(I_o)$
where: V_{OUT} = voltage to motor or load		
V_H = high voltage applied		
I_o = current into motor or load		
LOAD INDUCTANCE		
Min @ 155V	300 μH	150 μH
Min @ 80V	150 μH	75 μH
Compensation Switch	Up to 20 mH	Up to 10 mH
CURRENT LIMIT	Adjustable 1.5 to 30A	Adjustable 3 to 60A
INPUT CHARACTERISTICS		
Reference	Diff. ± 10V Max., 50KΩ Min.	"
Tachometer	Single-ended 50KΩ Min.	"
GAIN		
Diff. Amp	0.8V/V	"
Servo Preamp	Determined by internal components and potentiometers.	"
Current Source	4.3 A/V	8.7 A/V
BANDWIDTH		
Power stage, small signal	- 3 dB @ 1 kHz	"
Slew rate	0.19A/μs	0.38A/μs
SWITCHING FREQUENCY	22 kHz	"
REMOTE SHUTDOWN		
Enable	Switch closure enables output.	"
Positive enable	Switch closure enables positive output.	"
Negative enable	Switch closure enables negative output.	"
AMPLIFIER PROTECTION		
Current overload	Current limiter.	"
Heat sink temp.	Amplifier latched OFF, >90°C.	"
Over voltage shutdown	Temporarily, above + 165V.	"
Under voltage shutdown	Temporarily, below minimum.	"
Either output short to ground	Amplifier latched OFF.	"
Output short	Current limit	"
CURRENT MONITOR	± 0.2V/A or ± 6V_{Pk-Pk}/ ± 30A	± 0.1V/A or ± 6V_{Pk-Pk}/ ± 60A
LOGIC OUTPUTS/INPUTS		
Normal operation	Open collector.[2]	"
Overcurrent	HCMOS high indicates amplifier fault.[1]	"
Reset	Low will cause amplifier to attempt to reset every 50 ms.	"
LED INDICATORS		
Normal	Green LED	"
Over-Current	Red LED	"
POWER REQUIREMENTS		
High Voltage Supply	+ 24 to + 155V @ 30A	+ 30 to + 155V @ 60A
THERMAL REQUIREMENTS		
Case temperature	0 to 70°C	"
Power dissipation	40W @ 15A continuous	77W @ 30A continuous
Heat sink mount	Flat surface, 0 to 70°C	"
Forced air	0 to 50°C, 400 fpm	"
Ambient	0 to 45°C (240H)	"(241H)
Forced air	0 to 60°C, 400 fpm (240H)	"(241H)
Storage	- 30°C to + 85°C (240H)	"(241H)

APPENDIX G

PROGRAM FLOWCHART: HIALST

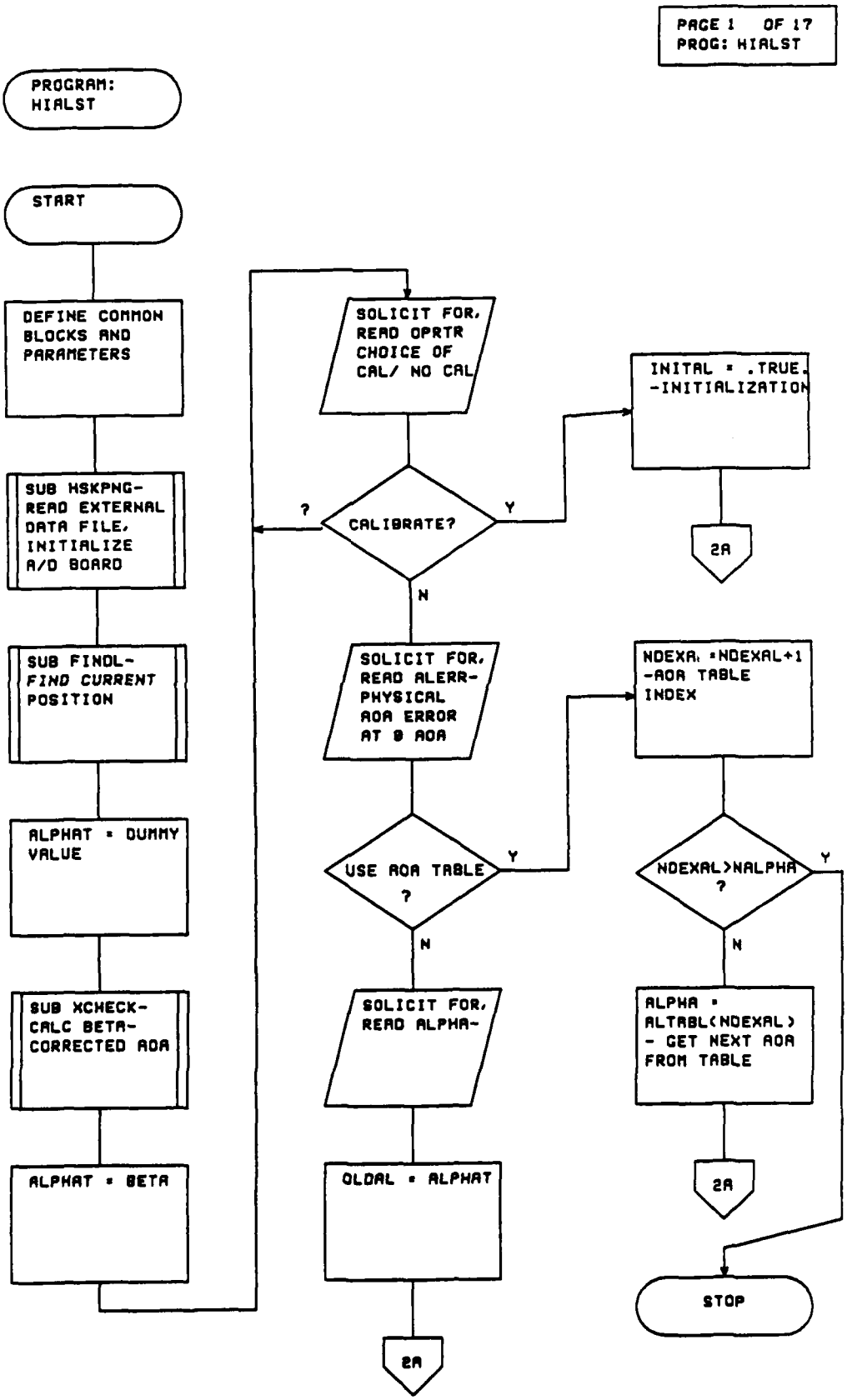
PAGE 1 OF 17
PROG: HIALST
PROGRAM: HIALST
START
DEFINE COMMON BLOCKS AND PARAMETERS
SUB HSKPNG- READ EXTERNAL DATA FILE, INITIALIZE A/D BOARD
SUB FINDL- FIND CURRENT POSITION
ALPHAT = DUMMY VALUE
SUB XCHECK- CALC BETA- CORRECTED AOA
ALPHAT = BETA
SOLICIT FOR, READ OPRTR CHOICE OF CAL/ NO CAL
CALIBRATE?
Y
N
INITAL = .TRUE. -INITIALIZATION
2A
SOLICIT FOR, READ ALERR- PHYSICAL AOA ERROR AT 0 AOA
USE AOA TABLE ?
Y
N
SOLICIT FOR, READ ALPHA-
OLDAL = ALPHAT
2A
NDEXA: =NDEXAL+1 -AOA TABLE INDEX
NDEXAL>NALPHA ?
Y
N
ALPHA = ALTABL(NDEXAL) - GET NEXT AOA FROM TABLE
2A
STOP

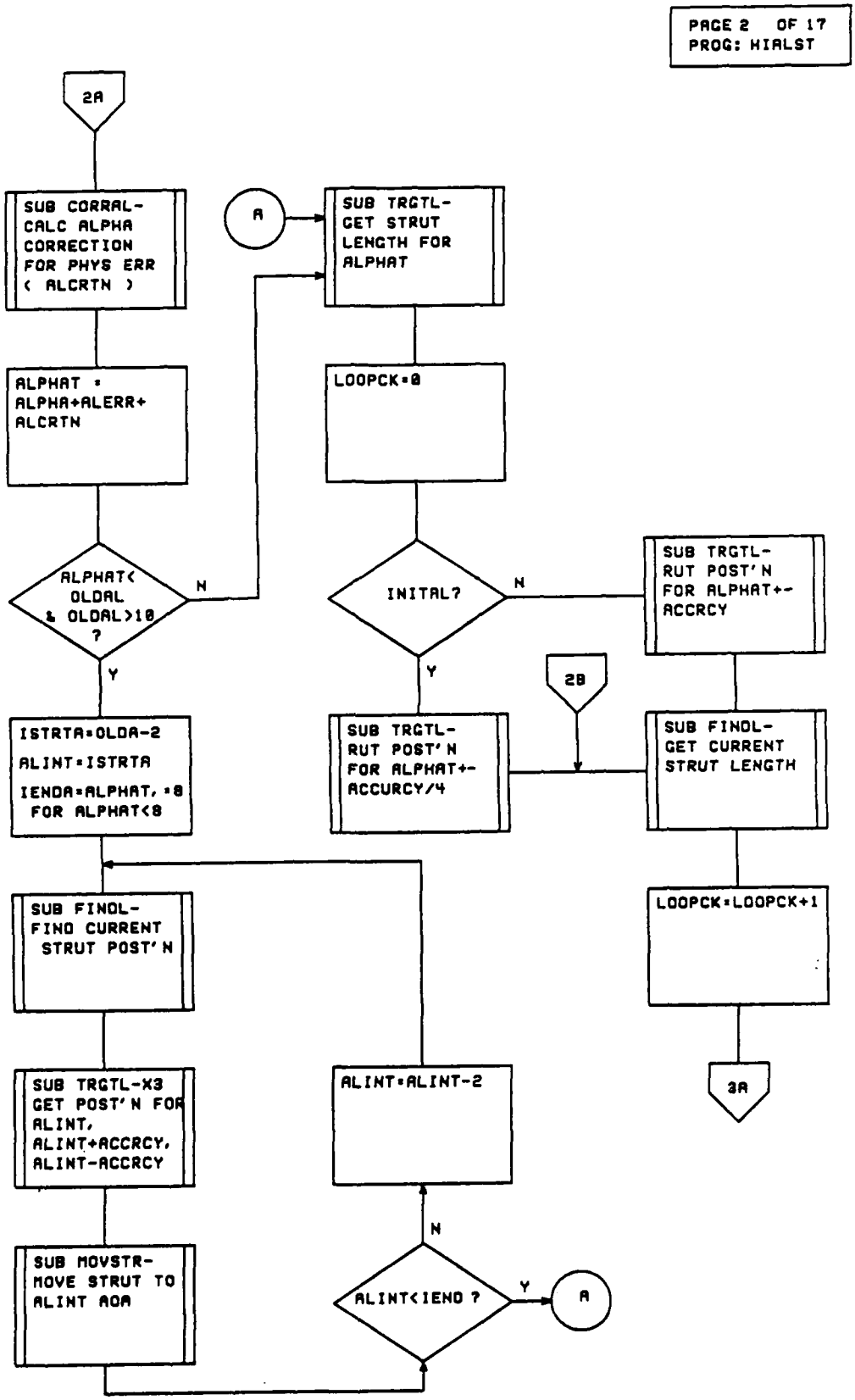
PAGE 2 OF 17
PROG: HIALST
2A
SUB CORRAL-
CALC ALPHA
CORRECTION
FOR PHYS ERR
(ALCRTN)
A
SUB TRGTL-
GET STRUT
LENGTH FOR
ALPHAT
ALPHAT =
ALPHA+ALERR+
ALCRTN
LOOPCK=0
ALPHAT<
OLDAL
& OLDAL>10
?
N
Y
INITAL?
N
Y
SUB TRGTL-
RUT POST'N
FOR ALPHAT+-
ACCRCY
2B
ISTRTA=OLDA-2
ALINT=ISTRTA
IENDA=ALPHAT, +8
FOR ALPHAT<8
SUB TRGTL-
RUT POST'N
FOR ALPHAT+-
ACCURCY/4
SUB FINDL-
GET CURRENT
STRUT LENGTH
SUB FINDL-
FIND CURRENT
STRUT POST'N
LOOPCK=LOOPCK+1
3A
SUB TRGTL-X3
GET POST'N FOR
ALINT,
ALINT+ACCRCY,
ALINT-ACCRCY
ALINT=ALINT-2
SUB MOVSTR-
MOVE STRUT TO
ALINT AOA
N
ALINT<IEND ?
Y
A

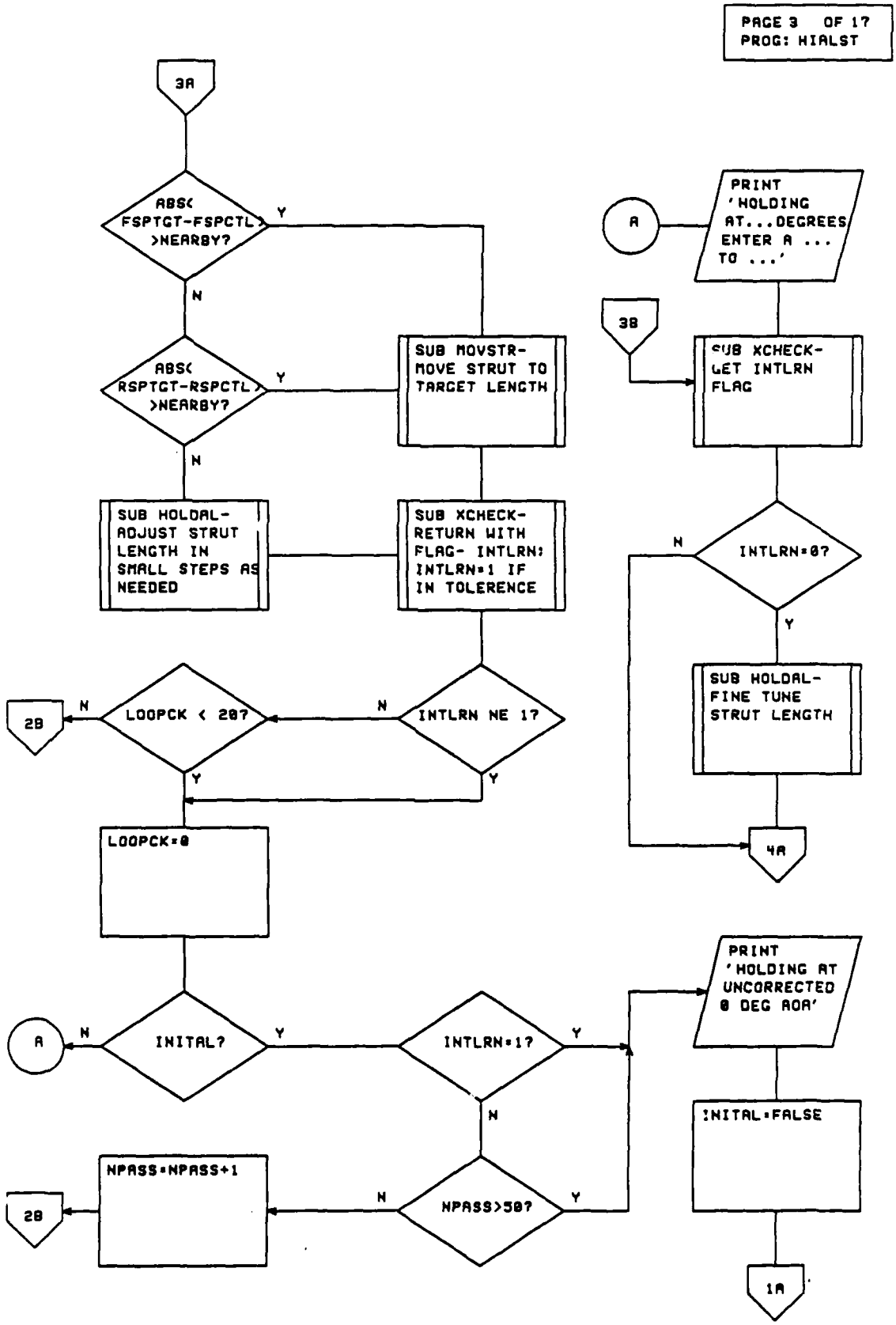
PAGE 3 OF 17
PROG: HIALST
3A
ABS(FSPTGT-FSPCTL) >NEARBY?
Y
N
ABS(RSPTGT-RSPCTL) >NEARBY?
Y
N
SUB MOVSTR- MOVE STRUT TO TARGET LENGTH
SUB HOLDAL- ADJUST STRUT LENGTH IN SMALL STEPS AS NEEDED
SUB XCHECK- RETURN WITH FLAG- INTLRN: INTLRN=1 IF IN TOLERENCE
INTLRN NE 1?
N
Y
LOOPCK < 20?
N
Y
2B
LOOPCK=0
INITAL?
N
Y
A
INTLRN=1?
Y
N
NPASS>50?
N
Y
NPASS=NPASS+1
2B
PRINT 'HOLDING AT UNCORRECTED 0 DEG AOA'
INITAL=FALSE
1A
A
PRINT 'HOLDING AT...DEGREES ENTER A ... TO ...'
3B
SUB XCHECK- GET INTLRN FLAG
INTLRN=0?
N
Y
SUB HOLDAL- FINE TUNE STRUT LENGTH
4A

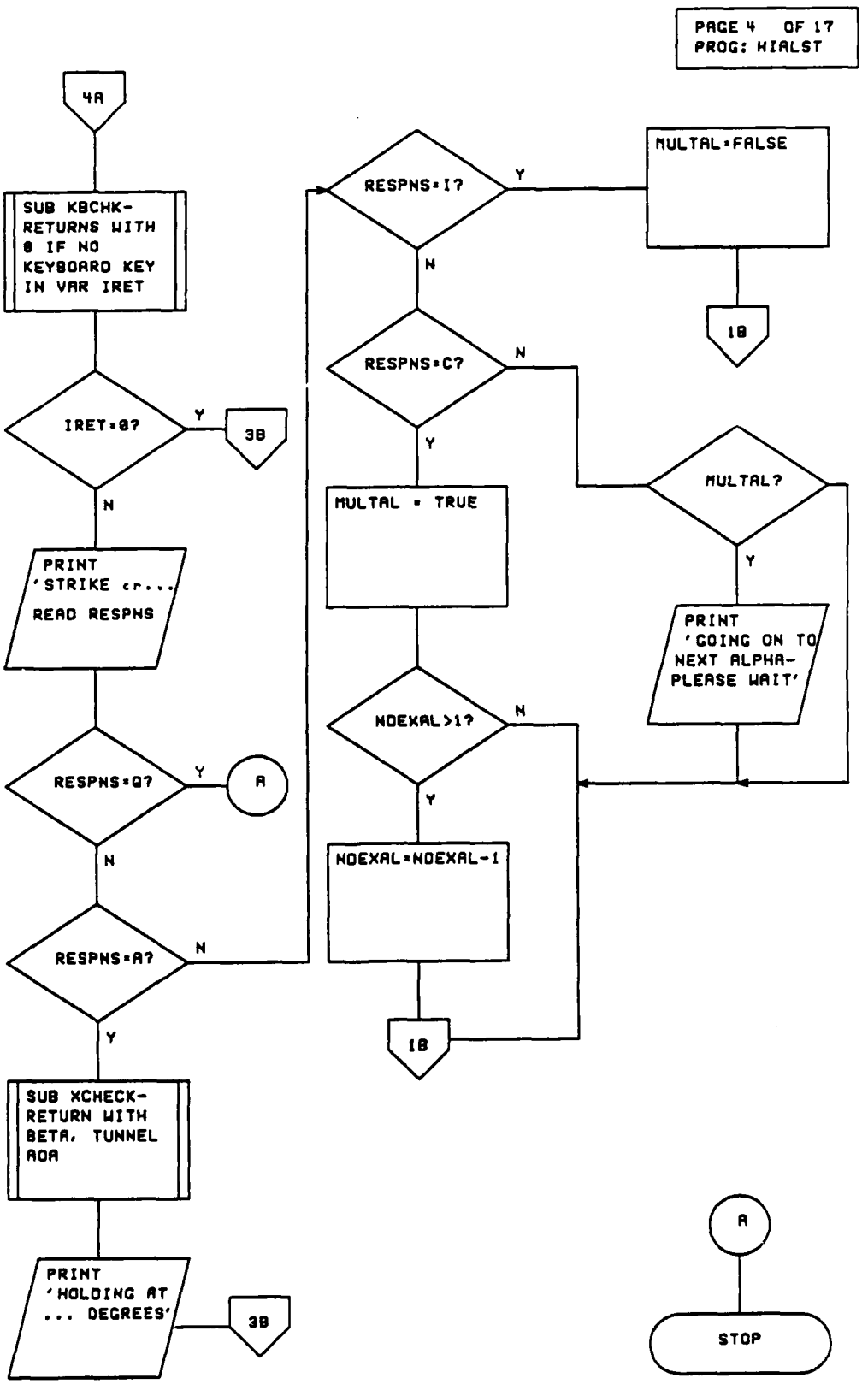
PAGE 4 OF 17
PROG: MIALST
4A
SUB KBCHK-
RETURNS WITH
0 IF NO
KEYBOARD KEY
IN VAR IRET
IRET=0?
Y
3B
N
PRINT
'STRIKE cr....
READ RESPNS
RESPNS=Q?
Y
A
N
RESPNS=A?
N
Y
SUB XCHECK-
RETURN WITH
BETA, TUNNEL
AOA
PRINT
'HOLDING AT
... DEGREES'
3B
RESPNS=I?
Y
MULTAL=FALSE
1B
N
RESPNS=C?
N
Y
MULTAL = TRUE
NOEXAL>1?
N
Y
NOEXAL=NOEXAL-1
1B
MULTAL?
Y
PRINT
'GOING ON TO
NEXT ALPHA-
PLEASE WAIT'
A
STOP

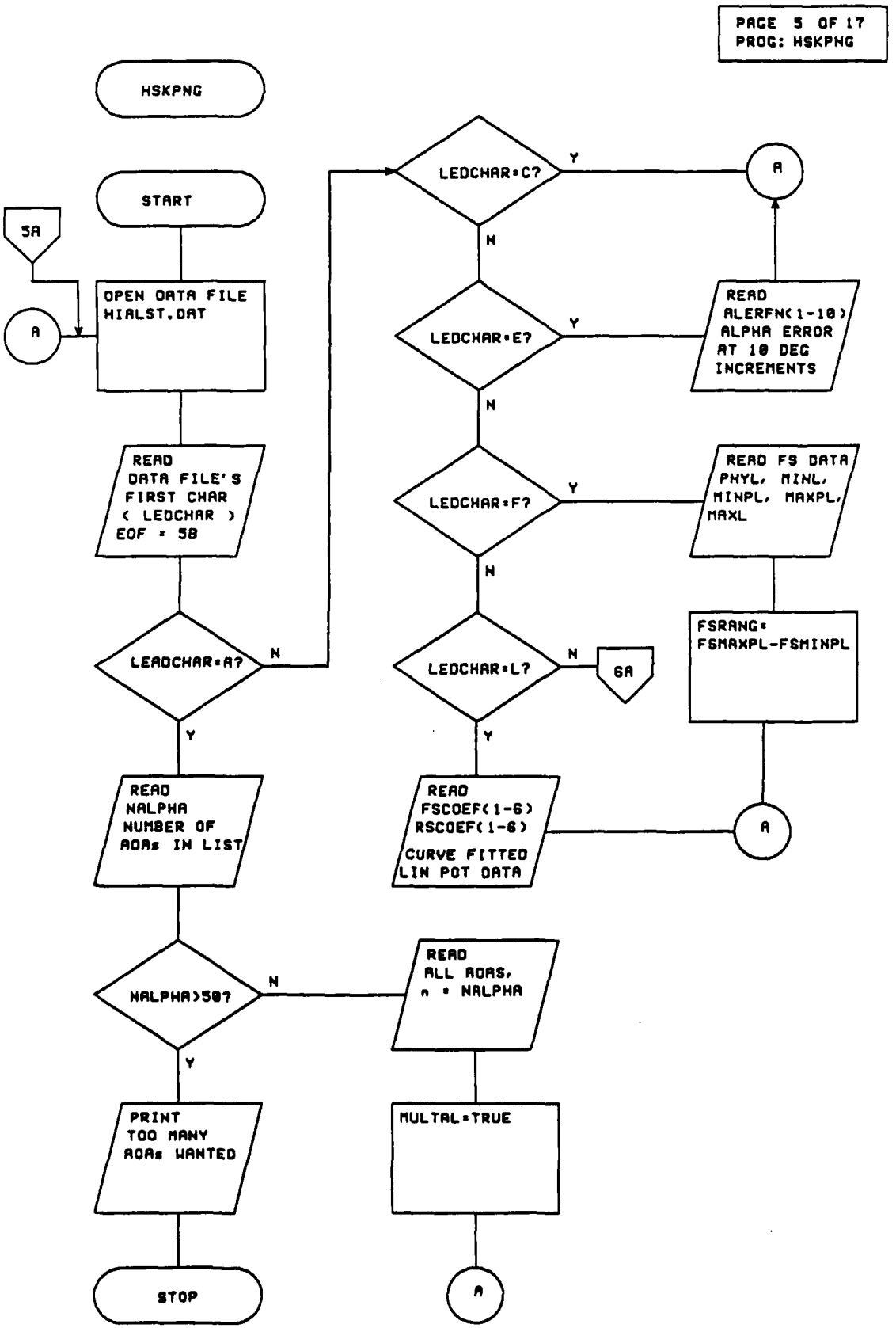
PAGE 5 OF 17
PROG: HSKPNG
HSKPNG
START
5A
A
OPEN DATA FILE
HIALST.DAT
READ
DATA FILE'S
FIRST CHAR
(LEDCHAR)
EOF = 58
LEADCHAR=A?
N
Y
READ
NALPHA
NUMBER OF
AOAs IN LIST
NALPHA>50?
N
Y
PRINT
TOO MANY
AOAs WANTED
STOP
LEDCHAR=C?
Y
A
N
LEDCHAR=E?
Y
READ
ALERFN(1-10)
ALPHA ERROR
AT 10 DEG
INCREMENTS
N
LEDCHAR=F?
Y
READ FS DATA
PHYL, MINL,
MINPL, MAXPL,
MAXL
N
LEDCHAR=L?
N
6A
Y
READ
FSCOEF(1-6)
RSCOEF(1-6)
CURVE FITTED
LIN POT DATA
FSRANG=
FSMAXPL-FSMINPL
A
READ
ALL AOAS,
n = NALPHA
MULTAL=TRUE
A

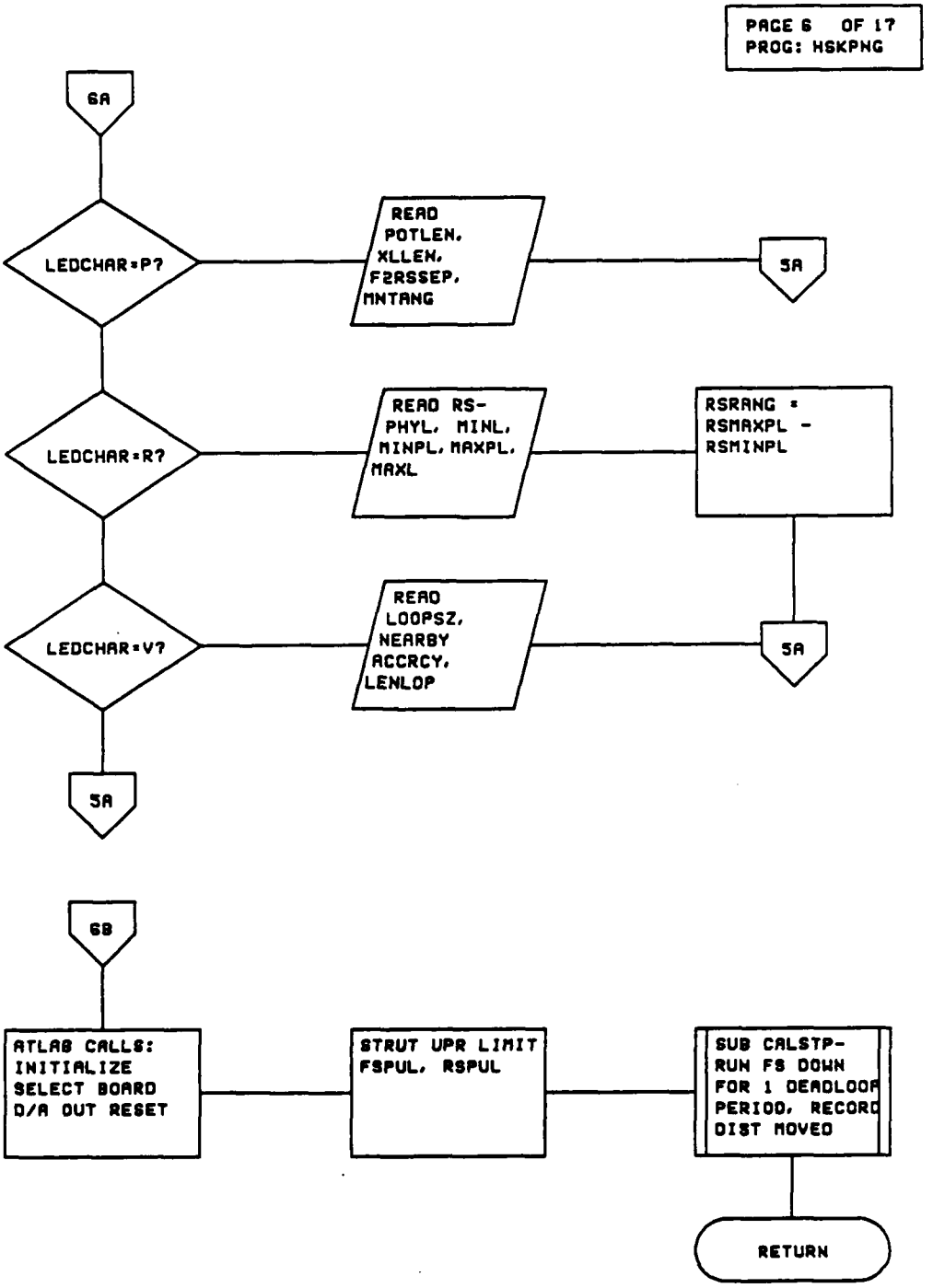
PAGE 6 OF 17
PROG: HSKPNG
6A
LEDCHAR=P?
READ POTLEN, XLLEN, F2RSSEP, MNTANG
5A
LEDCHAR=R?
READ RS-PHYL, MINL, MINPL, MAXPL, MAXL
RSRANG = RSMAXPL - RSMINPL
LEDCHAR=V?
READ LOOPSZ, NEARBY ACCRCY, LENLOP
5A
5A
6B
ATLAB CALLS: INITIALIZE SELECT BOARD D/A OUT RESET
STRUT UPR LIMIT FSPUL, RSPUL
SUB CALSTP-RUN FS DOWN FOR 1 DEADLOOP PERIOD, RECORD DIST MOVED
RETURN

PAGE 7 OF 17
PROG: TRGTL

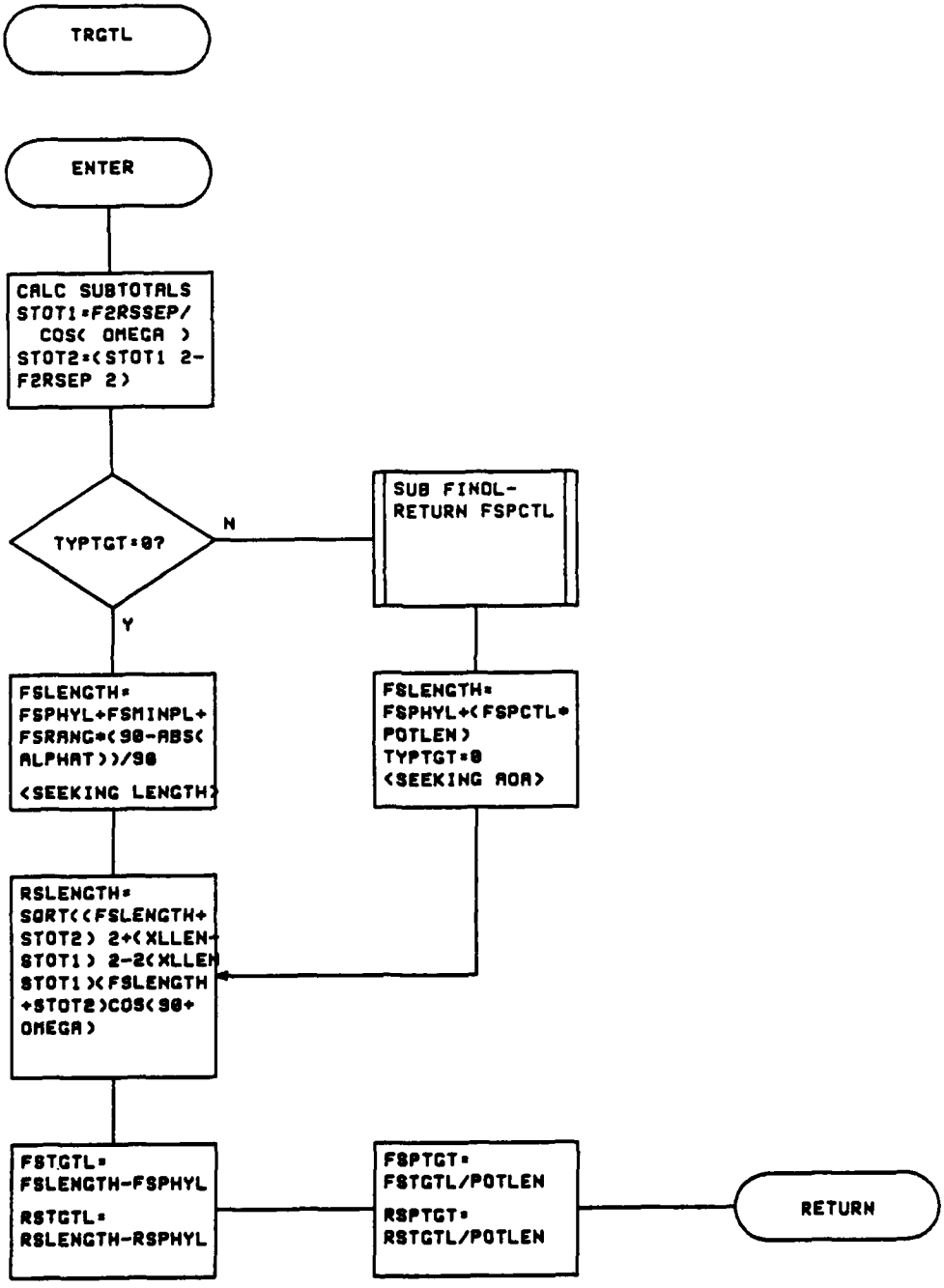

PAGE 0 OF 17
PROG: FINDL

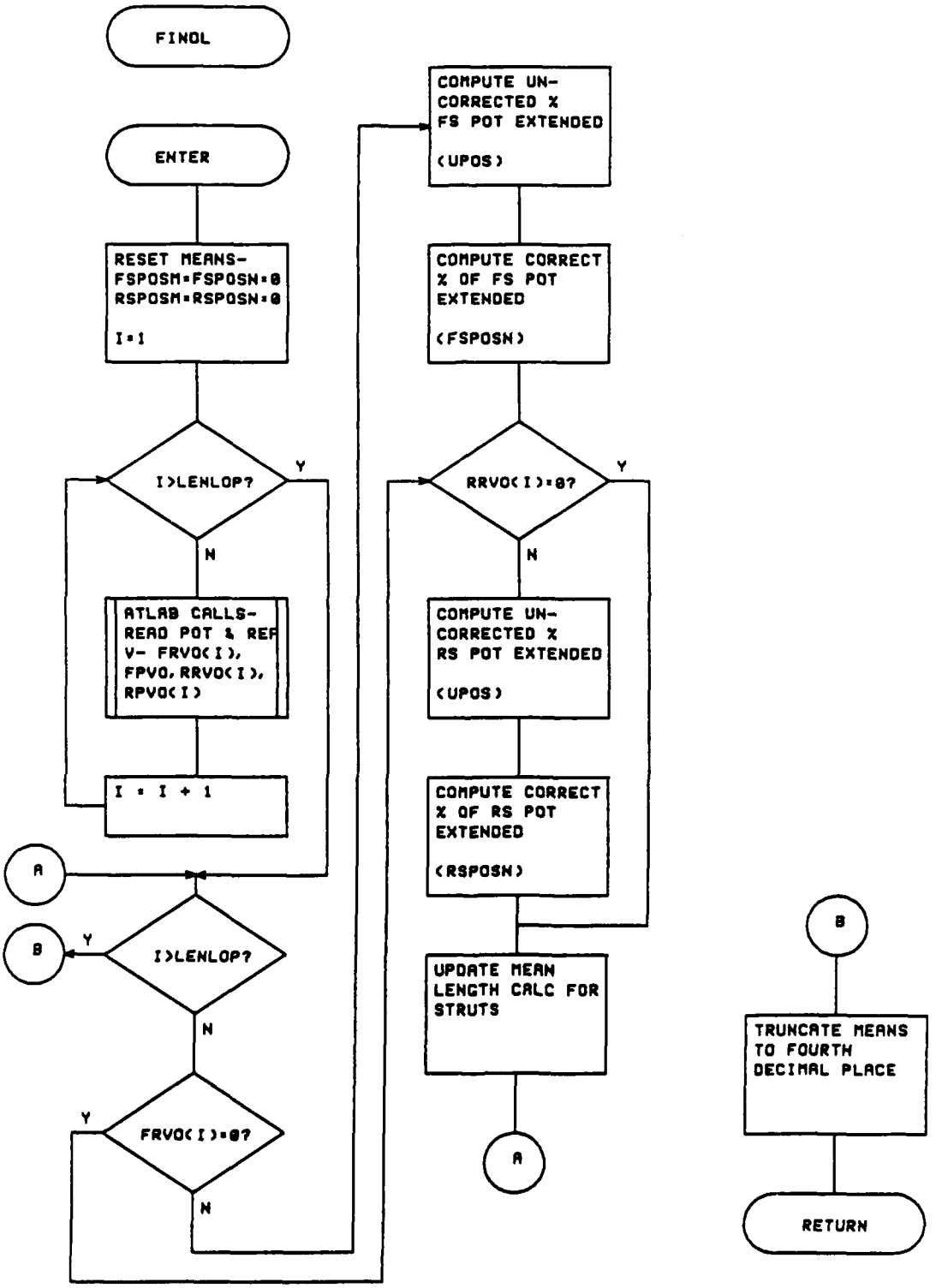

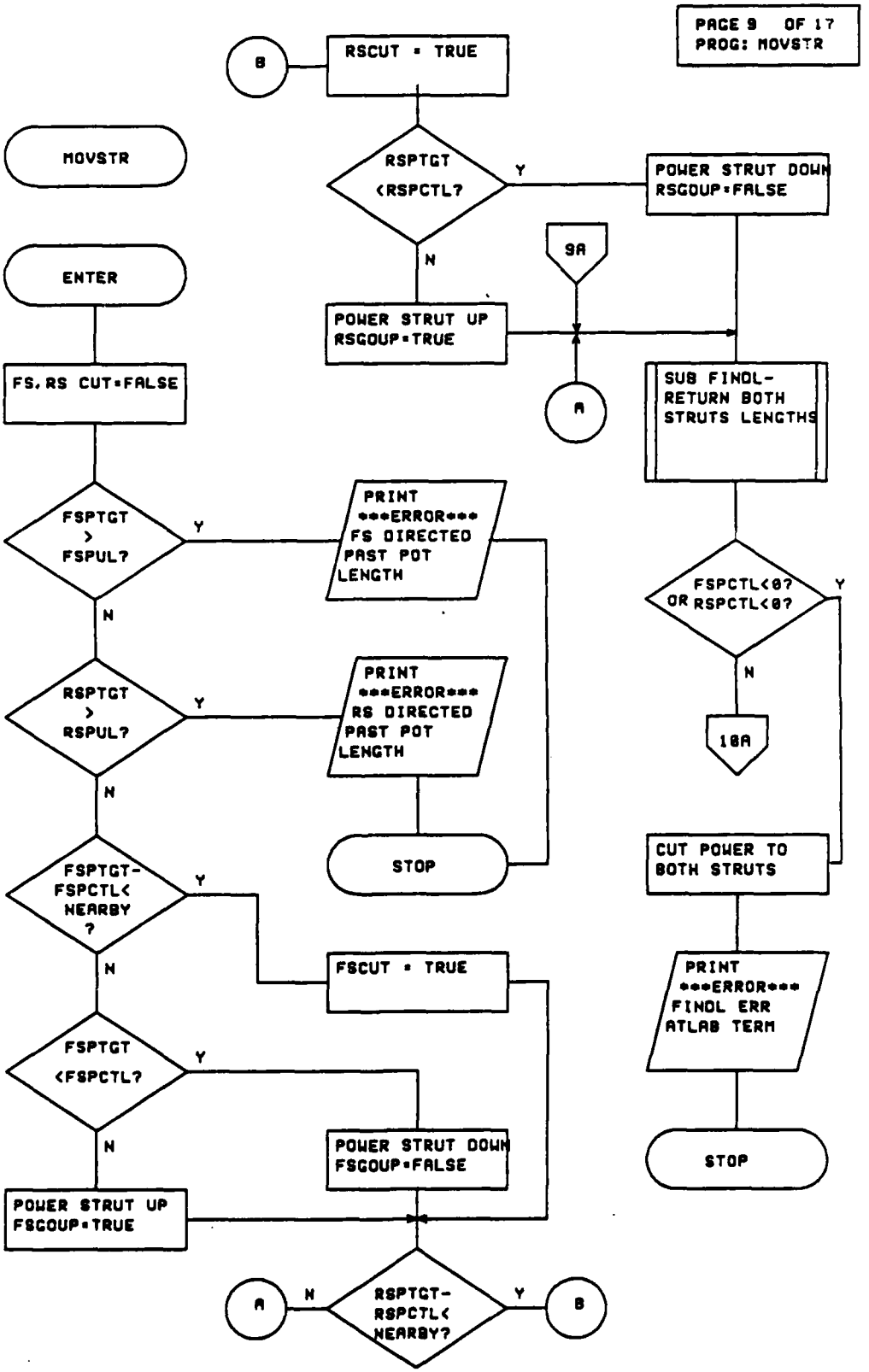
PAGE 9 OF 17
PROG: MOVSTR
MOVSTR
ENTER
FS,RS CUT=FALSE
FSPTGT > FSPUL?
Y
PRINT ***ERROR*** FS DIRECTED PAST POT LENGTH
N
RSPTGT > RSPUL?
Y
PRINT ***ERROR*** RS DIRECTED PAST POT LENGTH
N
STOP
FSPTGT-FSPCTL< NEARBY ?
Y
FSCUT = TRUE
N
FSPTGT <FSPCTL?
Y
POWER STRUT DOWN FSGOUP=FALSE
N
POWER STRUT UP FSGOUP=TRUE
B
RSCUT = TRUE
RSPTGT <RSPCTL?
Y
POWER STRUT DOWN RSGOUP=FALSE
N
POWER STRUT UP RSGOUP=TRUE
9A
A
SUB FINDL- RETURN BOTH STRUTS LENGTHS
FSPCTL<0? OR RSPCTL<0?
Y
N
10A
CUT POWER TO BOTH STRUTS
PRINT ***ERROR*** FINDL ERR ATLAB TERM
STOP
A
N
RSPTGT-RSPCTL< NEARBY?
Y
B

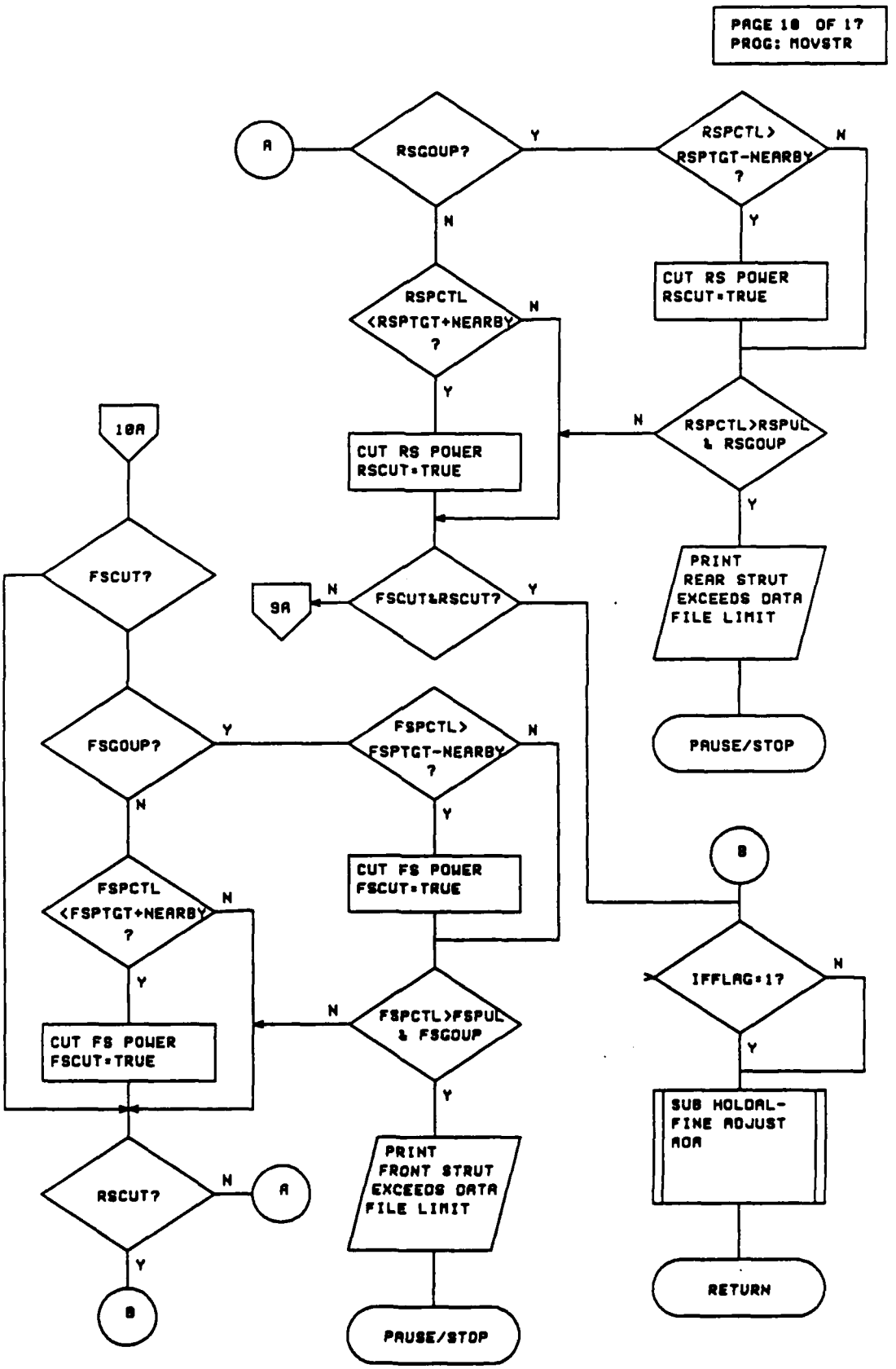
PAGE 10 OF 17
PROG: MOVSTR
A
RSGOUP?
Y
N
RSPCTL> RSPTGT-NEARBY ?
N
Y
CUT RS POWER RSCUT=TRUE
RSPCTL <RSPTGT+NEARBY ?
N
Y
CUT RS POWER RSCUT=TRUE
RSPCTL>RSPUL & RSGOUP
N
Y
PRINT REAR STRUT EXCEEDS DATA FILE LIMIT
PAUSE/STOP
10A
FSCUT?
9A
N
FSCUT&RSCUT?
Y
FSGOUP?
Y
FSPCTL> FSPTGT-NEARBY ?
N
Y
CUT FS POWER FSCUT=TRUE
FSPCTL <FSPTGT+NEARBY ?
N
Y
CUT FS POWER FSCUT=TRUE
FSPCTL>FSPUL & FSGOUP
N
Y
PRINT FRONT STRUT EXCEEDS DATA FILE LIMIT
PAUSE/STOP
B
IFFLAG=1?
N
Y
SUB HOLDAL- FINE ADJUST AOA
RETURN
RSCUT?
N
A
Y
B

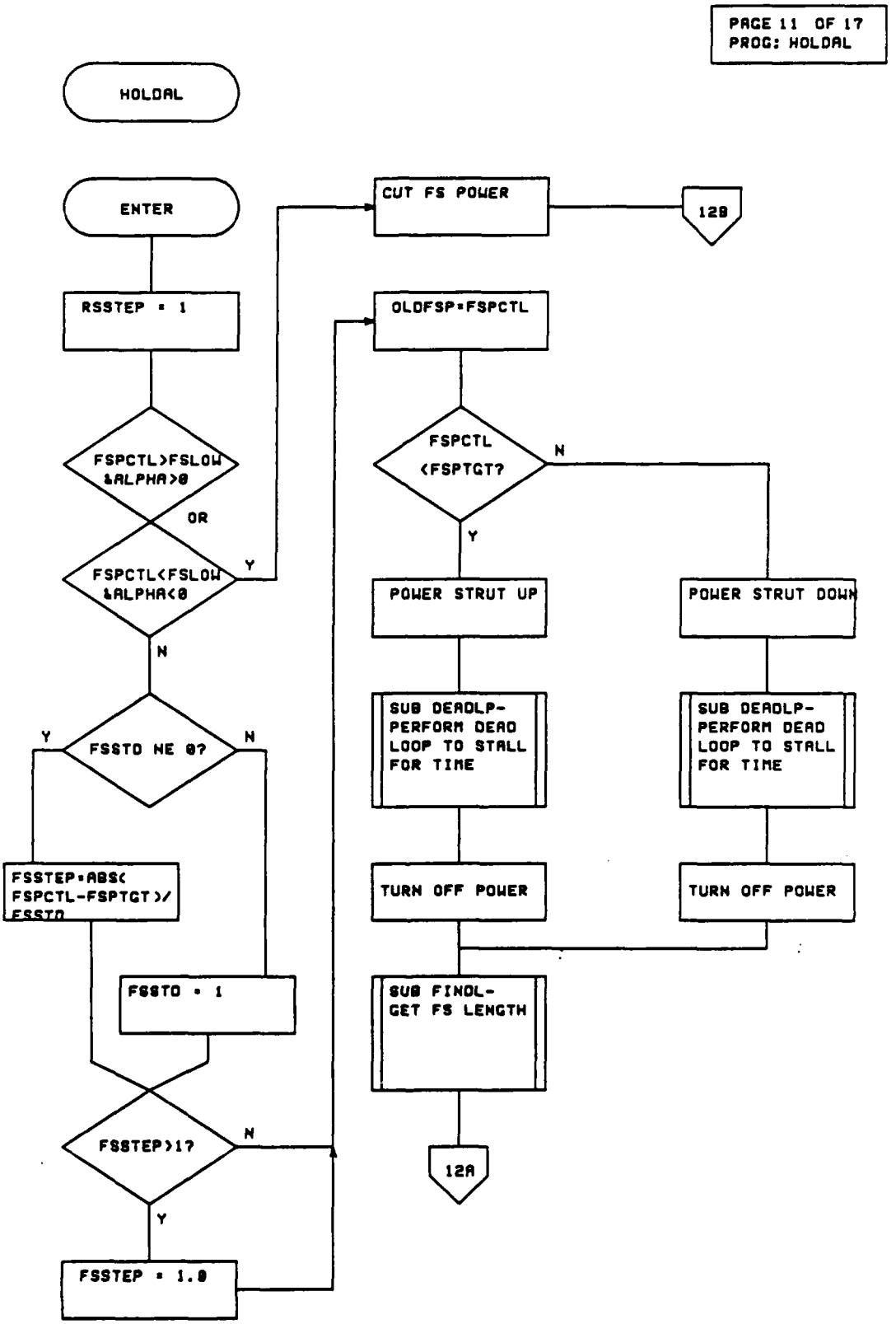
PAGE 11 OF 17
PROG: HOLDAL
HOLDAL
ENTER
RSSTEP = 1
FSPCTL>FSLOW &ALPHA>0
OR
FSPCTL<FSLOW &ALPHA<0
Y
N
FSSTO NE 0?
Y
N
FSSTEP=ABS(FSPCTL-FSPTGT)/ FSSTO
FSSTO = 1
FSSTEP>1?
N
Y
FSSTEP = 1.0
CUT FS POWER
12B
OLDFSP=FSPCTL
FSPCTL <FSPTGT?
N
Y
POWER STRUT UP
POWER STRUT DOWN
SUB DEADLP- PERFORM DEAD LOOP TO STALL FOR TIME
SUB DEADLP- PERFORM DEAD LOOP TO STALL FOR TIME
TURN OFF POWER
TURN OFF POWER
SUB FINDL- GET FS LENGTH
12A

PAGE 12 OF 17
PROG: HOLDAL

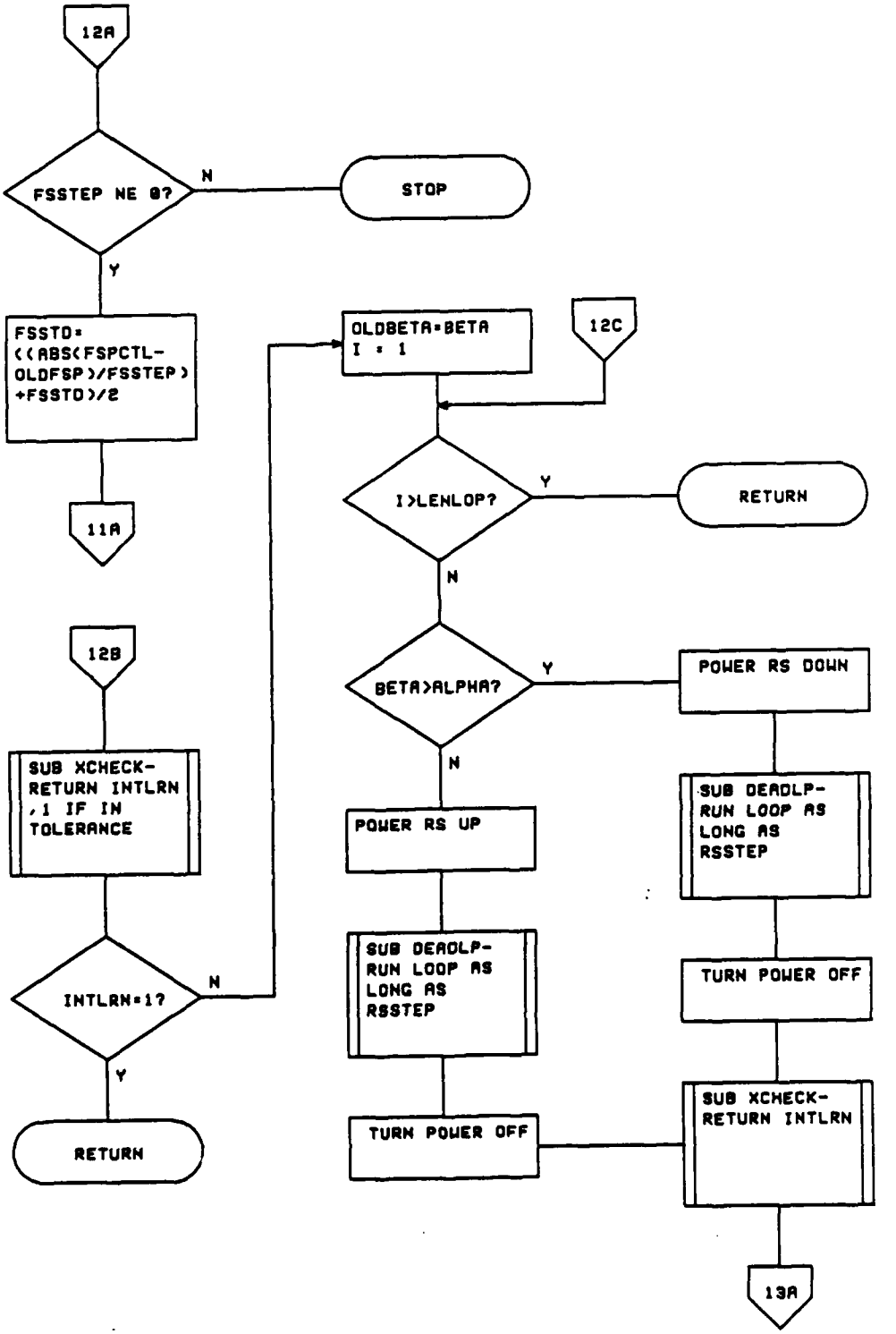

PAGE 13 OF 17
PROG: HOLDAL

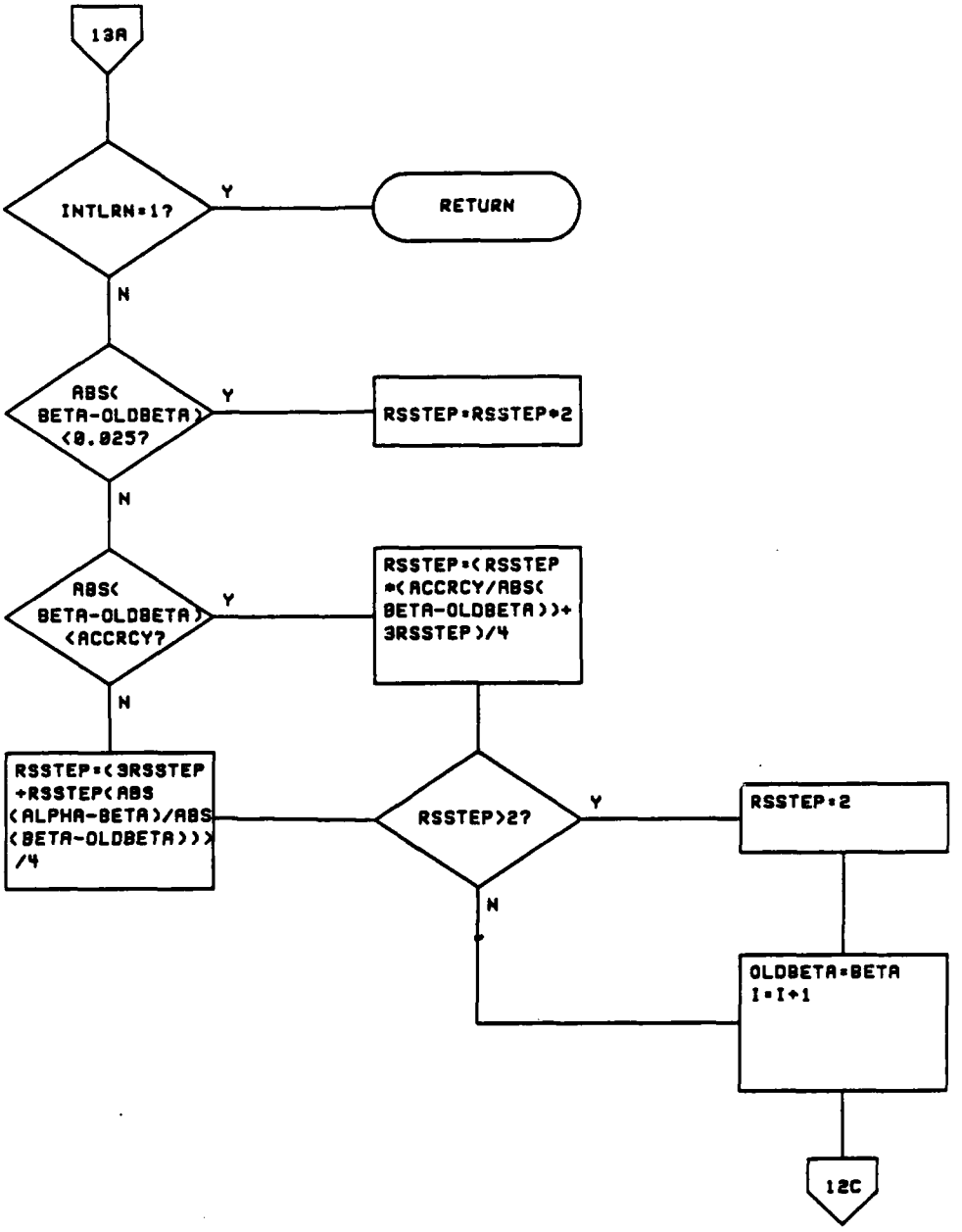

PAGE 14 OF 17
PROG: XCHECK

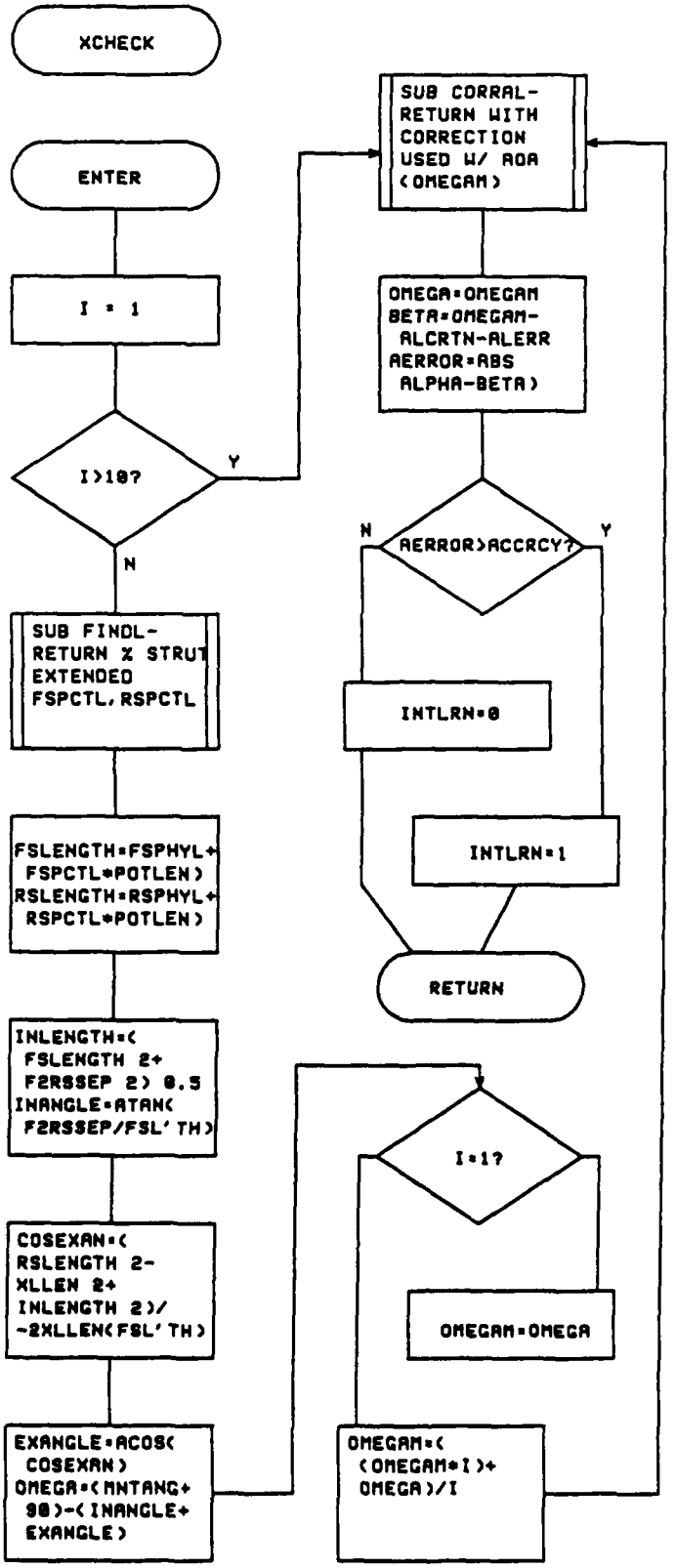

PAGE 15 OF 17
PROG: CALSTP

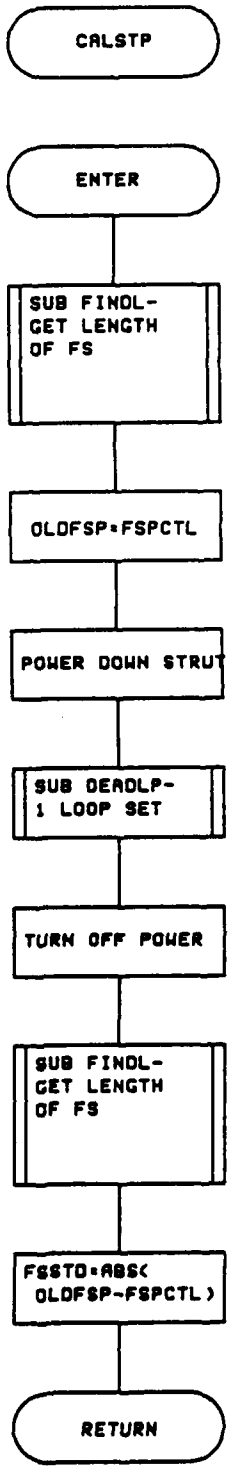

PAGE 16 OF 17
PROG: DEADLP

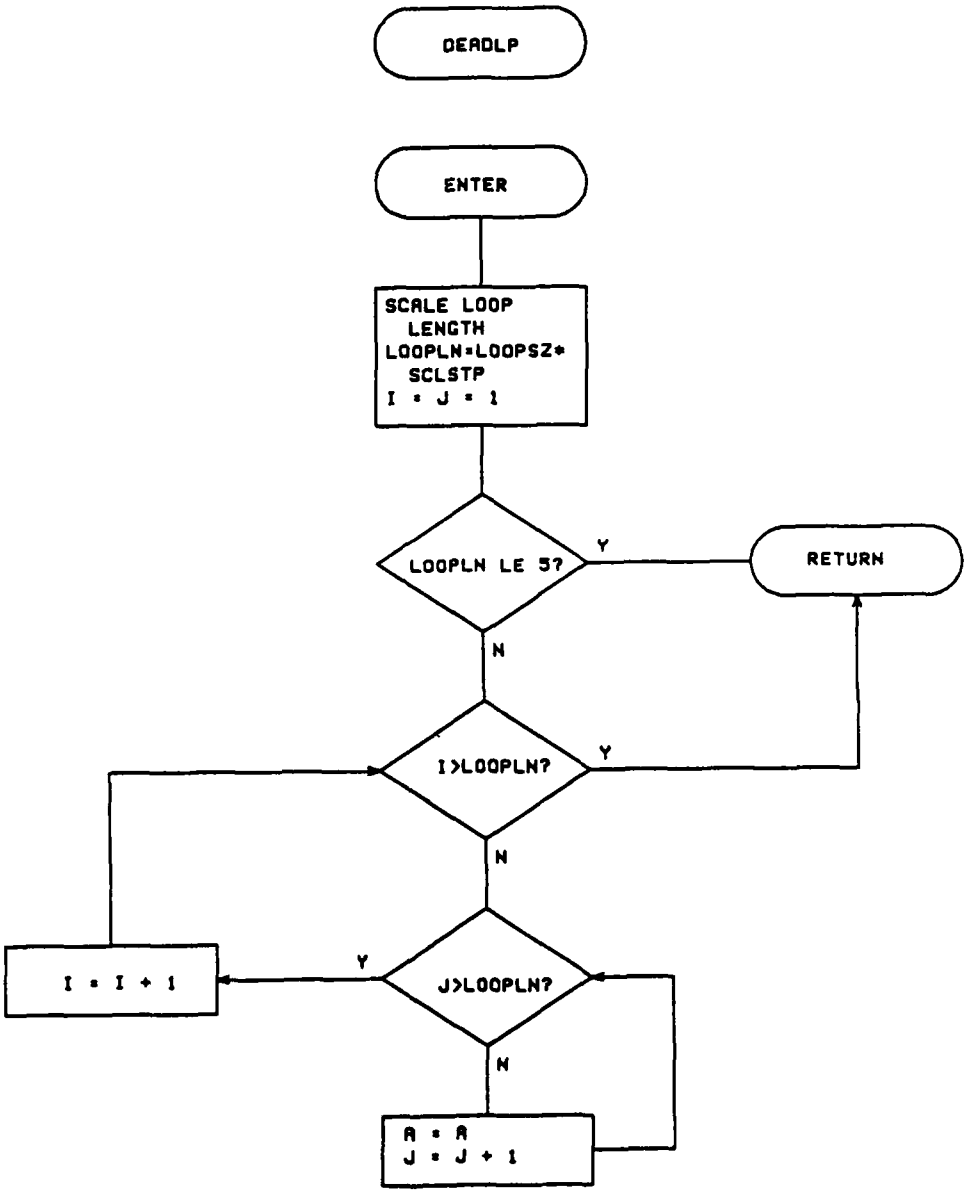

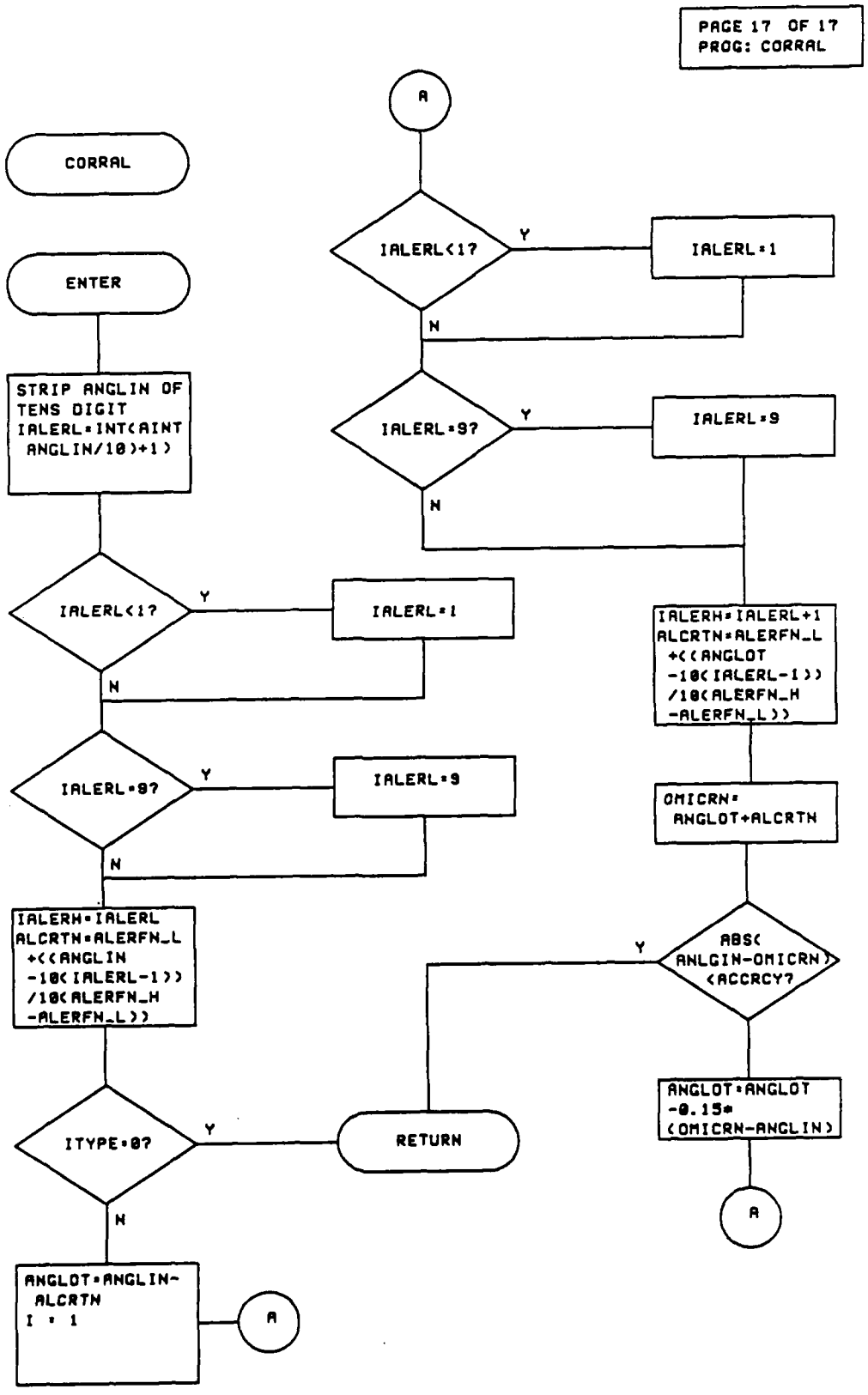
PAGE 17 OF 17
PROG: CORRAL
CORRAL
ENTER
STRIP ANGLIN OF TENS DIGIT IALERL=INT(AINT ANGLIN/10)+1)
IALERL<1?
Y
IALERL=1
N
IALERL=9?
Y
IALERL=9
N
IALERH=IALERL+1 ALCRTN=ALERFN_L +((ANGLOT -10(IALERL-1)) /10(ALERFN_H -ALERFN_L))
OMICRN= ANGLOT+ALCRTN
ABS(ANGLIN-OMICRN) <ACCRCY?
Y
ANGLOT=ANGLOT -0.15* (OMICRN-ANGLIN)
A
IALERL<1?
Y
IALERL=1
N
IALERL=9?
Y
IALERL=9
N
IALERH=IALERL ALCRTN=ALERFN_L +((ANGLIN -10(IALERL-1)) /10(ALERFN_H -ALERFN_L))
ITYPE=0?
Y
RETURN
N
ANGLOT=ANGLIN- ALCRTN
I = 1
A

APPENDIX H

HARS INSTALLATION PROCEDURES

TERMINOLOGY AND DEFINITIONS

RHS - right hand side - as looking upwind - side to back wall of tunnel

LHS - left hand side - as looking upwind - observation wall side of tunnel

FHSCS - flat head socket cap screw

SHCS - socket head cap screw

CS - cap screw

DIMENSIONS -

WASHERS : inside diameter × outside diameter (× thickness)

SCREWS : outside diameter - threads per inch(form/series- class of fit) note- dimensional information enclosed by parentheses is not typically used in this instruction set. Units are in inches

HARS INSTALLATION PROCEDURE

I. Prepare HARS Clearances and Calibrations

   A. Calibrate linear pots (refer to figure 1)

      1. Secure pot to bench top with 48 inches clearance to side for wiper bar extension
      2. Secure a tape measure atop the pot (duct tape, elastic, etc.)
      3. Fashion a pointer at some convenient point near the end of the pot
      4. Secure the tongue of the tape measure to the wiper bar by clamping the turn down edge between two 1/4 × 1 1/4 washers such that a unit of measure is aligned with the pointer when the wiper bar is fully seated

5. Attach the positive lead of a 10VDC filtered power supply to post 1 of the pot. Make sure the power supply is turned off and the power adjustment knob set to zero voltage
6. Attach the negative lead of the power supply to post 3 of the pot
7. Attach a digital voltmeter to the pot; ground to post 3
8. Turn on power supply and slowly turn up the voltage until the digital voltmeter reads a stable voltage as close to 10V as possible, record voltage
9. Move the positive lead of the voltmeter to post 2 of the pot, record voltage
10. Extend the wiper bar one inch at a time, recording the voltmeter reading until fully extended
11. Move the positive lead to post 1 of the pot, record voltage
12. If the voltage has varied from beginning the test linearly adjust the reference voltage for each inch of extension
13. Calculate the difference between percentage of reference voltage at each unit of extension and the percent of total extendible pot length at the point
14. Plot the difference in percentage of reference voltage *versus* percentage total pot length extended
15. Determine the coefficients of a sixth order polynomial curve fit of the curve values
16. Enter coefficients into the software data file, HIALST.DAT

B. Adjust wear pads

1. Front strut
    a. Lightly seat strut extension in fully retracted position
    b. Loosen **ALL** jam nuts and **ALL** retaining bolts at least two threads

c. Starting at the top, tighten all adjusting set screws to 15 inch-pounds. Be sure that the jam nut or retaining screw does not contact the casing and throw off the contact pressure. Adjust all four upper pads in this manner

d. Back each set screw off 1/2 turn and lock into position using the jam nut on all four upper pads

e. Tighten each retaining screw to 15 inch-pounds in the upper pads

f. Repeat the procedure for each succeeding set of pads until all pads have been adjusted

2. Rear strut

a. Lightly seat strut extension in fully retracted position

b. Loosen **ALL** jam nuts and **ALL** retaining SHCSs at least one thread

c. Starting at the top, gently tighten all adjusting set screws. Be sure that the jam nut or retaining screw does not contact the casing and throw off the contact pressure. Adjust all four upper pads in this manner

d. Back each set screw off 1/2 turn and lock into position using the jam nut on all four upper pads

e. Gently tighten each retaining screw in the upper pads

f. Repeat the procedure for each succeeding set of pads until all pads have been adjusted

C. Lubricate grease fittings (28 total)

1. Each pair under each front strut pad
2. In each casing cap
3. Idler gear shaft

D. Set electric motor to idler clearance

1. Secure the electric motors to the sliding motor mounts with 5/16-18 SHCSs using a 1/4 allen wrench

2. Secure the selected drive gear to the shaft of the electric motor
3. Secure the selected idler gear to the idler shaft
4. Making sure the adjustment screw jam nuts are free along the screw thread, push the motor mount into the transmission carrier plate until the teeth of the two gears are fully seated against each other
5. Using a 1/4 allen, wrench finger tighten the two SHCSs that serve as the motor mount adjusting screws
6. Alternating between screws, back each screw out a 1/4 turn while pulling outward on the sliding mount until there is approximately 0.030 inch clearance between the two gears
7. Using the allen wrench to insure the adjusting screw does not turn, tighten the jam nut against the motor mount
8. Using the allen wrench to insure the adjusting screw does not turn, tighten the jam nut against the transmission carrier plate

E. Adjust microswitch position

1. Secure microswitches to their proper positions on the strut casings
2. Starting from the outer most position, slowly close the clearance between the switch and the strut extension until there is an audible click from the switch closing. push the switch 1/32 of an inch closer and secure
3. Repeat for each switch

II. Install Mounting Platform/Upper Stabilizing Bar Mount

A. Attach base mount supports to mounting plate using 1/2-20 FHSCSs with a 3/16 allen wrench (eight required per tube)

B. Attach stabilizing bar to upper mount using two 7/16-20 bolts

C. Install mounting plate

1. 30 Degree mount angle

a. Position upper and lower turntables codirectional and longitudinally to the tunnel, pitch arm trunnion downwind

b. Lower mounting plate into turntable slot

c. Center mounting platform

d. Tighten balance clamps

e. Unlock upper and lower turntables from each other and rotate upper turntable 90°, balance clamp track upwind, pitch arm slot toward control room

f. Lock upper and lower turntables together

g. Attach upper stabilizing bar mount to end of mount extension bar that has been drilled with only four holes using four 1/2-20 bolts and nuts

h. Position the mount extension bar in the upper turntable slot with the bar dangling down forward of the large square turntable brace and the other end's six holes aligning with the six corresponding holes in the mounting plate. Attach the mount extension bar to the mounting plate with two short 1/2-20 bolts through the center hole on either side, insuring the other four holes are aligned

2. 0 Degree mount angle

a. Position upper and lower turntables 90 degrees to each other with the upper turntable slot longitudinal to the tunnel, the pitch screw upwind

b. Attach the upper stabilizing bar mount to the mounting plate using four 1/2-20 bolts and nuts, the bar mounting away from the end of the mounting plate that has four extra holes drilled and tapped into it

c. Lower mounting plate into turntable slot

d. Position the center of the mounting plate 11 inches aft of the center of the balance clamp track, the rear edge of the mounting plate should be approximately 12.5 inches forward of the rear edge of the track

e. Tighten the balance clamps

f. Lock the upper and lower turntables together

III. Main Strut Installation

A. Attach adapter to strut using six (6) 1/2-20 nuts and flat washers

1. 30 Degree mount angle - insure the mating surface to the mounting plate is facing up

2. 0 Degree mount angle - insure the mating surface to the mounting plate is facing down

B. Attach peripheral hardware

1. Wire guide

a. Attach aluminum wiring guide retaining clamp to strut extension using three (3) 1/4-28 SHCSs with a 3/16 Allen wrench

b. Attach plastic wiring guide locating collar to strut casing using two (2) 1/4-28 SHCSs with a 3/16 Allen wrench

c. Insert wiring guide through retaining clamp and locating collar leaving 10 - 12 inches of guide above the clamp

d. Lock guide in place by tightening 1/4-28 SHCS with a 3/16 Allen wrench

2. Linear potentiometer

a. Use only the linear pot with the plastic sleeve snapped over wiper rod

b. Attach 'L' brackets to RHS rear corner of casing using 12-32 phillips pan head screws, do not fully tighten

c. Attach linear pot as low as mounting slots will allow using four (4) 10-32 phillips pan head screws

d. Tighten 'L' bracket to casing phillips screws

e. Duct tape pot rod in seated position to prevent damage during installation

C. Install main strut

1. 30 Degree mount angle

a. Manually retract main strut extension to with in a foot of the fully retracted position

b. Place a person in the cradle (PIC) of the pyramidal balance to help position and stabilize the strut during installation

c. Use the hoist to slowly lower the strut between the mounting plate and the turntable's pitch arm. The PIC will need to provide the leverage necessary to tilt the strut such that the adapter can sink past the mounting plate and move forward to align the mounting studs of the adapter align with the holes in the mounting plate. A rope, lowered through the same hole which the stabilizer bar passes, should be looped around the exposed end of the front struts drive screw shaft, and pulled to assist the PIC

d. Maintaining the strut at the proper mounting angle, raise the strut until the studs protrude through the mounting plate and the mount extension bar

e. Secure the strut using 1/2-20 hex nuts and plain washers

2. 0 Degree mount angle

a. Manually extend main strut extension to within a foot of the fully extended position

b. Use the hoist to slowly lower the strut behind the mounting plate aligning the mounting holes of the adapter with the threaded holes in the mounting plate.

c. Secure the strut using 1/2-20 CSs

IV. Rear Strut Installation

A. Attach linear potentiometer

1. Attach linear pot as low as mounting slots will allow using four (4) 10-32 phillips pan head screws
2. Duct tape pot extension rod in seated position to prevent damage during installation

B. Install rear strut

1. Manually extend rear strut extension to within a foot of the fully extended position
2. Manually lower the strut behind the main strut while a person below insures the rear strut goes into the rear strut support collar
3. Install the rear keeper plate using two (2) 5/16-24 FHSCSs using a 3/16 allen wrench
4. Tighten the four (4) collar lock screws using a 1/2 wrench or socket
5. Support rear strut to keep from damaging linear pot until transverse link is installed

V. Transverse Link Installation

A. Lower transverse link into fork of main strut, aligning pivot holes of fork and brass bushings of the link

B. Insert large pivot pin from control room side of strut; fully seat pin

C. Support rear strut and lower link over the strut to align the pivot holes of the link and rear strut

D. Insert small pivot pin from control room side of strut; fully seat pin

E. Retain large pivot pin using plain washer and 3/4-10 self-locking nut with 1 1/8 wrench

F. Retain small pivot pin using plain washer and 9/16-18 self-locking nut with 13/16 wrench

VI. Motor Installation

A. Main strut

1. Secure transmission mount to strut casing - motor on the RHS of the struts - using 5/16-24 x 2 HHCSs with a 3/16 allen wrench
2. In order, install over strut screw shaft: lubricated face nylon washer, two steel spacer washers, spur gear
3. With weight compressing the main strut from above, raise the gear to remove any clearance and tighten set screw using a 5/64 allen wrench note: be sure the 1/8 key is in the shaft
4. Noting which side goes up by the engraved note on the lower surface, install the shaft end retaining collar
5. Install roll pin, leaving about 1/4 inch protruding
6. Measure gap between gear and collar. Any gap larger than 0.01 inch should be eliminated by spacer-washer or shim stock. Remove and replace collar as required
7. Tighten set screw in collar using 5/32 allen wrench

B. Rear strut

1. Attach transmission adapter plates to the strut casing using 5/16-24 x 2 FHSCSs with a 3/16 allen wrench, not tightening the screws
2. Secure transmission mount to strut casing - motor on the opposite side of the struts than the main strut motor - using 5/16-24 x 2 SHCSs with a 3/16 allen wrench
3. Tighten adapter plate screws
4. Follow steps 2 - 7 of main strut motor installation

VII. Electronics Installation

A. Microswitches

1. Mount terminal strips on top of mount extension bar

2. Slip slotted microswitch mounting brackets over mounting screws that are in place on strut casings
3. Tighten screws with appropriate driver
4. Route wiring to RHS of struts and attach to proper locations of terminal strip - refer to wiring guide, page 4, for details

B. Amplifiers

1. Attach amplifier feed wiring to terminal strip
2. Route the wiring down along the main strut to the balance cradle
3. Tape the foam amplifier cushion to the top of one of the pyramidal balances I-beam resolving arms
4. Refer to pages 1 and 5 of wiring guide for amplifier wiring details
5. Set the amplifiers atop the cushion. Plug in the amplifier feed wiring bundle
6. Attach power cables to the amplifiers - refer to wiring guide, page 5.
7. Attach positive motor power lead to post 1 of electric motor
8. Attach negative motor power lead to post 2 of the electric motor

C. Power Supply

1. Attach positive amplifier power supply leads to solenoid switch's #1 heavy duty posts. Refer to page 6 of wiring guide for details in this section
2. Attach amplifier power supply ground leads to the 28VDC power supply
3. Attach leads to positive side of 28VDC power supply
4. Attach 28VDC power supply leads to solenoid's #2 heavy duty posts as shown

5. Attach the 'panic button' harness to the solenoid switch. Red wire to post X1, black wire to post X2
6. Route 'panic button' harness to operators console
7. Attach harness red wire to push on/off 'panic button'
8. Attach harness black wire to negative post of 25VDC power supply
9. Attach free lead from on/off switch to the positive post of 25VDC power supply

D. Linear Pots

1. Attach color coded 'Y' harness to pots (6-pin connectors) - refer to page 3 of wiring diagram for connector wiring details
2. Attach linear pot feed harness to 'Y' harness' 16-pin connector
3. Route linear pot feed harness to operators console
4. Attach linear pot feed harness to A/D board and 10VDC power supply as detailed in page 2 of wiring guide

E. A/D Board

1. Attach strut motor feed to D/A ports - refer to page 2 of wiring guide
2. Route wiring to terminal strips secured to mount extension bar
3. Attach strut motor feed harness to terminal strips - refer to page 4 of wiring guide for details

VIII. System Startup

A. Power up

1. Make sure the 'panic' switch is off (open connection)
2. Turn on 25VDC power supply
3. Turn on 28VDC power supply
4. Turn on 10VDC power supply, wait 5 minutes before proceeding to allow voltage drop across linear pots to stabilize
5. Turn on computer

B. Operational calibration

1. Change directory to \ **ATLAB**
2. Make sure **HIALST.DAT** has zeros for entries in table of AOA corrections
3. Make sure data file properly defines strut extension positions for the installed configuration
4. Turn panic switch on (close connection)
5. While observing struts for movement, start program **HIALST**
6. **STOP!** The front strut should have moved down and the rear strut remained stationary for normal operation. If this is not the case, an electrical connection is crossed. Terminate the program. Double check connections at A/D board D/A ports, at terminal strips, amplifier power feed, and motor connections
7. Reply to "calibrate sting?" with a no
8. Enter 0 for AOA correction
9. Direct HARS to 0, 30, 45, 0, in turn **NOTE:** If the struts do not appear to be moving to the proper position, it may be caused by the connections to the linear pots being reversed. STOP!, if needed to reverse connections.
10. Record the AOA HARS states it is at, and measure of the true AOA of the transverse link for each AOA from 0 to 90° in 10° increments. Repeat test, in reverse, to 0° AOA
11. Repeat previous step
12. Compute mean error at each 10° increment
13. Terminate program **HIALST**
14. Reset A/D board by running program **ATLRST**
15. Enter error information into data file

C. Operation Check

1. Start program **HIALST**
2. Reply to "calibrate sting?" with a yes

3. Measure AOA of transverse link
4. Enter AOA error at request
5. Run HARS to 15° AOA
6. Run HARS to 0° AOA
7. Check AOA of transverse link, if error is present and doubled, the AOA error correction entered was of wrong sign. Terminate operation and restart operation check step 1

D. Operational Notes

1. The pots have been observed to change calibration if a large temperature variation from the time of operational calibration occurs. If the temperature varies by more than 10°F, double check the AOA offset at zero alpha
2. Problems of struts stopping movement prematurely have been traced to microswitch failure or misalignment.

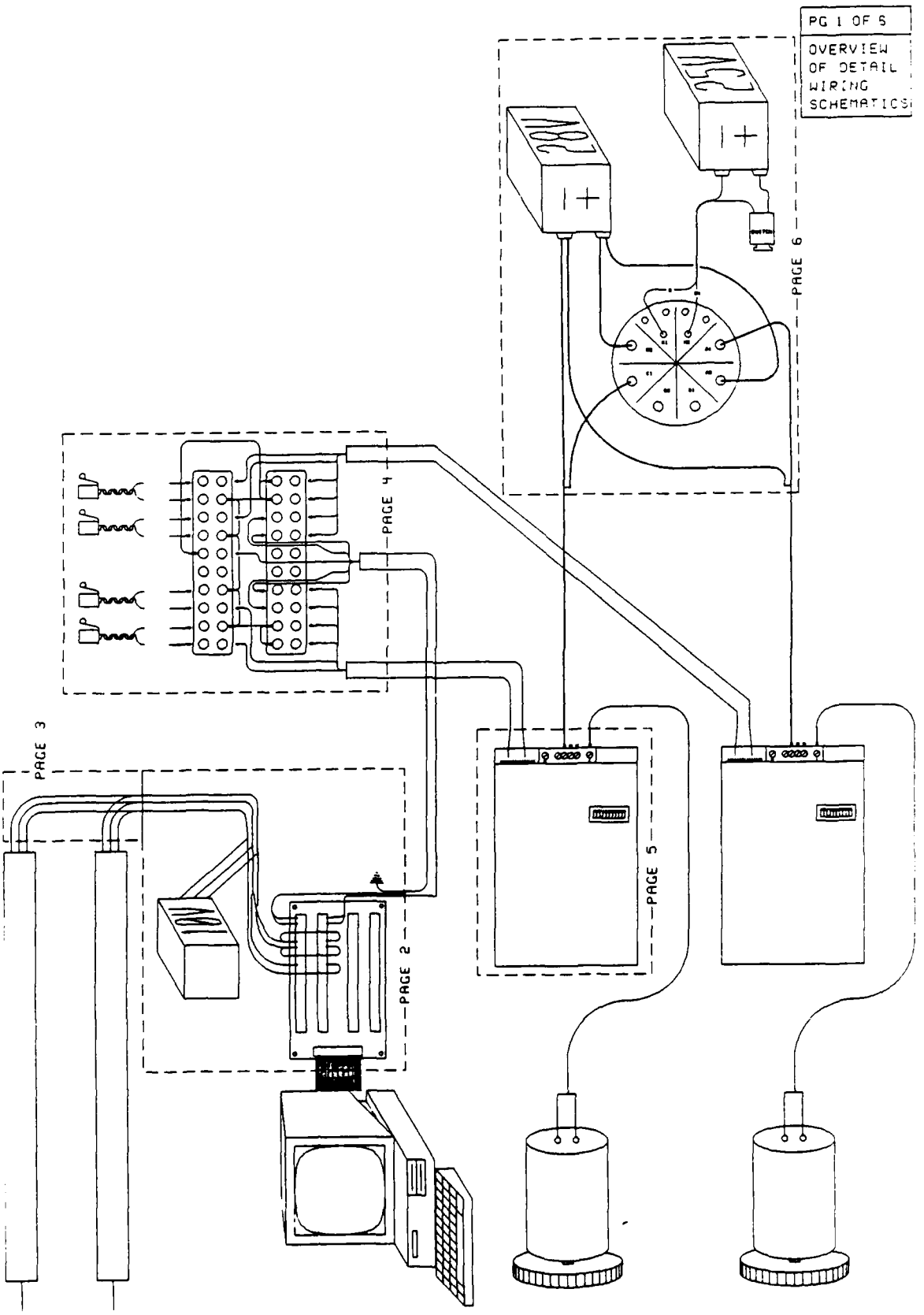
PG 1 OF 5
OVERVIEW
OF DETAIL
WIRING
SCHEMATICS
PAGE 6
PAGE 4
PAGE 3
PAGE 5
PAGE 2

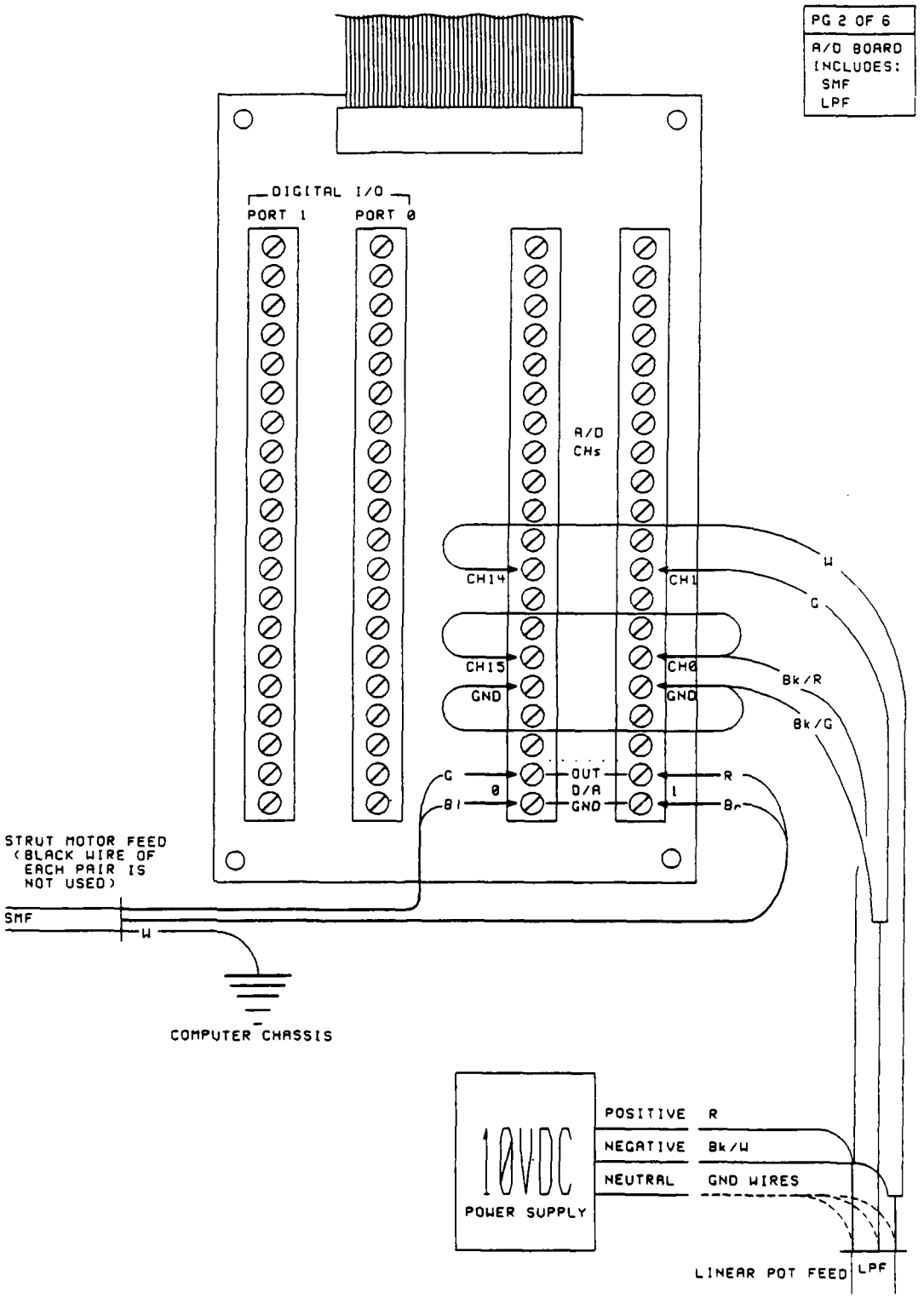
PG 2 OF 6
A/D BOARD
INCLUDES:
SMF
LPF
DIGITAL I/O
PORT 1
PORT 0
A/D
CHs
CH14
CH1
CH15
CH0
GND
GND
OUT
D/A
GND
STRUT MOTOR FEED
(BLACK WIRE OF
EACH PAIR IS
NOT USED)
SMF
COMPUTER CHASSIS
10VDC
POWER SUPPLY
POSITIVE
NEGATIVE
NEUTRAL
R
Bk/W
GND WIRES
LINEAR POT FEED
LPF
W
G
Bk/R
Bk/G

PG 3 OF 6

LIN' R POTS
INCLUDES
LPF

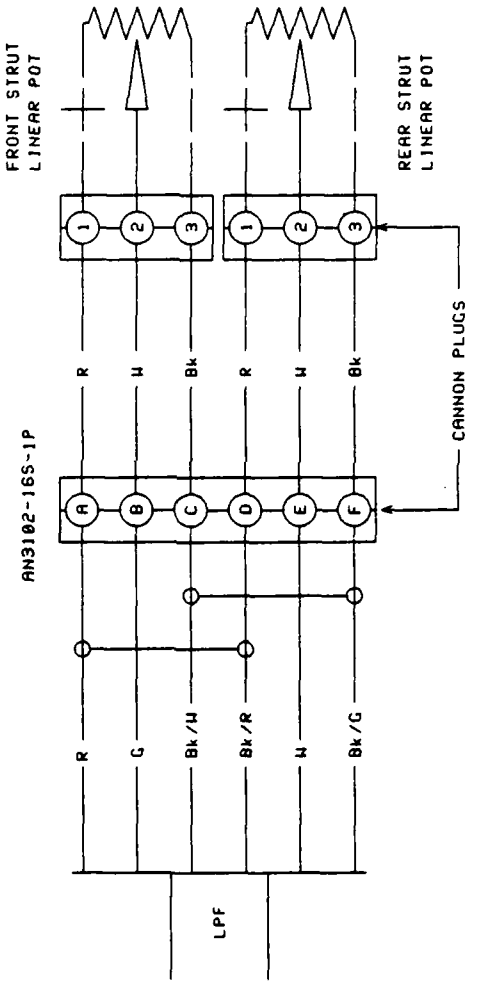

PG 4 OF 6

MICRO SWs
INCLUDES
AF
SMF

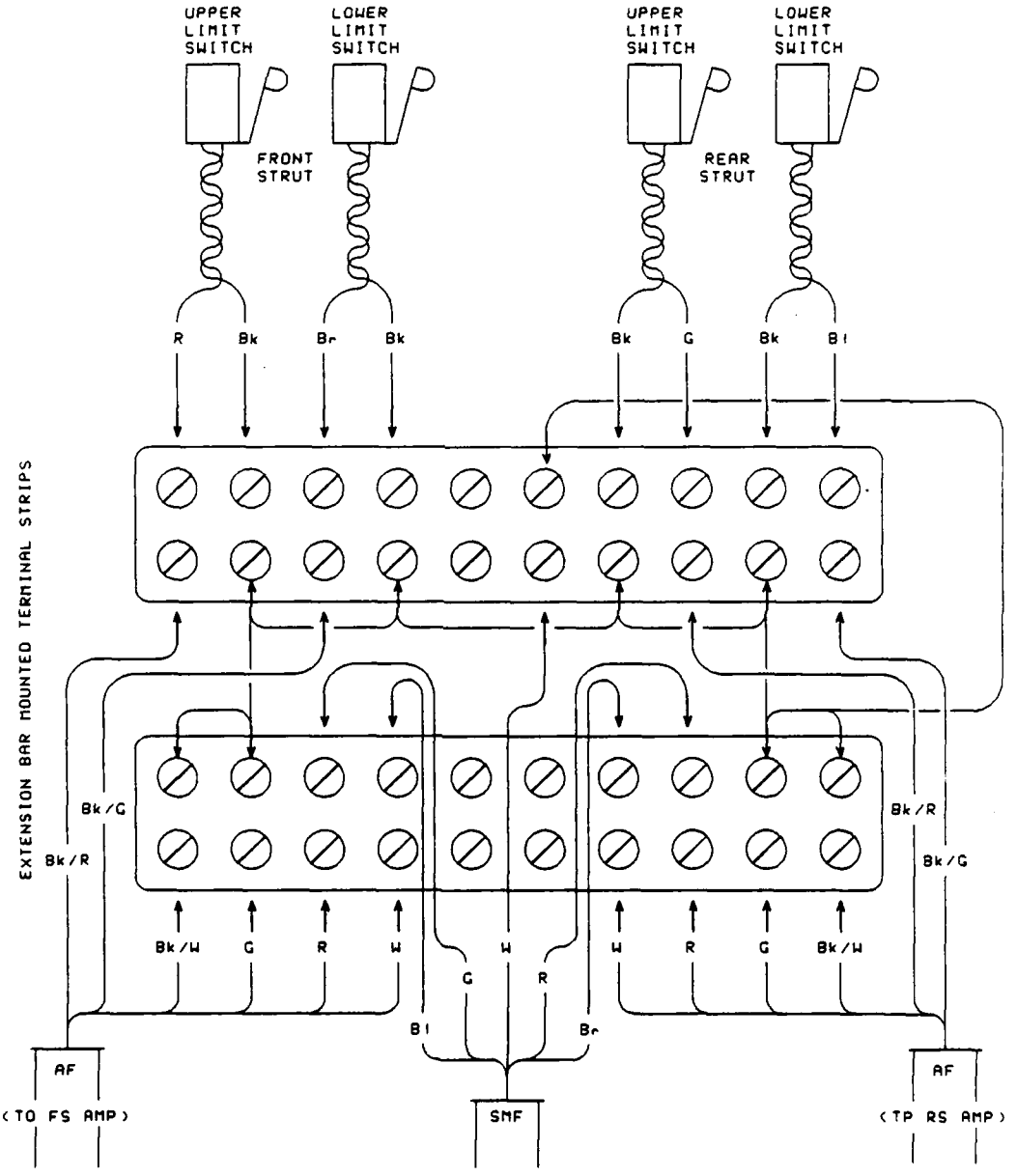

PG 5 OF 6

AMPLIFIERS
INCLUDES
AF
APS

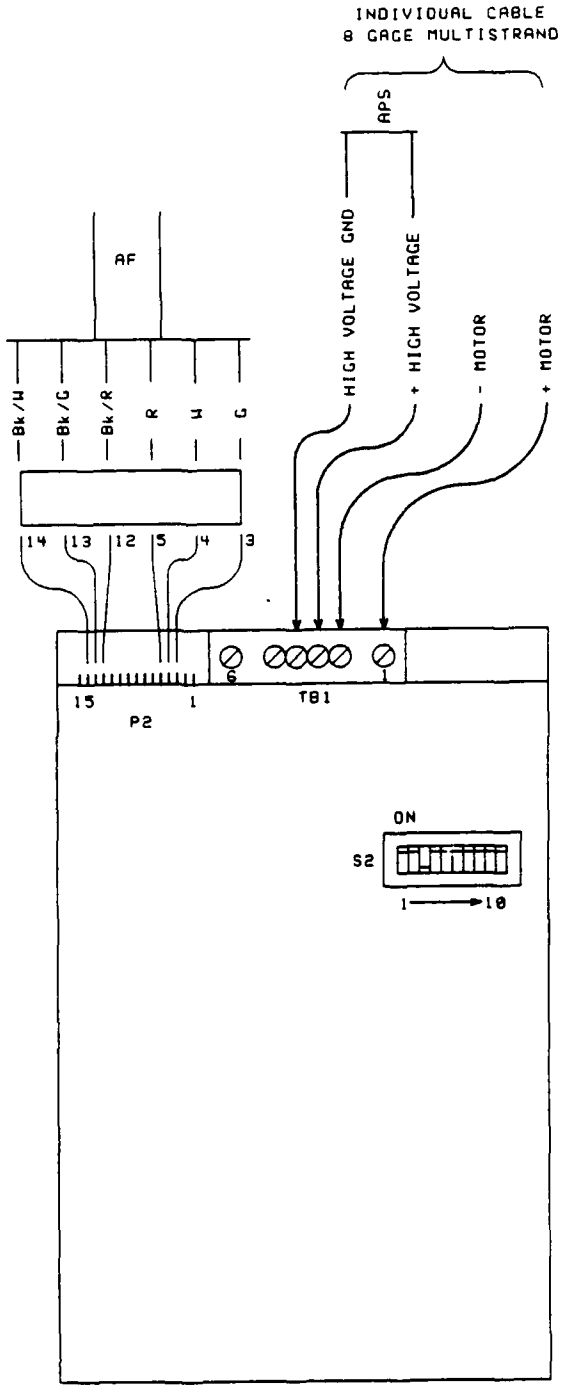

PG 6 OF 6

PANIC SW INCLUDES APS

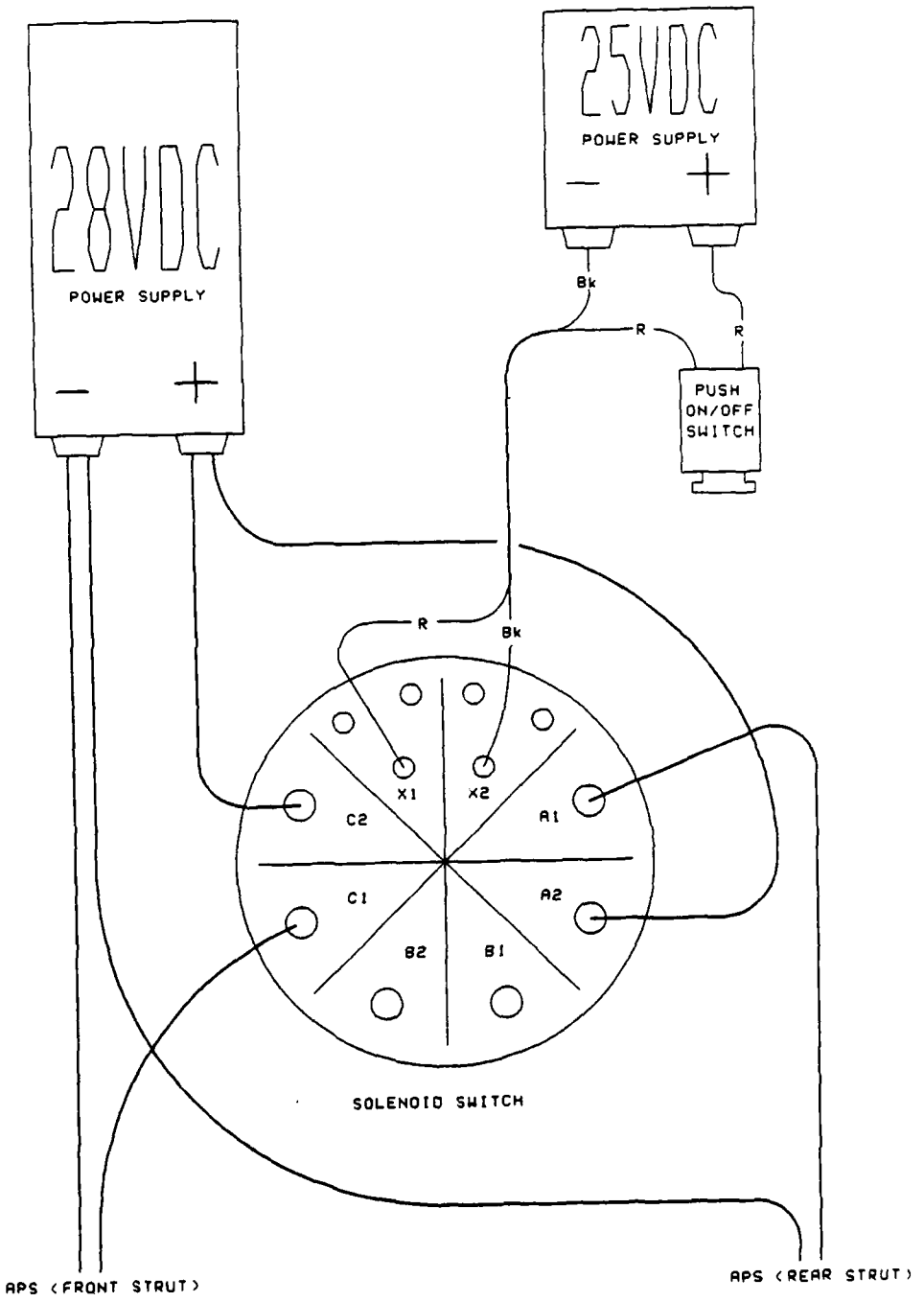

APPENDIX I

ASSEMBLY DRAWINGS

The following assembly drawings are extracts from the blueprints used to manufacture HARS. Copies of the blueprints are available upon request from Dr. Thomas C. Pollock. He can be contacted through the mail at Texas A&M University, Dept. of Aerospace Engineering, College Station, Texas, 77843; or by phone at (409) 845-7542.

0° ASSEMBLY

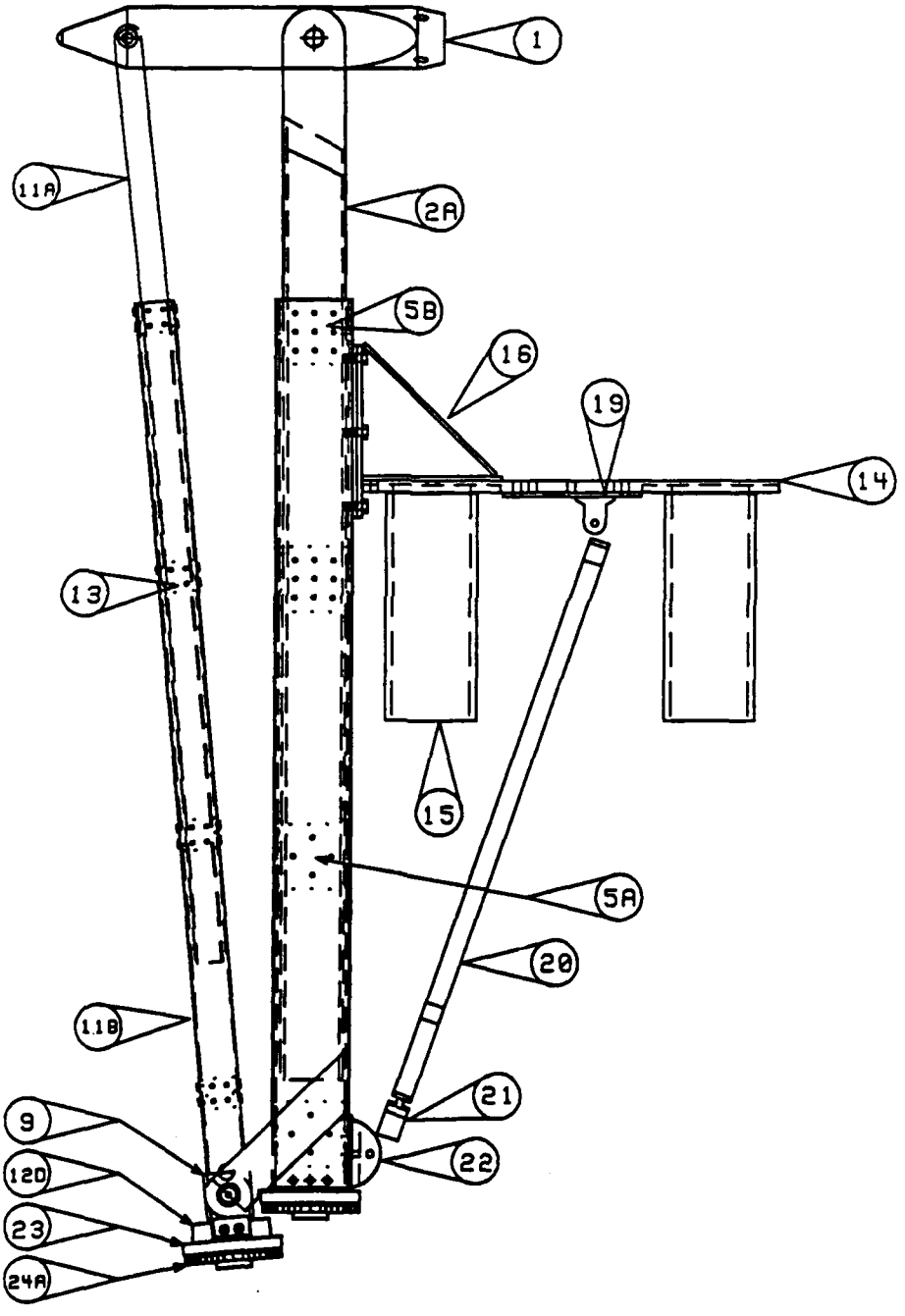

FOR NUMBERED PARTS IDENTIFICATION
REFER TO NEXT PAGE

0° ASSEMBLY

PART IDENTIFICATION BY NUMBER

1. TRANSVERSE LINK
2A. FRONT STRUT EXTENSION
2B. FRONT STRUT CASING
3A. FRONT STRUT EAR
3B. PIVOT BOLT
4A. FRONT STRUT SPLIT NUT
4B. FRONT STRUT CASING CAP
4C. FRONT STRUT SCREW
4D. NYLATRON WASHER
4E. STAINLESS STEEL WASHER
4F. PLAIN WASHER
4G. COTTER PIN
5A. FRONT STRUT BASE PAD (TYP)
5B. FRONT STRUT WEAR PAD (TYP)
6. FRONT STRUT MOUNT PLATE
8. REAR STRUT SUPPORT BRKT
9. REAR STRUT COLLAR
11A. REAR STRUT EXTENSION
11B. REAR STRUT CASING
12A. REAR STRUT SPLIT NUT
12B. REAR STRUT CASING CAP
12C. REAR STRUT SCREW
12D. TRANSMISSION ADAPTER BLOCK
13. REAR STRUT PADS (TYP)
14. MOUNTING PLATE
15. MOUNTING TUBE (TYP)
16. 0 DEG ADAPTER
17. 30 DEG ADAPTER
18. MOUNT EXTENSION BAR
19. UPPER BRACE MOUNT
20. BRACE
21. BRACE TURNBUCKLE
22. LOWER BRACE MOUNT
23. TRANSMISSION MOUNT
24A. GEAR (TYP)
24B. IDLER GEAR SHAFT
24C. STRAIGHT KEY
24D. SMALL NYLATRON WASHER
24E. SMALL STAINLESS STEEL WASHER
25A. WIRING GUIDE
25B. UPPER WIRING GUIDE CLAMP
25C. LOWER WIRING GUIDE LOCATOR

30° ASSEMBLY

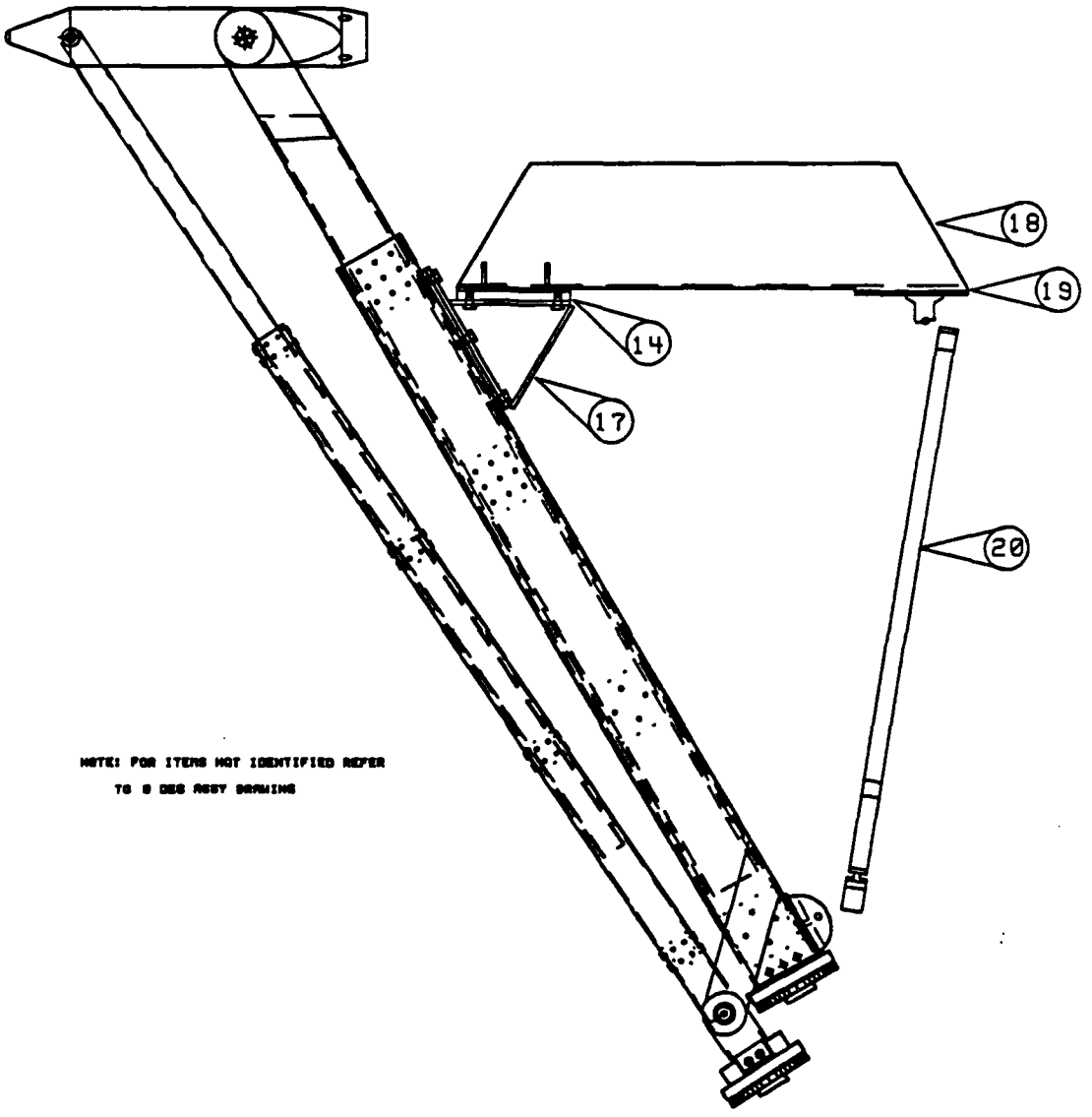

NOTE: FOR ITEMS NOT IDENTIFIED REFER TO 8 DEG ASSY DRAWING

REFER TO NEXT PAGE FOR PARTS IDENTIFICATION

30° ASSEMBLY

PART IDENTIFICATION BY NUMBER

1. TRANSVERSE LINK
2A. FRONT STRUT EXTENSION
2B. FRONT STRUT CASING
3A. FRONT STRUT EAR
3B. PIVOT BOLT
4A. FRONT STRUT SPLIT NUT
4B. FRONT STRUT CASING CAP
4C. FRONT STRUT SCREW
4D. NYLATRON WASHER
4E. STAINLESS STEEL WASHER
4F. PLAIN WASHER
4G. COTTER PIN
5A. FRONT STRUT BASE PAD (TYP)
5B. FRONT STRUT WEAR PAD (TYP)
6. FRONT STRUT MOUNT PLATE
8. REAR STRUT SUPPORT BRKT
9. REAR STRUT COLLAR
11A. REAR STRUT EXTENSION
11B. REAR STRUT CASING
12A. REAR STRUT SPLIT NUT
12B. REAR STRUT CASING CAP
12C. REAR STRUT SCREW
12D. TRANSMISSION ADAPTER BLOCK
13. REAR STRUT PADS (TYP)
14. MOUNTING PLATE
15. MOUNTING TUBE (TYP)
16. 0 DEG ADAPTER
17. 30 DEG ADAPTER
18. MOUNT EXTENSION BAR
19. UPPER BRACE MOUNT
20. BRACE
21. BRACE TURNBUCKLE
22. LOWER BRACE MOUNT
23. TRANSMISSION MOUNT
24A. GEAR (TYP)
24B. IDLER GEAR SHAFT
24C. STRAIGHT KEY
24D. SMALL NYLATRON WASHER
24E. SMALL STAINLESS STEEL WASHER
25A. WIRING GUIDE
25B. UPPER WIRING GUIDE CLAMP
25C. LOWER WIRING GUIDE LOCATOR

APPENDIX J

ACKNOWLEDGEMENTS

The author would like to acknowledge the the organizations and individuals responsible for making this project possible:

FUNDING was made available by General Dynamics/ Fort Worth, the Texas Engineering Extension Service (low speed wind tunnel facility), and Texas A&M University, College of Engineering, Department of Aerospace Engineering.

FABRICATION relied on the combined talents of a number of sources. Primary manufacturing credit goes to Brazos Technologies, Inc. of College Station, Texas. The fabrication of installation adapters, and the stabilization bar was done by Mr. Mike Birdsell and Mr. Paul Petty of the Flight Mechanics Laboratory, Texas A&M Department of Aerospace Engineering. The author made all small attachment hardware, wiring harnesses and guides, and subsequent modification machining to the original series of blueprints.

ASSISTANCE by Michael Niestroy during trial assembly, and installation of HARS proved invaluable. Additionally, Dr. Thomas Pollock provided timely machining expertise during the operational testing phase.

VITA

Tommy Jack Kubler [redacted] graduated from John Jay High School in San Antonio, Texas in May of 1974. In January, 1975 he enrolled in San Antonio Junior College, where he took general class work until enlisting in the United States Air Force a year later. For four and half years he worked as a computer programming specialist supporting the statistical research conducted by the Human Resources Laboratory, Brooks Air Force Base. In 1980 he was sponsored by the Air Force in an undergraduate degree program at Texas A&M University. Completing a Bachelor of Science in aerospace engineering in May 1983, he graduated from the Air Force's Officer Training School later that summer. His next assignment was with the Directorate of Material Management, San Antonio Air Logistics Center, Kelly Air Force Base. He initially served as Project Engineer for the TF-39 engines used on the C-5A and C-5B aircraft before transferring to the Aerodynamics and Performance Branch of the Directorate. In this position he performed aerodynamic performance prediction and mishap analysis support for the A-37, C-5, F-5, F-106, O-2, OV-10, T-37, and T-38 aircraft. He returned to Texas A&M again in the fall of 1987. During his return to course work, he worked under the direction of Dr. Thomas C. Pollock in the area of flight mechanics, specifically the design of a high angle of attack mounting mechanism for use in the low speed wind tunnel operated by the Texas A&M. Following successful completion of his degree program, he will be stationed at Eglin Air Force Base with the 3246th Test Wing. He will be maintaining his [redacted]

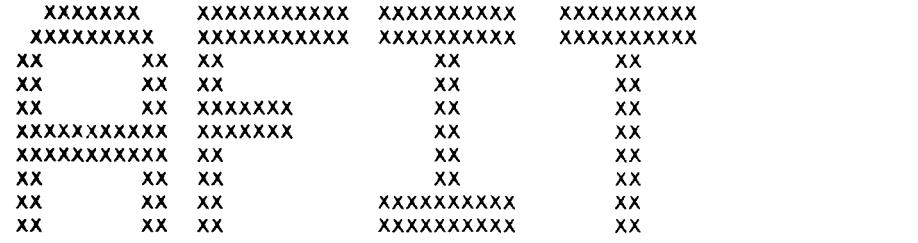

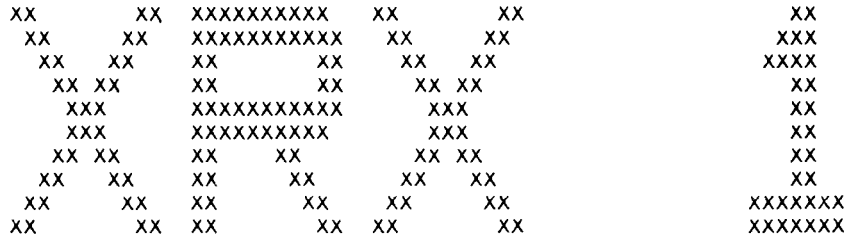

```
********** I T E M I Z E D   J O B   C O S T **********
*                                                      *
* BOX        JOB NAME          COMMENTS        DATE       JOB NUMBER *
* 100C       T1K7208        AFIT.XRX;1      15.25.13    89.180   2225  *
*                                                      *
* I T E M                   QUANTITY          COST     PREVIOUS       *
*                                                       BALANCE  57.858 *
* CPU                      0.36  SECONDS       0.133                  *
* XEROX SPECIAL FORM1       276  PAGES        15.180                  *
*                                                      *
*                                                      *
*                                                      *
*                                                      *
*                                                      *
*                                                      *
*                                                      *
*                                                      *
*                                                      *
*                                                      *
*                                                      *
*                                                      *
*                                                      *
*                                          TOTAL CHARGES   15.313 *
*                                                      *
* PRIORITY 5                DPSR B191    CURRENT BALANCE   42.545 *
*                                                      *
********************************************************
```

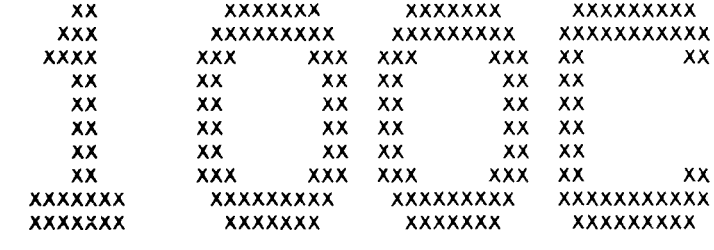

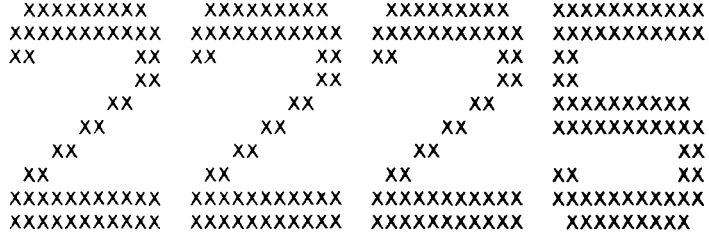

Texas A&M University
Analysis of Academic Progress
Office of Graduate Studies
MASTER OF SCIENCE IN AERO
Option: THESIS OPTION
Catalog 110, Academic Year 1987-88
Date Degree Plan Filed: 01/10/89

NOTE: See current Graduate Catalog for specific details relating to the degree requirements.

****
SECTION 1 - Selected Student Data
****

LOCAL ADDR. 1706 LEONA COLLEGE STATI TX 77840
PERM. ADDR. 223 JAMAICA SAN ANTONIO TX 78227
PHONE: (512)675-2976

CHAIR : POLLOCK, THOMAS C

CLASS	: G7	DATE OF BIRTH	: 05/31/56
COLLEGE	: GR	SEX	: M
DEGREE	: MS	MARITAL STATUS	:
DEPT	: AERO	CITIZENSHIP	: US
MAJORS	: AERO	VISA TYPE	:
OPTIONS	: THO	STATE OF ORIGIN	: TX
MINORS	:	ETHNIC ORIGIN	: W
CATALOG	: 110	ADMISSION DATE	: 06/05/87
SECOND DEGREE:		ADMISSION STATUS	: A
DEPT	:	ENTERING GPR	: 3.22
MAJORS	:	DEGREE CHECKOUT STATUS	: 3
OPTIONS	:	DEGREE CHECKOUT TERM	: 89A
MINORS	:	DEGREE EXPECTED TERM	: 89A
CATALOG	:	GRADUATION CODE	:

GRADUATE STUDENT DATA

COMMITEE MEMBERS:
CHAIR : POLLOCK, THOMAS C
WARD, DONALD T
MARONGIU, MAURICIO J

FIRST REGISTERED : 87C
LAST REGISTERED : 89A
RESEARCH PROPOSAL IN :
ADMITTED TO CANDIDACY :
PRELIMS :
ORALS :

PREVIOUS DEGREES	DEG	MAJ1	MAJ2	MINOR	HON	DATE
TEXAS A&M U MAIN CAMPUS	BS	AERO				5/83

TEST SCORES

GRE	6/87	520-GREV	800-GREQ	1320-GRET	650-GREA

DATE	DEPT	COMMENTS
1/10/89	CLGR	MARONGIU, MAURICE IS A MEMBER OF THE COMMITTEE

This evaluation is provided for advisement, it is not an official record. Please report any additions or corrections to your chair.

COURSE EXCLUSIONS

(Continued from previous page)

4. A maximum of 0 hours of seminar may be used.
5. A maximum of 6 hours of advanced undergraduate courses (300 or 400) may be used.
6. No correspondence study may be used.
7. No credit hours of 684 (Professional Internship) may be used.
8. A maximum of 12 hours of the following College of Medicine courses may be used: MANA 901, 911, 922, 985, 991; MBCH 911, 912, 985, 991; MPHY 901, 902, 985, 991; MPHM 924, 925, 985, 991; MMIM 923, 924, 985, 991; MPAT 923, 924, 925, 985, 991.
9. No more than 4 hours of OCNG 604 may be used in this degree program.
10. No more than 4 hours of OCNG 605 may be used for this degree program.
11. No more than 4 hours of OCNG 606 may be used for this degree program.
12. No more than 4 hours of OCNG 607 may be used for this degree program.
13. nomore than 9 hours of PSYC 682 may be used on this degree plan.
14. no more than 9 hours of BANA 688 may be used on this degree plan.
15. no more than 9 hours of FINC 688 may be used on this degree plan.

TIME LIMITS

All course work, final exam, and Thesis mus ,,e completed within seven consecutive years.

SECTION 3 - Academic Requirements Completed or in Progress

DEGREE PLAN

AERO 405	AEROSPACE STRUCTURES	88A	3.0	A	
AERO 601	PRIN OF FLUID MOTION	87C	4.0	B	
AERO 602	THEORY OF FLUID MECH	88A	4.0	B	
AERO 603	APPL MECH AERO ENGR	88C	3.0	C	
AERO 681	SEMINAR	87C	1.0	S	
AERO 681	SEMINAR	88A	1.0	S	
AERO 689	SP TP EXPER METH FLUIDS	87C	3.0	B	
AERO 691	RESEARCH	87C	1.0	S	
AERO 691	RESEARCH	88A	4.0	S	
AERO 691	RESEARCH	88C	3.0	S	
MATH 601	HGHR MATH ENGRS & PHYS	88B	4.0	B	
MEEN 689	SP TP DYN/CON ROBOTS	89A	(3.0)		Registered
	Total		34.0		GPR 3.000, Variance +0

SECTION 4 - Work Not Applicable to this Program

AERO 681	SEMINAR	88C	1.0	S	Not on Degree Plan
AERO 691	RESEARCH	88C	5.0	S	Not on Degree Plan

BIBLIOGRAPHY

1 Vinceint, J., "New Technologies for a European Fighter," *Aerospace America*, Vol. 24, Sept. 1986, p. 34.

2 Wright, O., Jr., "Squeezing the Testing Cycle," *Aerospace America*, Vol. 26, Feb. 1988, pp. 17-19.

3 Dietz, W.E., Jr. and Altstatt, M.C., "Experimental Investigation of Support Interference on an Ogive Cylinder at High Incidence," AIAA Paper 78-165, 16th Aerospace Sciences Meeting, Jan. 16-18, 1978.

4 Mouch, T.N., and Nelson, R.C., "The Influence of Aerodynamic Interference on High Angle of Attack Wind Tunnel Testing," AIAA Paper 78-827, 1978.

5 Johnson, J.L., Grafton, S.B., and Yip, L.P., "Exploratory Investigation of the Effects of Vortex Bursting on the High Angle-of-Attack Lateral-Directional Stability Characteristics of Highly-Swept Wings," AIAA Paper 80-0463, Mar. 1980.

6 Ericsson, L.E., and Reding, J.P., "Support Interference in Static and Dynamic Tests," *ICIASF 1981 Record*, pp. 213-223.

7 Rae, W.H., Jr., and Pope, A., *Low-Speed Wind Tunnel Testing*, Wiley and Sons, New York, 1984, p. 175.

8 Malcolm, G.N., "New Rotation-Balance Apparatus for Measuring Airplane Spin Aerodynamics in the Wind Tunnel," AIAA Paper 78-835, 1978.

9 Ericsson, L.E., "Reflections Regarding Recent Rotary Rig Results," AIAA Paper 86-0123, AIAA 24th Aerospace Sciences Meeting, Jan. 6-9, 1986.

10 Kreplin, H.P., Meier, H.U., and Maier, A., "Wind Tunnel Model and Measuring Techniques for the Investigation of Three-dimensional Boundary Layers," AIAA Paper 78-781, 1978.

11 Erb, R.E., *Evaluation of the Use of Hinged Strakes on a High Performance Fighter Aircraft*, thesis, Texas A&M University, May 1985.

12 *Low Speed Wind Tunnel Facility Handbook*, Texas Engineering Experiment Station, The Texas A&M University System, Jan. 1985.

[13] Bruhn, E.F., *Analysis and Design of Flight Vehicle Structures*, Jacobs Publishing, Carmel, Indiana, 1973, pp. A6.3-A6.6.

[14] Polakowski, N.H., and Ripling, E.J., *Strength and Structure of Engineering Materials*, Prentice-Hall, Inc., Englewood Cliffs, New Jersey, 1966, p. 401.

[15] DOD Publication FSC 1560, *Military Standardization Handbook - Metallic Materials and Elements for Aerospace Vehicle Structures*, Department of Defense, 1 Jun. 1983.

[16] Bertin, J.J., and Smith, M.L., *Aerodynamics for Engineers* , Wiley and Sons, New York, 1981, pp. 208-214.

[17] Nicolai, L.M., *Fundamentals of Aircraft Design*, Mets Inc., San Jose, Calif., 1975, pp. 11-5–11-23.

[18] Hoerner, S.F., *Fluid Dynamic Drag*, published by the author, Midland Park, New Jersey, 1958, p. 92.

[19] Perkins, C.D., and Hage, R.E., *Airplane Performance Stability and Control*, Wiley and Sons, New York, 1967, pp. 216-229.

Supplementary Sources Consulted

[1] *Plastics Reference Handbook* Regal Plastics Supply Company, National Association, 1987, pp. 183-196, (Private collection, T. Kubler).